Fall 2003

Development of supercritical processes for particle coating / encapsulation with polymers

Yulu Wang
New Jersey Institute of Technology

ABSTRACT

DEVELOPMENT OF SUPERCRITICAL FLUID PROCESSES FOR PARTICLE COATING/ENCAPSULATION WITH POLYMERS

by

Yulu Wang

This work presents the investigation of particle coating using supercritical fluid processes as novel coating approaches to coat particles from 20 nanometers to 500 microns with different polymers. Particle coating using different supercritical technologies of a modified rapid expansion of a supercritical solution (RESS) for particle coating and a supercritical antisolvent (SAS) process was described.

In the modified RESS process for particle coating, experiments were performed using a pilot-scale supercritical apparatus, glass beads as host particles and two different polymers as coating materials. By adjusting temperature and pressure, the polymer nucleated and precipitated onto the surface of the host particles in a precipitation chamber due to the significantly lowered solubility of polymer in supercritical CO_2. The glass beads were found coated with poly vinyl chloride-co-vinyl acetate (PVCVA) and hydroxypropyl cellulose (HPC) although the coating was not uniform and not continuously distributed over the surface of the particles.

The main part of this work is the study of the SAS process for particle coating. The supercritical fluid worked as an antisolvent in the SAS process instead of a solvent in the RESS. The SAS process is based on the principle of SC CO_2 induced phase separation in which the solute precipitates due to a high super-saturation produced by the mutual diffusion between organic solvent and SC CO_2 when an organic liquid solution comes

into contact with SC CO_2. Systematic study of the effects of process conditions on the coating of particles in the SAS process was performed. The polymer weight fraction and polymer concentration played critical roles in the agglomeration of coated particles and the thickness of coating. Higher pressure facilitated the T_g depression, enhancing the agglomeration of coated particles. Operating temperature had no visible effect on the coating effect when the temperature was below T_g. The coating quality also was independent of spraying velocity. Surfactants had adverse effects on the coating quality.

The application of SAS particle coating process in the design of drug delivery system was studied. A biopolymer of poly lactide-co-glycolide (PLGA 50/50) and hydrocortisone were selected as the coating material and the model drug, respectively. The hydrocortisone particles were successfully coated with PLGA. At higher polymer loading ratios, the coated drug particles showed sustained release behavior. Higher polymer loading ratio produced higher encapsulation efficiency.

DEVELOPMENT OF SUPERCRITICAL FLUID PROCESSES FOR PARTICLE COATING/ENCAPSULATION WITH POLYMERS

by
Yulu Wang

A Dissertation
Submitted to the Faculty of
New Jersey Institute of Technology and
Rutgers, The State University of New Jersey-Newark
In Partial Fulfillment of the Requirements for the Degree of
Doctor of Philosophy in Environmental Science

Department of Chemistry and Environmental Science

January 2004

APPROVAL PAGE

DEVELOPMENT OF SUPERCRITICAL FLUID PROCESSES FOR PARTICLE COATING/ENCAPSULATION WITH POLYMERS

Yulu Wang

Dr. Robert Pfeffer, Dissertation Advisor Date
Distinguished Professor of Chemical Engineering, New Jersey Institute of Technology

---

Dr. Rajesh Dave, Dissertation Co-advisor Date
Professor of Mechanical Engineering, New Jersey Institute of Technology

---

Dr. Zafar Iqbal, Committee Member Date
Professor of Chemistry and Environmental Science
New Jersey Institute of Technology

Dr. Jing Wu, Committee Member Date
Assistant Professor of Chemical Engineering, New Jersey Institute of Technology

---

Dr. Barbara Kebbekus, Committee Member Date
Professor of Chemistry and Environmental Science
New Jersey Institute of Technology

BIOGRAPHICAL SKETCH

Author: Yulu Wang

Degree: Doctor of Philosophy in Environmental Science

Date: January 2004

Undergraduate and Graduate Education:

- Doctor of Philosophy in Environmental Science,
  New Jersey Institute of Technology, Newark, NJ, 2004
- Master of Science in Chemical Engineering,
  Dalian University of Technology, Dalian, P. R. China, 1995
- Bachelor of Science in Chemical Engineering,
  Hefei University of Technology, Hefei, P. R. China, 1992

Major: Environmental Science

Presentations and Publications

Yulu Wang, Yiping Wang, Jun Yang, Robert Pfeffer, Rajesh Dave, Bozena Michniak, "Application of Supercritical Antisolvent Process for Controlled Drug Delivery System Design", in preparation.

Yulu Wang, Robert Pfeffer, Rajesh Dave, Robert Enick, "Encapsulation of Ultrafine Particles in polymer by a Supercritical Antisolvent (SAS) Process", submitted to AIChE J.

Yulu Wang, Rajesh Dave, Robert Pfeffer, "Nanoparticle Encapsulation with Heterogeneous Nucleation in A Supercritical Antisolvent Process", *J. Supercrit. Fluids*, 28, 2004, 85-99.

Yulu Wang, Dongguang Wei, Rajesh Dave, Robert Pfeffer, Martial Sauceau, Jean-Jacques Letourneau, Jacques Fages, "Extraction and Precipitation Particle Coating Using Supercritical CO_2", *Powder Technol.*, 127, 2002, 32-44.

Jun Yang, Yulu Wang, Rajesh Dave, Robert Pfeffer, "Mixing of Nano-particles by Rapid Expansion of Supercritical Suspensions (RESS)", *Adv. Powder Technol.*, 14, 2003, 471-493.

Yulu Wang, Rajesh Dave, Robert Pfeffer, "Preparation of Microencapsulated Ultra-Fine Particles by Supercritical Solvent (SAS) Process", presentation at AIChE Annual Meeting, Nov. 1-7, 2002, Indianapolis, IN

Yulu Wang, Rajesh Dave, Robert Pfeffer, "Fine Particle Coating/Encapsulation with Polymer using Supercritical Anti-Solvent (SAS) Process", presentation at AIChE Annual Meeting, Nov 4-9, 2001, Reno, NV.

Yulu Wang, Baohua Yue, Dongguang Wei, Michael Huang, Rajesh Dave, Pfeffer, "Nano-Particle Coating/Encapsulation with Polymers by Supercritical fluid Processing", CD-ROM Proceedings of 4th World Congress on Particle Technology, July 21-25, 2002, Sydney, Australia.

Jun Yang, Rajesh Dave, Robert Pfeffer, Yulu Wang, "Investigation of Nano-Particle Mixing and Characterization", CD-ROM Proceedings of 4th World Congress on Particle Technology, July 21-25, 2002, Sydney, Australia.

To my beloved son, Yunpeng Wang; Wife, Yun Wang; my parents, Chenglan Gu and Zijin Wang.

ACKNOWLEDGEMENT

My sincere gratitude goes to Dr. Robert Pfeffer, who not only gave me the utmost freedom in the laboratory and opened up a new area of interest, but also provided constant support, guidance, and encouragement. He has been more than an advisor, a mentor whom I learned so much from. Special thanks are also due to Dr. Rajesh Dave for his constructive comments and resourceful suggestions. I appreciate his guidance, knowledge and support during the course of this work.

I would like to thank Dr. Barbara Kebbekus, Dr. Zafar Iqbal, and Dr. Jing Wu for actively participating in my committee, and for giving many helpful suggestions and corrections.

The modified RESS coating experiment was done at Particle Technology Center in Ecole des Mines d'Albi-Carmaux, France. I would like to thank Prof. John Dodds for providing me the opportunity. I also thank Prof. Jacques Fages, Dr. Jean-Jacques Letourneau, Martial Sauceau, Maryse Collado for their advice and help during my stay in France.

During my graduate research, I was fortunate to receive help from a number of people, Dr. Michael Huang, Dr. Larisa Krishtopa, Dr. Jun Yang, Dr. Dongguang Wei, Dr. Xueyang Zhang, and Dr. Dong-June Park. I truly appreciate their assistance.

Special thanks to my peers, Baohua, Caroline, Yueyang for their support, friendship and "simulating" conversations. They made my stay at NJIT pleasant and productive.

Lastly, I am deeply indebted to my parents, Chenglan Gu and Zijin Wang, my wife and son, Yun Wang and Yunpeng Wang for their sacrifices and support during my many years of study.

TABLE OF CONTENTS

TABLE OF CONTENTS
(Continued)

Chapter **Page**

TABLE OF CONTENTS
(Continued)

Chapter **Page**

TABLE OF CONTENTS
(Continued)

Chapter **Page**

TABLE OF CONTENTS
(Continued)

Chapter **Page**

LIST OF TABLES

Table **Page**

LIST OF FIGURES

Figure **Page**

LIST OF FIGURES
(Continued)

Figure **Page**

LIST OF FIGURES
(Continued)

Figure **Page**

LIST OF FIGURES
(Continued)

Figure **Page**

NOMENCLATURE

a	Parameter in Peng-Robinson equation of state, gram·m^5/sec^2·mol^2
b	Parameter in Peng-Robinson equation of state, m^3/mol
x	Molar fraction in gas phase
y	Molar fraction in liquid phase
c	Critical value
r	Reduced value
m	Mass, gram
t	Thickness of coating, μm
ρ	Density, gram/ml
V	Expanded liquid volume, ml
V_0	Initial liquid volume, ml
ΔV	Expansion rate, %
A	Antisolvent
R	Radius of particles, μm
R	Relative velocity
T	Temperature, °C
P	Pressure, bar
C	Coating material
H	Host particles
D	Droplet diameter, m
S	Solubility, mole/ml

NOMENCLATURE

(Continued)

Z	Compress factor
i	Component index
j	Component index
k_{ij}	Interaction parameter,
lij	Secondary interaction parameter
ν	Compress factor
ω	Accentric factor
σ	Surface tension, N/m^2
Nw_e	Weber number, $Nw_e = \rho_A v_R^2 D/\sigma$
Φ	Phase
$\overline{\upsilon}$	Partial molar volumes, ml/mol

CHAPTER 1

BACKGROUND

1.1 Introduction

Particulate materials are critical to many industries, such as chemicals, pharmaceuticals, agriculture and cosmetics, since over 60 % of their products are either in the form of particles or related to particles, which act as important intermediates in the product cycle. In 1993, the US Department of Commerce estimated that particle products contribute $1 trillion annually to the US economy. The surface properties of particulate materials are very important because most of the properties of bulk materials, such as solubility, stability, wettability, durability, dispersability, and flowability are dependent on surface properties. Therefore, surface modification of particles to produce desirable properties is of great interest and has become an important topic for research.

Coating or encapsulation of particles is most widely used for particle surface modification. Coating or encapsulation is defined as the application of a layer of another material on the surface of a particle, forming a barrier or film between the particle and its environment. Coating of particles are required for a variety of reasons. Coating of drug particles provides controlled release behavior, achieving targeted release and more effective therapies, while eliminating the potential for both under and overdosing. For example, Ike et al., 1992, showed that encapsulated cisplatin (an anti-cancer agent) in poly lactide (D, L-PLA) provided controlled release in vivo for 21-42 days.

Film coating of particles made of sensitive materials provides protections from degradation due to moisture, oxygen, light, or acids. For instance, the surface of titanium dioxide particles is coated with alumina to protect photoactivation by sunlight. Silica

coating on the surface of titanium dioxide for pigment application suppresses surface reactions when particles are dispersed in resins and polymers (Iler, 1959, Allen, 1978, Jacobson, 1980). Antistatic coating improves powder handling; poly vinyl alcohol particles coated with an antistatic agent can make these powders safe from explosion in pneumatic transport and bulk storage. The coating of titanium dioxide pigment with naphthenic acid improves its flowability (Davis, et al., 1998). Surface modification of drug loaded microspheres with polyethylene oxide (PEO) or poly vinyl alcohol (PVA) was reported (Lück, et al., 1998) to improve the biocompatibility and bio-distribution of the drug delivery carriers.

1.2 Particle Coating or Encapsulation Techniques

Particle coating or encapsulation is achieved by a number of wet or dry coating methods. Traditional particle coating employs wet coating methods. Wet approaches include emulsion evaporation, double emulsion evaporation, spray drying, fluidized bed coating, sol-gel process, coacervation, melting solidification, interfacial polymerization, and others.

1.2.1 Emulsion Evaporation

The emulsion evaporation technique is widely used in the fabrication of microsphere drug delivery systems. Depending on the properties of the active drugs, a variety of emulsions can be used. Oil-in-water (O/W) emulsion is suitable for the encapsulation of drug compounds with very limited solubility in an aqueous system. In this emulsion method, the active agent and a polymer are dissolved in an organic solvent. The resulting solution is dispersed into an aqueous solution containing a surfactant. After complete evaporation

of the organic solvent, the solidified drug loaded microspheres are filtered and vacuum dried. For example, Yen, et al., 2001 reported the production of nalbuphine propionate loaded microspheres for controlled release using this method. Ko, et al., 2002, applied this approach to microencapsulate drug components for controlled drug delivery. For water-soluble material, a non-aqueous emulsion is used for the encapsulation process. The aqueous phase is replaced by a solvent, which is a non-solvent for the active ingredient. With this method, Ogawa, et al., 1988, efficiently entrapped leuprolide acetate into microcapsules of poly (lactic acid) or poly (lactic-co-glycolic acid).

1.2.2 Double Emulsion

A double emulsion method is a modification of emulsion evaporation employing a multiple emulsion. It is quite popular in the design of microspheres for drug delivery systems. In the double emulsion method, the active agent is first dissolved in an aqueous solution and then added into an organic polymer solution to form a primary emulsion under stirring. The resulting primary emulsion is added to the aqueous solution containing a surfactant and subjected to mixing. The formed microspheres are collected by filtration after evaporation of the organic solvent. For double emulsion systems, the encapsulation rate of active compounds is a function of the surfactant concentration and the ratio of the aqueous phase to the organic phase. Compared with emulsion evaporation, double emulsion methods favor higher loading of active drug. Yamaguchi, et al., 2002 and Blanco-Prieto, et al., 1997 used this approach to make protein and peptide loaded microspheres for drug delivery. The encapsulation of plasmid DNA in

microspheres for gene delivery system using the same technique was demonstrated in the work of Wang, et al., 1999 and Capan, et al., 1999.

1.2.3 Spray Drying

Spray drying has been used for coating and encapsulation of particles for some time. In the encapsulation of drug component, the active ingredient is dissolved or dispersed in an organic or aqueous solution. The suspension or solution is atomized by spraying through a nozzle into hot air (150-200 ^{o}C), which is used to evaporate the solvent and produce microspheres of the active drug compound and polymer. The spray drying approach is a single step process, which is easy and cost-effective to operate. Numerous drug compounds can be encapsulated by using this method. Fang-Jing and Chi-Hwa, 2002 used spray-drying technique to produce sustained release of etanidazole in microspheres. Walter, et al., 1999 prepared a DNA vaccine delivery system by DNA encapsulation in polymer microspheres using spray drying. Bergna, 1987 patented an approach using a spray drying process to coat catalyst granular particles with a porous thin layer of silica.

1.2.4 Fluidized Bed Techniques

A fluidized bed equipped with a spray nozzle has been widely utilized in the coating of particles. The Wurster Coater is a well known technique used by the pharmaceutical, chemical, food, and agricultural industries. This method has the advantages of uniformity coating, good controllability, versatility, and operability. It is a very efficient and cost-effective coating method for the coating of granules, tablets, pellets, and large particles. For example, Wan and Lai, 1992, using a fluidized bed, demonstrated multilayer coated

particles for drug controlled release. Kage, et al., 1996, reported the coating of seed particles in a fluidized bed. Sudsakorn and Turton, 2000 also showed particle coating using a fluidized bed coater.

1.2.5 Coacervation

The coacervation process makes use of the partial precipitation of macromolecules and their aggregation induced by a chemical or physical change in a dispersing medium. The aggregation of polymer chains leads to a phase separation within an initially uniform colloidal solution. This operation proceeds with the presence of a solid or liquid dispersion, resulting in the formation of microspheres or microcapsules. Host particles are dispersed in a solution of coating material at a high temperature and the temperature of the dispersion is step-wise decreased, while the dispersion is stirred. Due to the cooling effect, the polymer precipitates onto the surface of the host particles. The encapsulation of a water-soluble drug of clomipramine HCl in ethylcellulose was done by Wieland-Berghausen, et al., 2002, using the coacervation method. Özyazici, et al., 1996 reported a very similar coacervation technique to produce microcapsules of nicardipine hydrochloride in ethyl cellulose.

1.2.6 Sol-Gel Process

The sol-gel approach is a well known method for the preparation of complex coating and encapsulation of fine particles. The method was demonstrated by Ruys and Mai, 1999 to coat nanoparticles. A core-shell structure was observed in the coated particles by TEM characterization. Zhang and Gao, 2001 described a heterogeneous nucleation in a sol-gel

process to coat SiC nanoparticles with $Al(OH)_3$ for the fabrication of nanocomposite powders. Chang, et al., 1994 also used the sol-gel method to produce monodisperse colloidal silica-cadmium sulfide nanocomposites with tailored morphology.

1.2.7 Melting Solidification

Melting solidification is used to produce a matrix of microspheres to encapsulate an active component. In the melting solidification process, the active component is dissolved or dispersed in a molten substance. The mixture is then emulsified in a dispersing phase, such as water, organic solvent, or vegetable oil. The dispersing phase is not a solvent for the molten polymer and the active component. As the temperature is lowered, the liquid droplets solidify, encapsulating the active compound. Benita, et al., 1986 studied this approach for the encapsulation of chemoembolization in carnauba wax microspheres.

1.2.8 Interfacial Polymerization

Interfacial polymerization was initially developed by Pennwalt Corp. (Ivy and Pencap, 1972) to encapsulate pesticide. The interfacial polymerization approach involves preparation of an organic or aqueous solution of the active component containing monomer A. The solution is then dispersed and emulsified in a continuous phase containing monomer B. The polycondensation at the interface between A and B results in the formation of a film, which isolates the solution from the active component. The resulting encapsulated particles are separated by filtration or centrifugation. This approach has been applied to produce carbon free paper (Baxter, 1977) and to encapsulate perfume (Curt, 1987).

Suspension polymerization for microencapsulation is similar to the previously described interfacial polymer approach except that only one monomer is used. Polymerization in a suspension of the monomer is carried out around the active component in the presence of an initiator. Most studies focus on the encapsulation of inorganic particles. Luna-Xavier, 2002 did research on surface coating of silica particles with PMMA using an emulsion interfacial polymerization approach. In their research, silica particles were coated using a cationic initiator, 2,2'-azobis (isobutyramidine) dihydrochloride (AIBA), and a nonionic polyoxyethylenic surfactant (NP_{30}) in the emulsion polymerization. The coated particles showed a core-shell structure. Shim, 2002 reported similar work of the surface modification of zinc oxide particles with polymethylmethacrylate (PMMA) using suspension interfacial polymerization. The encapsulation of active component in polymer nanoparticles for anticancer treatment was illustrated by Chiannikulchi, 1989. A similar research was carried out (Fattal, 1989) for ophthalmological use.

Although the above described wet coating methods are widely utilized for particle coating or encapsulation in chemical, pharmaceutical, food, agrochemical, and advanced materials industries, there are many drawbacks associated with them. Usually, a large amount of organic solvent is required in the wet coating processes. In addition, some other chemicals, such as surfactants, monomers, initiators, etc., are involved in the wet approaches. These lead to volatile organic compounds (VOCs) emissions and other waste streams. Furthermore, heavy down stream processes, for example, separating, drying, milling, and sieving, etc., are also required to manufacture the final products.

When coating or encapsulation using wet methods are applied for pharmaceutical purposes, there are some other concerns regarding the safety and maintenance of bioactive agents. During the emulsion preparation, the organic solvent, strong shearing forces, temperature, pH, and the interface between the oil and water phases may affect and/or alter the structure of the bioactive agents (Leong, et al., 1998, Jong, et al., 1997, Yang, et al., 1999, Fu, et al., 1999). Moreover, residual organic solvent in the final product might cause toxic effects for patients. Spray drying is appealing for coating of pharmaceutical agents because it is a single step process and low cost operation. However, it is not suitable for the coating of thermally labile drug entities due to the high temperature employed in this process. A fluidized bed equipped with a spray nozzle is well accepted for the coating of tablets, pellets, and granules. However, for particles less than 30 microns (Group C), agglomeration of particles due to strong cohesive forces becomes serious. Hence, it is difficult to fluidize fine particles of size less than 30 microns.

1.2.9 Dry Coating

As environmental regulatory statutes became more stringent, relatively new dry coating approaches attracted a lot of attention. Since no solvent is required, not even water, drying and separating processes are no longer problems and dry coating processes are environmentally benign. Pfeffer, et al., 2001 comprehensively, described the subject of dry particle coating. Dry particle coating involves the coating of submicron-sized guest particles onto the surface of larger host particles by mechanical forces. The size of the guest particles is so small (sub-micron) that van der Waals interactions between guest and

host particles are strong enough to keep them firmly attached on the surface of the host particles, resulting in surface coating. In this coating process, agglomerates of fine particles must first be broken into primary fine particles so that these fine particles can adhere onto the surface of the larger host particles. The exchange and redistribution of fine particles among the host particles proceed until a random distribution is achieved.

Dry particle coating methods can be utilized to change the properties of the host particles. For example, the absorption of moisture from the air by wax coated magnesium powder using a dry coating method was significantly reduced (Pfeffer, et al., 2001). Ishizaka, et al., 1988 reported that, when aspirin was coated onto potato starch by this approach, the dissolution rate of the aspirin was accelerated. Since there is no drying step required, energy consumption is substantially reduced. Also it is environmentally benign as no organic or aqueous waste is produced.

There are some other dry coating methods to modify the surface properties of particles such as: (a) physical vapor deposition (PVD) (Zhang, et al., 2000), (b) plasma treatment (Shi, et al., 2001, Vollath, et al., 1999), (c) chemical vapor deposition (CVD) (Takeo, et al., 1998), and (d) pyrolysis of polymeric or non-polymeric organic materials deposition (Sglavo, et al., 1993). However, all of these require high energy input.

Although dry particle coating processes are attractive from the point of view of environmental concern and require less downstream operating procedures, they are not suitable for coating particles for pharmaceutical applications since it is difficult to control the film structure on the surface of the host particles, such as the film thickness, uniformity, texture and robustness of the coating. In addition, in dry coating processes, the high shear and compressive forces employed and the local increase in temperature

would cause some bio-active particles, such as, proteins and peptides, to lose much of their bio-activity.

Based on the discussion of the various available particle-coating methods presented above, it is imperative to develop a new coating or encapsulation technique to overcome the drawbacks of these methods. The new process should be environmentally benign, with much less organic solvent required than in wet coating methods. It should be capable of operating at ambient temperature without any heavy downstream processing and be able to encapsulate fine particles less than 30 microns and down to nanosize.

1.3 Supercritical Fluid

1.3.1 Fundamentals

The phase of a substance depends on the temperature and pressure to which it is subjected. Freezing and boiling are frequently observed phenomena during which a

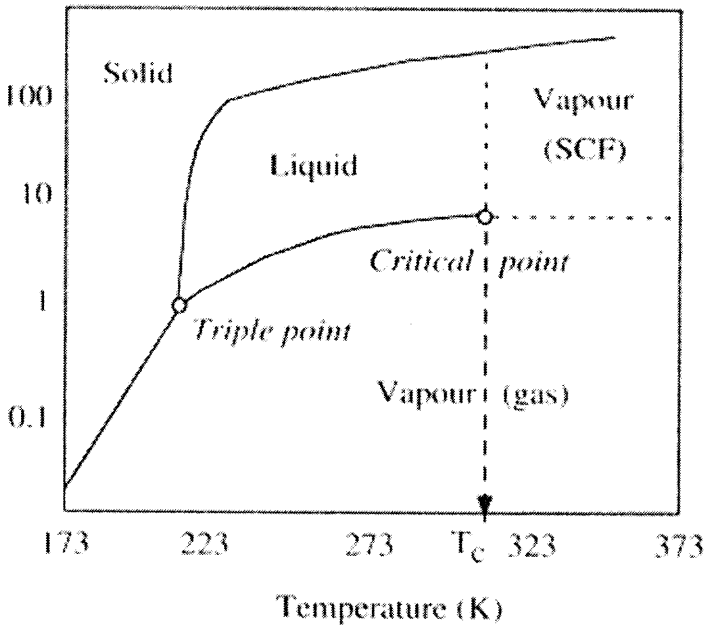

Figure 1.1 Schematic phase diagram of carbon dioxide.

phase change occurs as a function of temperature and pressure. A given substance, below a certain temperature, can be brought into the liquid state if it is subjected to sufficient pressure. However, about this temperature, it cannot be liquefied no matter what pressure is applied. This temperature is called critical temperature (T_c). At this temperature, the pressure at which the liquid phase and gas phase of a substance are in equilibrium is defined as the critical pressure (P_c). When a substance is subjected to conditions where both the temperature and pressure are above the critical temperature and critical pressure simultaneously, the substance is said to be in the supercritical fluid state

Table 1.1 Critical Temperatures and Critical Pressures of Various Substances

Substances	T_c (°C)	P_c (bars)
Inorganics		
Helium	-269.9	1.1
Nitrogen	-147	34
Carbon Dioxide	32	74
Water	374	221
Nitrous	37	72
Ammonia	132	114
Organics		
Ethane	32	49
Propane	97	43
Butane	152	38
Methanol	239	81
Ethanol	491	61
Ethyl Acetate	250	38
Acetone	215	74
Dimethyl ether	127	52
Diethyl ether	193	36
Perfluoorobutane	14	23

as illustrated in Figure 1.1. Each substance has a unique critical temperature and critical pressure (T_c and P_c). For example, T_c and P_c of carbon dioxide are 32 °C and 74 bars, respectively and water's critical point is at 374 °C and 221 bars. The critical points of a variety of substances are listed in Table 1.1.

1.3.2 Properties of Supercritical Fluid

A supercritical fluid has a very high compressibility. The density and viscosity of a substance in the supercritical state are between their values in the gas and liquid state. A plot of the variation in density with pressure and temperature is schematically shown in Figure 1.2. In the vicinity of the critical point, the fluid density changes dramatically with an increase in pressure. As can be seen in Figure 1.2, below the critical pressure the fluid

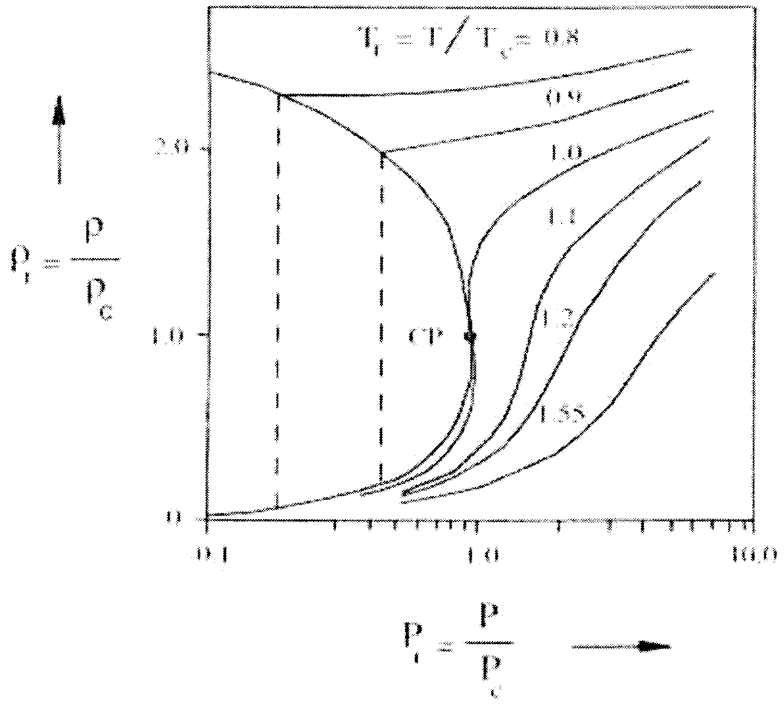

Figure 1.2 Schematic diagram of the density of a fluid change with pressure (McHugh and Krukonis, 1986).

is in the gaseous state and has a low density. However, above the critical pressure the fluid is in the supercritical region and has a relatively high liquid-like density. Although a supercritical fluid possesses liquid-like density, it has high compressibility as illustrated in Figure 1.3 in the range of 60-120 bars.

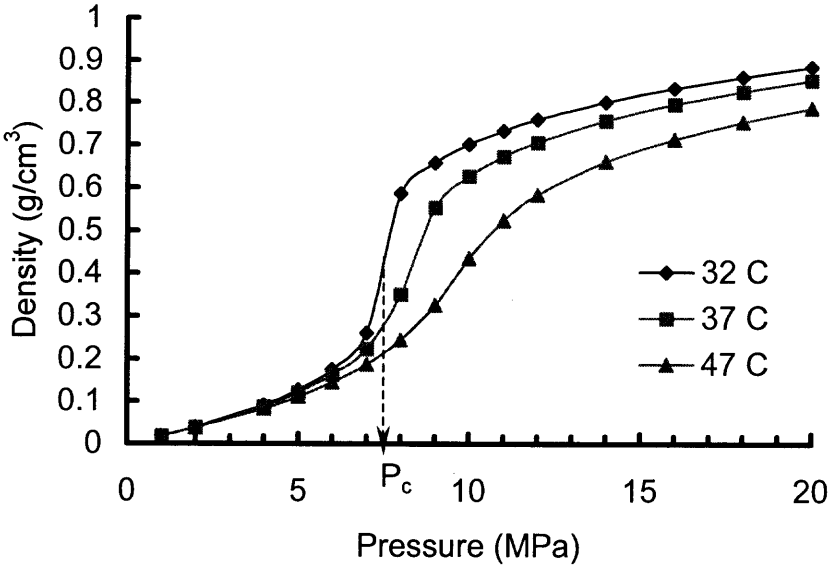

Figure 1.3 CO_2 density as a function of pressure and temperature calculated using the Peng-Robinson equation of state (Peng and Robinson, 1976).

The compressibility of a supercritical fluid can be used to manipulate the density by adjusting pressure. The solvent strength is related to the density of a fluid; hence, the solvent properties of a supercritical fluid can be adjusted by simply changing the pressure. The solubility of acridine in supercritical CO_2 is illustrated in Figure 1.4. It is found that the solubility initially decreases slightly and then increases sharply as the pressure is raised above the critical pressure. At high pressure the solubility gradually levels off. This corresponds with the density profile as a function of pressure.

A supercritical fluid also possesses other attractive physicochemical properties, such as high diffusivity and low viscosity. The diffusivity of a supercritical fluid is greater than that of a liquid but lower than that of a gas. McHugh and Krukonis, 1986

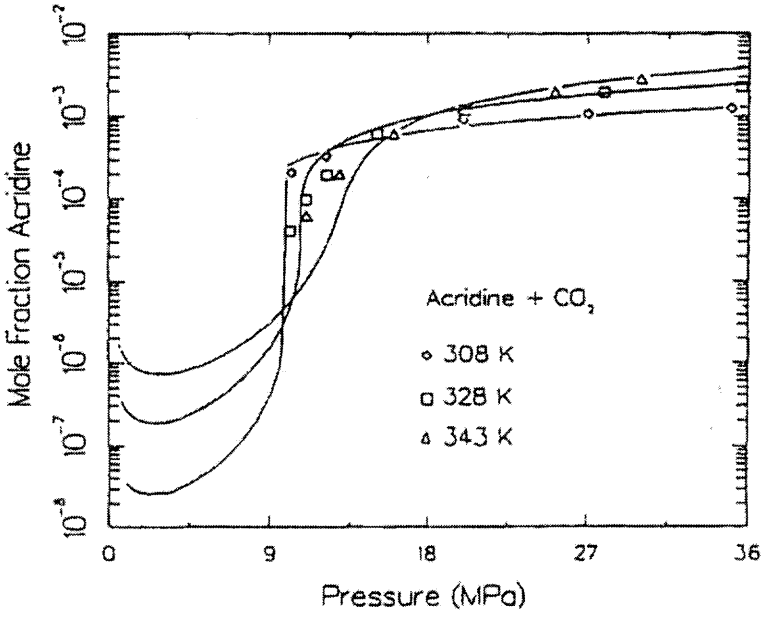

Figure 1.4 Solubility of acridine in supercritical CO_2 (Debenedetti and Kumar, 1986).

compared typical diffusivities of small organic solutes in supercritical CO_2 over a wide range of pressure and temperature with those of small organic solutes in liquids. As shown in Figure 1.5, the diffusivity in CO_2 at 40 °C in the range between 70-200 bars was found to be from 10^{-3} to 10^{-4} cm^2/sec. However, the diffusivity in a typical liquid is around 10^{-5} cm^2/sec. The viscosity of the supercritical fluid falls in between that of a gas and a liquid. Figure 1.6 illustrates the viscosity of CO_2 as a function of temperature and pressure. Below the critical point, the viscosity of CO_2 behaves as a gas and is very low.

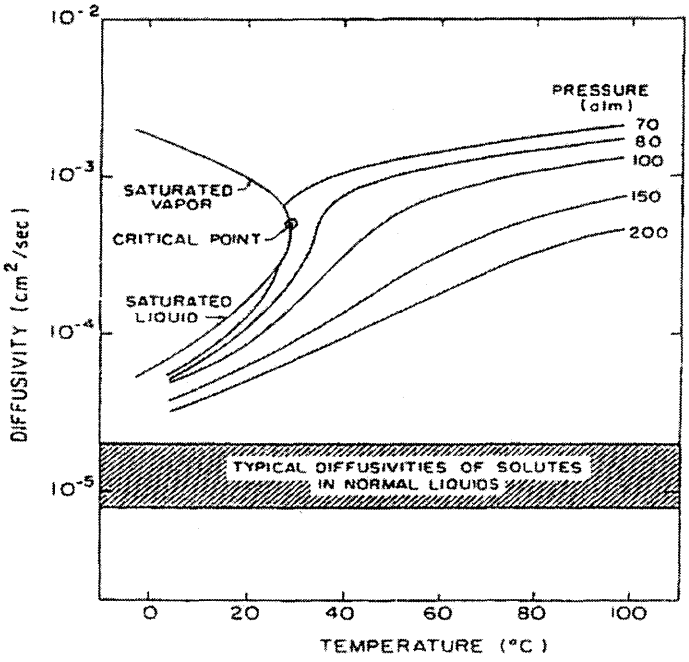

Figure 1.5 Diffusivity of small organic solutes in CO_2 (McHugh and Krukonis, 1986).

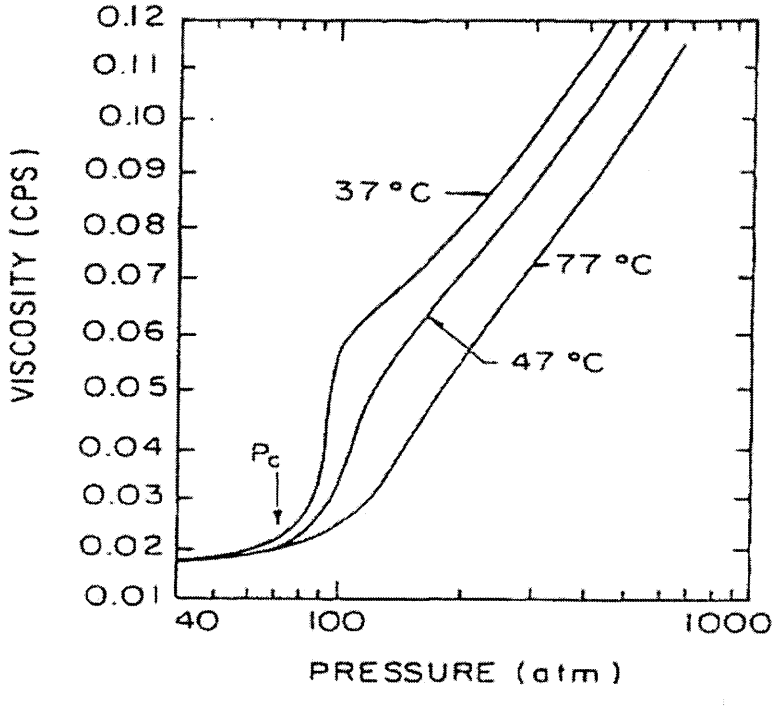

Figure 1.6 Viscosity of CO_2 as a function of pressure and temperature (McHugh and Krukonis, 1986).

Above the critical point, the viscosity of supercritical CO_2 increases as the pressure goes up, but it is still lower than that of liquid even at high pressure. For example, at 300 bars and 47 °C the viscosity of supercritical CO_2 is 0.09 centipoise, roughly one order of magnitude lower than that of liquid (McHugh and Krukonis, 1986).

As discussed above, the liquid–like density, high compressibility, high diffusivity, and low viscosity of supercritical fluids make them appealing solvents.

1.4 Supercritical CO_2 Properties and Applications

Many organic solvents are hazardous and harmful to the environment. Water is the most desirable solvent, but it cannot dissolve less polar substances at ambient conditions. Although supercritical water is a good solvent for organics, its high critical temperature (374 °C) and critical pressure (221 bars) make it less attractive due to safety and operating cost issues.

1.4.1 Supercritical CO_2 Properties

Supercritical CO_2 is of interest as a solvent because it is inexpensive, essentially nontoxic, nonflammable, recyclable, and environmentally acceptable. In addition, the temperature and pressure critical conditions, T_c = 32 °C and P_c = 74 bars, are easily accessible. In addition, supercritical CO_2 has a relatively high solvent strength (dissolving power). In some cases, it can be utilized as an environmentally benign solvent substitute for hydrocarbons, chlorofluorocarbons, and other organics (McHugh and Krukonis, 1988). Nitrogen also has low critical parameters (T_c = -147 °C, P_c = 33.9 bars); it is inert,

nontoxic, nonflammable and inexpensive. However, its dissolving power is lower than that of supercritical CO_2 (Ghaderi, et al., 2000).

1.4.2 Applications of Supercritical CO_2

1.4.2.1 Extraction and Separation. Because of its remarkable solvent strength, supercritical CO_2 is an attractive solvent for extraction and separation in the food and pharmaceutical industries. By careful control of process conditions (temperature and pressure) to adjust the solvent power, supercritical CO_2 can be used to extract specific compounds of interest from raw materials. For example, supercritical CO_2 tea and coffee decaffeination processes have been commercialized since the 1960s. General Foods runs a coffee decaffeination plant in Houston, Texas and SKW/Trostberg has a tea decaffeination facility in Meunschmeunster, Germany (Brennecke, 1996). Supercritical CO_2 is also used to extract hops, spices, and flavors; Germany, France, and UK have led in this area. Pfizer built a hop extraction plant in Nebraska in the US in 1985 (McHugh and Krukonis, 1994).

Supercritical CO_2 has also been used to extract pharmaceutical components and various health supplements. Jennings, et al., 1992 did the extraction of taxol, which is an effective drug for the treatment of ovarian cancer, from the ground bark of *Taxus brevifolia* using supercritical CO_2. King and his co-workers at the US Department of Agriculture in Peoria, Illinois, found that gamma-linolenic acid, which is used as a health aid, could be extracted from evening primrose oil seeds (Jennings, et al., 1992). In addition, a variety of flavors and fragrances can be extracted using supercritical CO_2.

Moyler, et al., 1993 showed that more than 80 varieties of roots, barks, leaves, flowers, fruits and seeds have been successfully extracted with either supercritical or liquid CO_2.

1.4.2.2 Environmental Applications. Supercritical CO_2 has also been extensively used for environmental applications. As an environmentally friendly solvent, supercritical CO_2 has been used to replace many organic solvents for extraction and separation, as a reaction medium, and for material processing. A new discovery showed that supercritical CO_2 could be utilized to extract hazardous compounds from soil and slurries (Agkerman and Yeo, 1989, Andrews, et al., 1991). Another interesting application is the use of supercritical CO_2 to clean oils and greases from electronic materials and sophisticated machineries. The high solubility of greases and oils in supercritical CO_2 and the high diffusivity and low surface tension of the supercritical CO_2 allow complete cleaning without any residue left on the parts (Jennings, et al., 1992). In addition, because of its very low surface tension, supercritical CO_2 can get into very fine pores of micro-chips for rinsing without damaging them while normal liquids would destroy them due to their high surface tension (Gallagher-Wetmore, et al., 1994).

1.4.2.3 Reaction medium. The high diffusivity and low viscosity of the supercritical CO_2 make it an appealing solvent for chemical reactions due to enhanced mass transfer. In addition, the physical properties, such as dielectric constant, density, solubility parameter, are highly sensitive to pressure, especially in the near-critical region. Therefore, it is possible to optimize the chemical reaction rate, conversion, and selectivity by conveniently changing pressure. Free radical polymerization in supercritical CO_2 had

been extensively studied by DeSimone, et al., 1992. Fluoropolymers are traditionally synthesized in chlorofluorocarbon (CFC) solvents; however, DeSimone successfully carried out free radical polymerization of highly fluorinated acrylic monomers in supercritical CO_2. A review article by Kendall, et al., 1999 introduces a more comprehensive description of polymerization reactions in supercritical CO_2, including chain growth polymerization, precipitation polymerization, ring-opening polymerization, step-growth polymerization, dispersion and emulsion, etc. Jessop, et al., 1999 summarized the homogeneous catalytic reactions carried out in supercritical CO_2 in a review article. This article describes in great detail the hydrogenation, isomerization, hydrosilylation of CO_2, olefin metathesis, cyclization and other C-C bond forming reactions, and phase-transfer catalysis, etc.

1.4.2.4 Material processing. Recent discoveries show that supercritical CO_2 is a good processing medium either acting as solvent or as an anti-solvent in material processing. When supercritical CO_2 is used as solvent to dissolve a substance of interest and then the resulting supercritical solution is depressurized to low pressure or ambient condition, this process is called rapid expansion of supercritical solution (RESS). If supercritical CO_2 is used as an anti-solvent to precipitate the substance of interest, the process is known as the supercritical anti-solvent (SAS) process. The RESS process is suitable for substances that have reasonably good solubility in supercritical CO_2, while supercritical CO_2 insoluble substances can be processed using SAS. Both RESS and SAS can be utilized for particle generation and particle coating. A more detailed overview of supercritical CO_2 for particle generation and coating will be discussed in the next chapter.

1.5 Objectives, Outline, and Environmental Significance of This Thesis

1.5.1 Objectives

As described above, traditional wet coating methods are associated with many drawbacks, such as VOC emissions and other waste streams, the need for drying and other extensive down-stream processes, residual organic solvents in the final products, and possible drug component damage. Dry coating approaches do not provide a satisfactory coating structure and could have destructive effects on active agents. Thus it is necessary to develop an environmentally friendly coating method, which can provide good coating quality without harsh conditions involved. The new coating process should be able to be operated simply with no further downstream processing required.

Supercritical CO_2 has a wide variety of applications in extraction and separation, as a reaction medium, and material processing due to its attractive properties as a solvent. Thus it is interesting to investigate the use of supercritical CO_2 as a solvent for particle coating or encapsulation. Therefore the objectives of this research are two-fold. The first is to develop a supercritical coating process for fine particle coating or encapsulation. The second is to apply this coating technique to the area of drug delivery system design.

1.5.2 Environmental Significance of Supercritical Coating Processes

As discussed before, conventional wet coating processes require large amounts of organic solvents, surfactants and additives. Thus, wet-coating processes can lead to substantial VOC emissions and other waste streams. They are also associated with high-energy consumption because further down-stream processing, including milling and sieving, would be usually required. Therefore wet coating processes are environmentally

unfriendly. However SC CO_2 is nontoxic, nonflammable, easily recyclable, and environmental friendly. It has proven to be an ideal processing medium for many processes, such as reaction (DeSimone, et al., 1992, Jessop, et al., 1999), extraction and separation (Agkerman and Yeo, 1989, Andrews, et al., 1991), solvent free dyeing (Kazarian, et al., 1999), and cleaning (Jennings, et al., 1992, Gallagher-Wetmore, et al., 1994). For example, the UNICARB spray-coating process utilizing CO_2 as suspension medium for automobiles, furniture, and other products can reduce VOC emissions as much as 70 % (Brennecke, 1996). Shim, et al., 1999 even reported a rapid expansion of supercritical suspensions (RESS) in SC CO_2 for spray coating without using any organic solvent.

The proposed extraction and precipitation particle coating (modified RESS) process (Chapter 3) using SC CO_2 as a solvent for the coating material can eliminate the need for organic solvents. Although a co-solvent is sometimes used to improve the solubility of coating material in a SC CO_2 (RESS process), the amount of solvent used is usually very low, 1.0 wt. % (Tom and Debenedetti, 1991) and 1.4 mole % (Chang and Randolph, 1989). Therefore, the amount of organic solvent used is significantly reduced, more than 90%.

The proposed SAS coating process (Chapter 4, 5 and 6) involves dissolving of coating material in an organic solvent and extraction of the organic solvent by SC CO_2. It is difficult to make an exact comparision of the organic solvent usage in a SAS type process with wet coating processes since the amount of organic solvent required is dependent on a number of factors, such as the specific coating process, coating materials, and thickness of coating desired, etc. However, based on the SAS coating experiments

and literature describing wet coating or encapsulation processes, a simple comparison could be made. In the proposed SAS coating process, when particles are coated with polymer at a polymer concentration of 0.4 % (wt/v), 50 ml acetone is required to produce 1.0 gram of silica particles coated at a polymer weight fraction of 18.2 %. When the double emulsion approach is used to encapsulate plasmid DNA (Wang, et al., 1999; Capan, et al., 1999) with PLGA, 1800 ml and 2500 ml organic solvent are required to produce 1.0 gram DNA encapsulated with PLGA at a drug loading of 0.66 % and 0.2 %, respectively. In the spray drying process, 3330 ml organic solvent is required to encapsulate 1.0 gram etanidazole at a loading rate of 1.0 % (Wang and Wang, 2002). From this simple calculation, it is clear that the SAS coating process requires much less (above 97 %) organic solvent than the double emulsion and the spray drying approaches do. In addition, the production of free flowing coated particles in the one-step SAS coating process does not require any further down-stream treatment where VOCs will also be generated. Therefore, the SAS coating process is an environmentally friendly coating process.

1.5.3 Outline of This Thesis

Following this Introduction, Chapter 2 presents a literature survey of supercritical processes for particle engineering. First, a brief description of supercritical processes for particle formation and a review of previous work in this area are presented. Next, a detailed summary of supercritical coating work is given. In this part a variety of coating techniques using supercritical CO_2, either as a solvent or an anti-solvent, are reviewed.

Chapter 3 describes a new modified RESS process for particle coating using a solution of polymer in supercritical CO_2. This technique involves extracting the polymer with supercritical CO_2, with or without a co-solvent in an extraction vessel, and then precipitating the polymer onto the surface of host particles in a second precipitation vessel by adjusting the pressure and temperature inside the precipitator to lower its solubility. The study is performed using a pilot-scale supercritical apparatus, glass beads as host particles and two different polymers as coating materials. Results show that the coating of glass beads with poly vinyl chloride-co-vinyl acetate (PVCVA) and hydroxypropyl cellulose (HPC) was successfully achieved.

Chapter 4 presents a new method using supercritical CO_2 as an anti-solvent (SAS) for nanoparticle coating/encapsulation. A model system, using silica nanoparticles as host particles and Eudragit polymer as the coating material, is chosen for this purpose. The SAS process causes a heterogeneous polymer nucleation with the nanoparticles acting as nuclei and a subsequent growth of polymer on the surface of the nanoparticles induced by mass transfer and phase transition. A polymer matrix structure of encapsulated nanoparticles is formed by agglomeration of the coated nanoparticles.

Chapter 5 focuses on the coating and encapsulation of synthesized sub-micron silica particles with poly lactide-co-glycolide (PLGA). A systematic study of operating parameters that have an effect on the coating process, such as polymer to particle weight ratio, polymer concentration, temperature, pressure, flow rate of polymer solution, and the addition a SC CO_2 soluble surfactant are performed. It is found that the polymer weight fraction and the polymer concentration are critical for the successful encapsulation of silica particles with minimum agglomeration.

Chapter 6 describes an application of the supercritical antisolvent coating process to a drug delivery system design. In this work a biopolymer of poly lactide-co-glycolide (PLGA 50/50) is chosen as the coating material and hydrocortisone is used as the model drug. Results of HPLC assay analysis reveal that the hydrocortisone particles are successfully coated with PLGA. The coated drug particles show sustained release behavior at high polymer loading ratios of 33 % and 50 %. This research demonstrates that the SAS coating process is a very promising technique for drug coating or encapsualtion for the design of solid and inhalation drug delivery systems.

Chapter 7 presents recommendations based on this research and suggestions for future work.

CHAPTER 2

SUMMARY OF PREVIOUS WORK

Because of its remarkable solvent power and its easy adjustability by simply tuning operating conditions (temperature and pressure), supercritical CO_2 has received a lot of attention for both particle synthesis and particle coating in both the academic and industrial arena. Since the 1980's, extensive research efforts have been made in particle engineering using supercritical processes. In this chapter, a brief description and review of particle formation using different supercritical processes is presented first. Then the previous work in particle coating or encapsulation using supercritical CO_2 is described and reviewed.

2.1 Particle Formation Using Supercritical Processes

Particle size and particle size uniformity (distribution) of pharmaceutical compounds are important in pharmaceutical formulation development. Smaller particles provide higher surface area; thus, the dissolution rate and bioavailability, which depend on surface area, can be improved. In aerosol drug delivery applications, small particles (less than 5 μm) with a narrow size distribution are required to achieve effective delivery of drug to the lungs with a dry powder inhaler (DPI), a metered dose inhaler (MDI) or a nebulizer.

Conventional approaches for particle size reduction, including milling, grinding, crystallization, freeze-drying and spray drying, have some disadvantages for these applications. It is difficult to produce very small particles (less than 5 μm) with a narrow size distribution by grinding or milling. Spray drying is good for controlling particle size; however, the high temperature required in the spray drying process may detrimentally

affect the bioactivity of pharmaceutical active ingredients. Freeze drying produces particles with a wide size distribution, requiring further processing. Crystallization uses large amount of liquid solvents and separation of particles from the liquid involves filtration, centrifugation, and extensive drying to remove the solvent.

It is attractive to use SC CO_2 as a processing medium since CO_2 has a low critical temperature; this allows for particle processing at ambient temperatures. SC CO_2 behaves as a low-density gas after decompression making separation of the final product very easy. Furthermore, using SC CO_2 either as a solvent (RESS) or as an antisolvent (GAS/SAS) can be utilized to produce very small particles with a narrow size distribution.

2.1.1 Rapid Expansion of Supercritical Solutions (RESS)

Particle formation using the RESS process takes advantage of the fact that the solvent strength of supercritical CO_2 is a function of processing parameters, such as pressure, temperature and nozzle geometries. In a RESS process, typically, a solute is dissolved in supercritical CO_2 and the resulting supercritical solution is depressurized through a nozzle. A very high degree of supersaturation is obtained in a very short period of time since the expansion occurs very rapidly. This leads to nucleation of the solute and small particles with narrow size distribution are formed.

To better understand this process, a schematic diagram of the RESS process is presented below. For particle generation, the quality of the final products, such as size, size distribution, crystalline structure and morphology, depends not only on the solubility

of the solute in supercritical CO_2, but also on the operating parameters. Since the solvent power of the supercritical CO_2 is a function of density, the operating pressure and

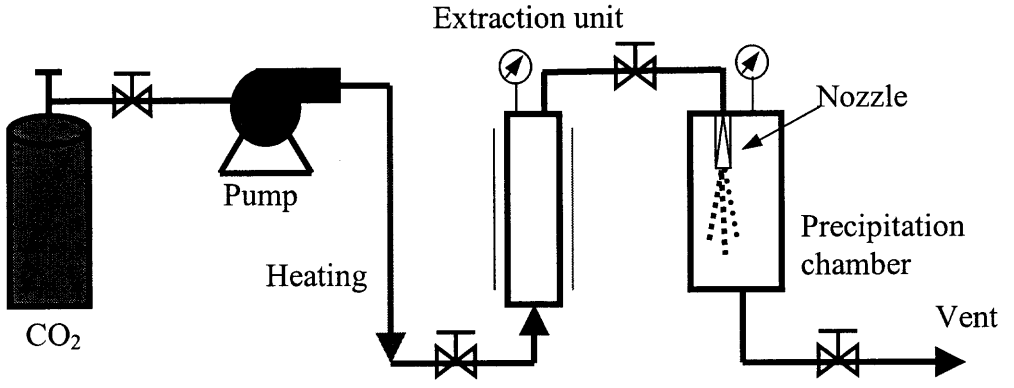

Figure 2.1 Schematic diagram of RESS process.

temperature need to be tuned carefully to dissolve the solute. For those substances that have very limited solubility in supercritical CO_2, a small amount of organic solvent can be used as a co-solvent to improve the solubility, sometimes significantly. Nozzle geometry, such as the inside diameter and ratio of length to the inside diameter, also plays a critical role in the RESS process for particle formation.

Hannay and Hogarth, 1879 first reported the formation of solids as a result of the expansion of a supercritical solution. They observed the precipitation of solids as "snow" or "frost" in a gas by a quick decompression. This was considered the first RESS experiment ever performed.

About 100 years later, Krukonis, 1984 first initiated a comprehensive study of RESS to produce a variety of powders, which included pharmaceutical compounds, polymers, dyes, organic catalysts, biological compounds, and surfactants. The work he

did led to an active research field focused on exploring further applications of RESS for particle engineering and obtaining a theoretical understanding of this process as well. Since then, numerous studies have been performed using the RESS process for particle generation. Matson et al., 1987 studied the precipitation of silicon dioxide (SiO_2) and germanium dioxide (GeO_2) from supercritical water. In his work a stainless steel capillary tube with a dimension of 5 mm in length and 60 μm I.D. was used as a spray nozzle. At the conditions of 300 °C (autoclave temperature), 590 bars (system pressure) and 470 °C (pre-expansion temperature), 0.1-0.5 μm spheres of SiO_2 were produced by the RESS process. Similarly, GeO_2 spheres (0.5-1.3 μm) were generated. He and his co-workers also studied the precipitation of polymers using RESS. However, polymer fibers with a dimension of about 1 μm in diameter and 100-1000 μm in length were generated. In his study solute concentration among other variables was found to have the greatest effect on the particle size.

Lele and Shine, 1994 carried out a study of the effect of RESS dynamics on polymer morphology. In their RESS process for polymer precipitation four parameters, pressure, dissolution temperature, pre-expansion, and inside diameter of the capillary nozzle, were studied. They found that the time scale for phase separation during RESS governed the morphology of the precipitated polymers. When precipitation took place over microseconds inside the nozzle, 0.2-0.6 μm polymer particles were produced. When the precipitation occurred over tens of seconds, the polymer had a chance to grow as 1-13 μm particles and fibers. These findings can be utilized to adjust the dynamics of RESS to control the shape and morphology of polymer precipitants.

A carefully designed study of operating parameters in RESS was performed by Mawson, et al., 1995 to understand the mechanism of the RESS process. In their study, experimental variables and procedures were carefully designed. The concentration of polymer solution was held constant at 0.5 and 2.0 %. The pre-expansion temperature was varied above and below the cloud point, and the ratio of the length to diameter (L/D) of the spraying nozzle from 8.5 to 508. The results supported the mechanism proposed by Lele and Shine, 1994. The earlier the phase separation in the nozzle, the greater the time for coalescence and fiber formation of the polymer. The L/D was found to be the most influential factor in determining the shape of the final product of the polymer precipitants, fibers or particles. The polymer solution concentration and pre-expansion temperature also had an important effect on the sizes of the particles and fibers produced.

Mohamed, et al., 1989 did a systematic study of the effect of operating conditions on the final solid products. In this study naphthalene was used as the model solute. Pre-expansion and post-expansion temperature, pressure and composition were systematically investigated. It was found that the pre-expansion temperature had a remarkable effect on the particle size. A higher pre-expansion temperature favored larger particles. An increase in solution concentration resulted in a decrease in the particle size. This was in good agreement with classic nucleation theory; higher solution concentration resulted in higher nucleation rate, leading to higher degree of supersaturation. Consequently, smaller particles were produced. The effect of pressure was also examined in this study and the particle size was found to be insensitive to the change of post-expansion pressure.

Domingo, et al., 1996 studied ultra-fine particle formation using the RESS process. In their work, benzoic acid was dissolved in SC CO_2 and was sprayed through a

porous sintered plate nozzle (pore size 0.5-5 μm) instead of through an orifice or a capillary tube. The results showed that the spray nozzle determined the particle size and crystal formation. With a porous sintered metal plate as the spray nozzle, less than 1 μm particles were produced. However, at the same operating conditions, 2-6 μm particles were generated when a capillary tube (62 μm) was used as the spray nozzle. They determined that the time scale for a solution to reach supersaturation was one of the most important factors in determining the crystal size.

Charoenchaitrakool, et al., 2000 investigated the RESS process for the micronization of a pharmaceutical compound to increase its dissolution rate. In their work ibuprofen was used as a model drug and its solubility was determined at different temperatures. The particle size of the ibuprofen product was studied as a function of spraying distance, pre-expansion pressure, and nozzle length. Results showed that less than 2.5 μm ibuprofen particles were generated in the RESS process. They found that the particle size and morphology were independent of pre-expansion pressure and nozzle length within the range of their study. An increase in spraying distance generated slightly smaller particles with less aggregation. The dissolution rate of micronized ibuprofen in RESS was 5 times greater than that of the original ibuprofen because the particle size and crystallinity of micronized ibuprofen were reduced compared with the original material.

The major drawback of the RESS process is the fact that the solubility of most substances in SC CO_2 is very low. To overcome this problem a co-solvent, such as acetone, methanol or ethanol can be used to assist the dissolution of the substance of interest in SC CO_2. Chang and Randolph, 1989 showed that the addition of toluene up to 1.4 % mole fraction as a co-solvent in supercritical ethylene enhanced β-carotene

solubility. Submicron β-carotene particles (0.5 μm) were produced in this study. However, an increase in toluene concentration resulted in a two-phase expansion, which produced larger particles with a wide particle size distribution. This was attributed to the re-crystallization of β-carotene from liquid toluene after expansion. Therefore, it is important to limit the mole fraction of co-solvent in the RESS process so as to maintain a single phase after depressurization.

Although most of the RESS work has been experimental studies focusing on applications to various materials and the influence of process conditions on the final products, some fundamental theory and simulation of RESS has also been proposed to better understand the process. Kwauk and Debenedetti, 1993 proposed a simulation model of the RESS process based on compressible fluid dynamics, thermodynamics, nucleation kinetics and an equation describing crystal growth. This model calculated the solute nucleation and particle growth for a partial expansion of a dilute supercritical solution in a subsonic converging nozzle in a steady, one-dimensional, and inviscid flow. According to the model, the particle size was found to be related to changes in both the extraction and pre-expansion temperatures. An increase in pre-expansion temperature favored larger particles. However, particle size decreased with an increase in extraction temperature or in pressure. Other effects of process variables, for example, nozzle length and flow rate on particle size and particle size distribution were tested as well. The model was helpful in understanding the relationship between the particle size and the process condition in RESS, in interpreting experimental results, and in providing guidelines for equipment design.

A recent modeling work of the RESS process was done by Türk, 2000. In this model, the calculation was based on a steady-state one-dimensional flow model, which includes heat exchange in the capillary and the free jet, friction in the capillary and isentropic flow in the capillary inlet area. The resulting pressure and temperature along the expansion path were used for the calculations of solubility and supersaturation. In the calculation of the nucleation rate, an equation based on classical nucleation theory was used with arguments extended to fluid-phase non-ideality. The calculation results showed that at the beginning of the free jet, supersaturation went up steeply and reached a maximum of 10^8. The maximum nucleation rate was about 10^{26} for an interfacial tension of 0.02 Nm^{-1}. In the calculation, it was found that the nucleation rate was dependent on the solubility and the surface tension. In addition, classical nucleation theory was found to be unsuitable to describe the correlation between particle size and RESS process conditions.

Helfgen, et al., 2001 recently simulated particle formation in RESS. They set up a model to calculate the flow field based on mass, momentum and energy balances and the extended generalized Bender equation of state (Platzer & Maurer, 1989). The particulate phase was calculated using the general dynamic equation, providing that the particle size distribution was lognormal, the method of moments coupled with the transport equations and a population balance. The mechanisms for particle formation and growth were nucleation, condensation and coagulation. According to their calculations, the conditions inside the expansion chamber were most likely the key factor, which influenced particle characteristics, since particle growth by coagulation continued in the expansion chamber.

Although RESS is attractive for its simplicity and easy implementation, the very limited solubility of most compounds of interest severely limits the application of RESS. Furthermore, proper nozzle design, scale-up, and controllability in a RESS operation pose large challenges in applying this process.

2.1.2 Supercritical Antisolvent and Gas Antisolvent Processes (SAS and GAS)

When the substance of interest does not dissolve in SC CO_2, an antisolvent process is usually considered. Antisolvent approaches are operated on the basis that two solvents have good miscibility. The substance of interest is soluble in the first solvent, but not soluble in the second solvent. By adding the antisolvent into the solution the two solvents are dissolved in each other while the solution becomes supersaturated. The supersaturation achieved is the driving force for the solute to nucleate and precipitate out.

Thermodynamics should be considered first when one decides to utilize the antisolvent process for particle generation. The choice of solvent is critical in a successful antisolvent process. The solvent should not only dissolve the solute up to a reasonable concentration, but also should have very good miscibility with the antisolvent. Usually, the volume expansion of the solvent is used to determine the miscibility of the solvent and antisolvent. The expansion rate ($\Delta V\%$) is defined as:

$$\Delta V\% = \frac{V(P,T) - V_0}{V_0} \times 100\% \qquad (1)$$

where V(P, T) is the volume of solvent expanded by CO_2 and V_0 is the volume of pure solvent before the antisolvent addition.

The Peng-Robinson equation of state (PR-EoS) (Peng and Robinson, 1976) can be used to predict the expansion behavior of a binary system, e.g., of CO_2-acetone. The PR-EoS is expressed as:

$$P = \frac{RT}{v-b} - \frac{a(T)}{v(v+b)+b(v-b)} \tag{2}$$

where a and b are parameters of the mixture of the binary system. Originally, the PR-EoS had only one interaction coefficient, k_{ij}. However, as suggested by Kordikowski, et al., 1995, it is necessary to have a second interaction parameter l_{ij} to account for a polar compound in the binary system. In the acetone-CO_2 system, k_{ij} is –0.007 and l_{ij} is –0.002, which were regressed from the experimental data reported by Katayama, 1975. The mixing rules are given as:

$$a = \sum_i \sum_j x_i x_j a_{ij} \tag{3}$$

$$b = \sum_i x_i x_j b_{ij} \tag{4}$$

$$a_{ij} = (1-k_{ij})\sqrt{a_i a_j} \tag{5}$$

$$b_{ij} = \frac{(b_i + b_j)}{2}(1-l_{ij}) \tag{6}$$

where the pure component values can be determined as:

$$b_{ii} = 0.07780\frac{RT_{ci}}{P_{ci}} \tag{7}$$

$$a = 0.45724\frac{R^2 T_{ci}^{\ 2}}{P_{ci}}[1+(0.37464+1.54226\omega_i - 0.26992\omega_i^{\ 2})\times(1-\sqrt{T/T_{ci}})]^2 \tag{8}$$

and P_{ci}, T_{ci}, and ω_i are the critical pressure, critical temperature, and accentric factor of component *i*, respectively.

The calculated volume expansion rate as a function of pressure at different temperatures is shown in Figure 2.2. The volume of acetone increases slowly with system pressure from 0 to 60 bars at 32.5 °C. When the system pressure is above 60 bars, the acetone is fully expanded. The expansion behavior of acetone results in a decrease in the

partial molar volume of the solvent so that the solvent strength is reduced considerably. Consequently, the solution reaches supersaturation and the solute nucleates and precipitates out.

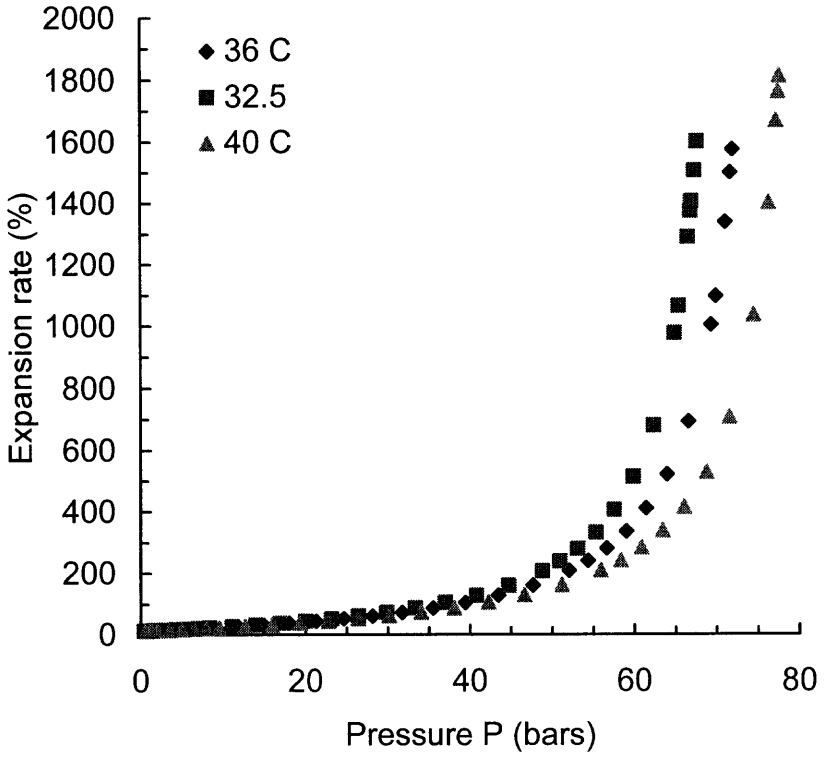

Figure 2.2 Liquid solvent expansion by CO_2.

2.1.2.1 Compressed Gas Antisolvent Process (GAS). Compressed CO_2 can be dissolved in most organic solvents, and hence it can be used as an antisolvent for particle generation. When compressed CO_2 acts as an antisolvent the process is called GAS. In a typical GAS process, compressed CO_2 is bubbled through a liquid solution. Due to the dissolution of compressed CO_2, the solvent is expanded and its solvent strength is lowered. Consequently, the solution becomes supersaturated and the solute nucleates and precipitates in the form of microparticles. The processing parameters, such as

temperature, pressure, agitation, nozzle geometry, solution concentration and flow-rate of CO_2 have direct effects on the particle size, size distribution, crystalline structure and morphology of the resulting particles. Figure 2.3 schematically shows the GAS process.

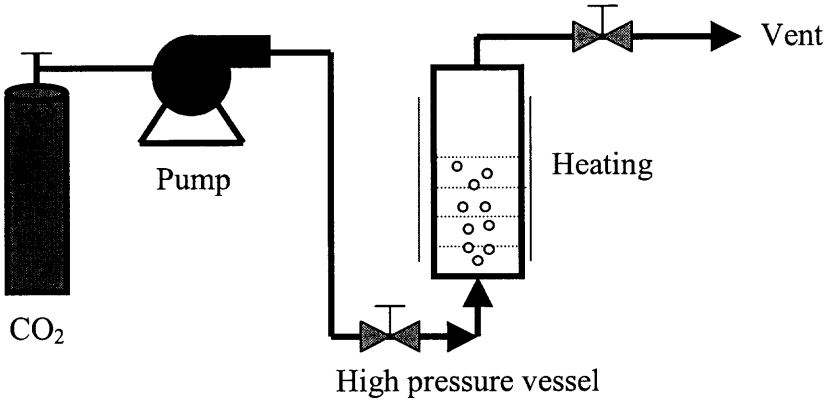

Figure 2.3 Schematic diagram of GAS process.

Krukonis, 1988, first proposed the GAS process for fine particle production, such as highly energetic materials (explosives) and other substances that are difficult to pulverize. Gallagher, et al., 1992 used this approach to recrystallize nitroguanidine from N-methylpyrrolidone and N, N-dimethylformamide. It was found that adjusting the addition rate of gas anti-solvent could control the particle size, morphology, and size distribution.

Berends, et al., 1996 performed a study of crystallization of phenanthrene from toluene using the GAS process. The size of the produced particles ranged from 160 to 450 μm depending on the stirrer speed and growth time. The residual toluene in the final product was about 70 ppm, significantly lower than that of normally prepared

phenanthrene. They also found that stirrer speed determined the degree of attrition and mass transfer of the gas anti-solvent into the liquid solution. A theoretical model was proposed in this study to predict the liquid expansion by GAS and the solubility of solute in expanded solvent very well.

Yeo, et al., 2000 reported the formation of crystals of barium chloride ($BaCl_2$) and ammonium chloride (NH_4Cl) produced from solutions of dimethyl sulfoxide (DMSO) in a GAS process. CO_2 was introduced into the solutions at different flow-rates and the crystals were produced with various particle sizes, crystal habits and crystalline structures. As the CO_2 delivery rate was increased the average size of the crystals produced decreased for both compounds. When the CO_2 delivery rate was increased, the crystal habits of $BaCl_2$ and NH_4Cl were found to change from an equant to an acicular habit and from an equant to a tabular habit, respectively. In addition, the $BaCl_2$ crystal structure was changed from orthorhombic to hexagonal based on XRD patterns. These findings showed that the GAS process could be used for crystal modification or polymorph screening.

Cocero and Ferrero, 2002 carried out a systematic study of the effects of operating parameters on the particle size and size distribution. In this GAS work, β-carotene was recrystallized from ethyl acetate and dichloromethane solutions. It was found that higher agitation and a higher CO_2 addition rate favored smaller particles with narrower size distribution. This was consistent with the conclusions of Berends, et al., 1996. The initial solution concentration and operating temperature also affected the particle size of the final product. A dilute initial solution at low operating temperature (25 ^{o}C) produced less than 1 μm size particles with a very narrow size distribution. However, a high initial

concentration at high temperature (40-60 °C) resulted in a high yield of the final product with a particle size of 5 μm.

In a recent study of gas antisolvent recrystallization of an organic compound, Muhrer, et al., 2003, discussed the influence of the initial solution concentration and antisolvent addition rate on the final product quality in terms of particle size and size distribution. As reported before (Berends, et al., 1996, Cocero and Ferrero, 2002), the average size of produced particles varied from 0.36 to 8.1 μm as the antisolvent addition rate changed. However, it was interesting to find that the particle size distribution was unimodal and narrow for low and high addition rates, while it was bimodal for an intermediate addition rate. The particle size and size distribution were insensitive to the initial solution concentrations. This finding did not agree with the results of Cocero and Ferrero, 2002. Scale-up of the GAS process from a 300 ml to a 1000 ml precipitator was demonstrated and the particles produced from the two different sized precipitators were very close. This finding showed that the GAS process was very promising for industrial applications.

Muhrer, et al., 2002 developed a mathematical model describing the GAS recrystallization process. In this work, phenantrene and toluene were used as a model system to study the GAS process. It was shown that the particle size was strongly dependent on the addition rate of the antisolvent. This work clarified the importance of secondary nucleation with respect to primary nucleation and was very significant for the development and optimization of the GAS process.

2.1.2.2 Supercritical Antisolvent Process (SAS). The second technique, in which supercritical CO_2 acts as an antisolvent to induce the nucleation and precipitation of a solute, is known as the SAS process. Variations of this process, include precipitation from compressed antisolvent (PCA) solution, enhanced dispersion by supercritical fluids (SEDS), and aerosol solvent extraction systems (ASES). In the SAS process, a liquid solution is delivered by an HPLC pump and is sprayed through a nozzle into a high-pressure chamber, which is filled with supercritical CO_2. Once the solution comes out of the nozzle and contacts the supercritical CO_2, a very fast mutual diffusion between the bulk supercritical CO_2 and the solution takes place. Therefore, the solution reaches a very high degree of supersaturation practically instantaneously, resulting in the nucleation and precipitation of the solute. A schematic diagram of SAS process is shown in Figure 2.4.

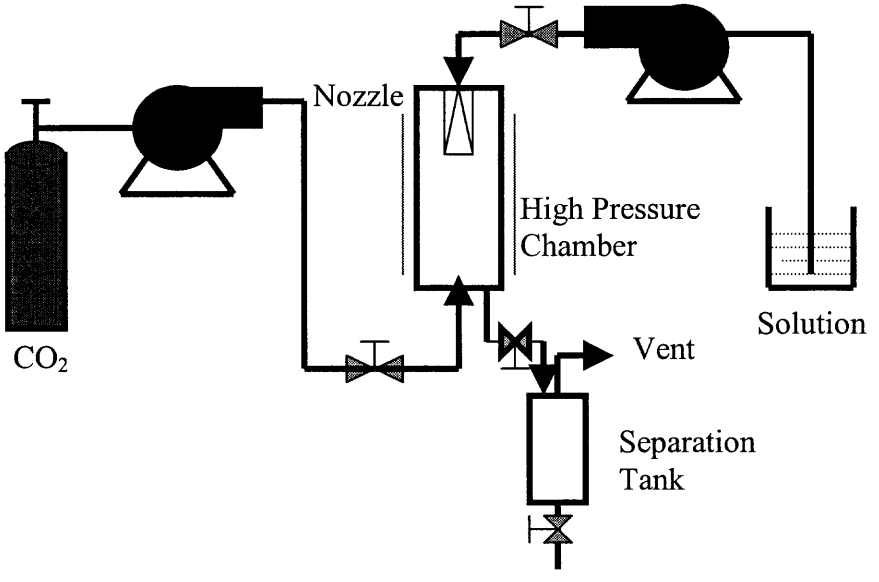

Figure 2.4 Schematic diagram of SAS process.

The operating parameters, such as temperature, pressure, solution concentration, CO_2 flow rate, solution flow rate and nozzle design are important in controlling the particle size, distribution, morphology, and crystalline structure. In particle formation, particle size and particle size distribution are the most important parameters to be controlled. The SAS process is very complicated since thermodynamics, mass transfer, kinetics and hydrodynamics are coupled and are all important. However, understanding the mechanism of particle formation in the SAS process is very useful in controlling the final product.

Hydrodynamic theory has been applied to the SAS process in an attempt to relate particle size to antisolvent density (Dixon, et al., 1993). The Weber number (N_{We}) is defined as the ratio of the deforming external pressure forces and the reforming surface tension forces experienced by a liquid droplet encountering flowing air (Lefebvre, 1989). It is expressed by:

$$Nw_e = \rho_A v_R^2 D/\sigma \qquad (9)$$

where ρ_A is the density of the antisolvent, v_R is the relative velocity, D is the droplet diameter and σ is the surface tension. In the SAS process, the spray of solution through the nozzle into the supercritical CO_2 phase produced fine droplets due to the jet break-up effect. The initial droplet size determined the particle size of final product. According to theory, the higher the antisolvent density, the smaller the droplets that are formed. Dixon, et al., 1993 and Thies and Müller, 1998 found that particle size decreases with increase in antisolvent density. Their findings were in good agreement with the hydrodynamic theory.

However, Randolph et al., 1993, in their research found that nucleation and growth of the solute induced by mass transfer played a critical role in the determining the particle size. Similarly, Bristow, et al., 2001 proposed that the supersaturation rate rather than the initial droplet size was directly related to the particle size.

Enhancing the rate of mass transfer in the SAS process favors a higher degree of supersaturation, leading to the formation of smaller particles. The rate of mass transfer can be enhanced by efficiently mixing the sprayed solution with the bulk supercritical CO_2. To improve the rate of mass transfer, different nozzle designs have been reported. Hanna and York, 1994 designed a coaxial nozzle and applied this nozzle in the SAS process, which is termed as SEDS. This specially designed nozzle improved the mass transfer rate due to the intense mixing of the supercritical CO_2 with the solution. A schematic of the coaxial nozzle used in SEDS s shown in Figure 2.5. Chattopadhyay and Gupta, 2002 combined the use of an ultrasonic vibration surface with the spray nozzle to enhance mass transfer.

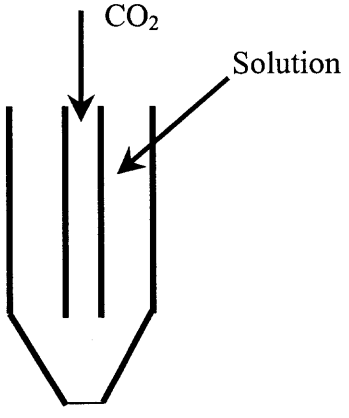

Figure 2.5 Schematic of the coaxial nozzle used in SEDS.

The SAS process offers the advantage of flexibility in choosing the solvent and the antisolvent. In addition, high throughput and mild operating conditions are enticing for pharmaceutical compounds. The SAS process has received a lot of attention and a large number of studies were published. Most of the research effort focuses on the formation of particles of pharmaceutical agents. Yeo, et al., 1993 studied the formation of protein powders (insulin) using the SAS process. The protein was dissolved in dimethylsulfoxide (DMSO) and N, N-dimethylformamide (DMFA) and the solutions were sprayed into SC CO_2 through a nozzle having an ID of 30 μm. Amorphous protein powders were produced in the continuous SAS process with 90 % of the particles less than 4 μm and 10 % of the particles less than 1 μm. The results of in vivo tests on rats showed that the micronized insulin maintained the same biological activity as that of unprocessed insulin. Thus the SAS process is suitable for the micronization of bio-active agents of proteins and peptides.

Reverchon and Porta, 1999 reported the production of antibiotic micro and nano-particles by the SAS process. In this work, griseofulvin, ampicillin, amoxicillin, and tretracycline in organic solvents of N-methylpyrrolidone (NMP), DMSO, ethyl alcohol, and methylene chloride were used in the SAS process. The micronization of tetracycline using NMP as the solvent was successfully achieved and sub-micron particles were produced. The other combination of solutes and solvents failed due to the formation of either long needle-shaped crystals or serious aggregation of the precipitated particles. The effect of SAS parameters on morphology, particle size and size distribution was also investigated using the system of tetracycline and NMP. It was found that higher operating

pressure reduced the coalescence of tetracycline particles, and that higher solution concentration favored size enlargement of the tetracycline aggregates.

In another study Revechon, et al., 2001 performed research on SAS precipitation of salbutamol microparticles. In their SAS work, salbutamol was tested in different solvents of DMSO, methyl alcohol, and ethanol-water mixture. Rod-like particles with a dimension of 1-3 μm in length and 0.2-0.35 μm in diameter were produced when DMSO was used as the solvent. Sintering of precipitated particles occurred with the other two solvents. It was interesting to notice that the length of particles decreased as the solution concentration increased. In addition, the residual organic solvent in the final product was low enough so that it was below the detection limit of the FT-IR.

Steckel, et al., 1997 investigated the ASES process for the micronization of several steroids (triamcinolone acetonide, flunisolide, prednisolone, budesonide, and fluticasone-17-propionate, beclomethasone-17, 21-dipropionate, beclomethasone-17-valerate) for pulmonary delivery. The drugs were dissolved in dichloromethane, methanol, and a mixture of both. The median particle size of the micronized steroid (triamcinolone acetonide, flunisolide, prednisolone, budesonide, and fluticasone-17-propionate) particles was mostly less than 5 μm. No particles were obtained with the drugs of beclomethasone-17, 21-dipropionate and beclomethasone-17-valerate in the ASES process due to extraction by SC CO_2. HPLC tests revealed that no chemical decomposition occurred during SAS processing. However, some of the micronized drugs, such as triamcinolone acetonide, flunisolide, prednisolone, and fluticasone-17-propionate, changed their crystallinity and polymorphism. The addition of a surface-

active ingredient, phosphatidylcholine, in the solution resulted in a slight increase in particle size, but considerably reduced the contact angle, improving wettability.

Moshashaée, et al., 2000 studied lysozyme precipitation from organic solution using the SEDS process. The hen egg lysozyme in a solution of DMSO was sprayed through a specially designed coaxial nozzle, shown schematically in Figure 2.5. The primary particle size was in the range of 1-5 μm. The residual DMSO in the final product was less than 20 ppm. It was noticed that a lower operating pressure favored the maintenance of bio-activity of the processed lysozyme. Also the lower pressure resulted in the formation of well-defined 1-5 μm particles while a higher pressure gave rise aggregates of particles.

Chattopadhyay and Gupta, 2002 recently reported SAS with an enhanced mass transfer technique. In this study lysozyme was dissolved in DMSO and the resulting solution was sprayed onto a vibrating surface, which was in a high pressure chamber filled with SC CO_2. The solution jet was deflected by the surface vibrating at an ultrasonic frequency, atomizing the jet into much smaller droplets so that lysozyme nanoparticles and microparticles were produced. It was found that the ultrasound field generated by the vibrating surface not only enhanced the mass transfer, but also prevented the agglomeration of precipitated particles through improved mixing. The vibration intensity of the surface, which was a function of the power supplied to the ultrasound transducer, affected particle size. The biological activity of the protein was retained during the SAS processing. In a similar study (Chattopadhyay and Gupta, 2001), tetracycline was micronized to 125 nm using this SAS with enhanced mass transfer technique.

The SAS process is also capable of micronizing biopolymers, e.g., poly (L-lactic acid) (PLA), which is very popular for pharmaceutical drug delivery applications, has been micronized by the SAS process (Thies and Müller, 1998; Randolph, et al., 1993; Reverchon, et al. 2000; Breitenbach, et al. 2000, Mawson, et al., 1997). In these SAS studies PLA microparticles were produced with various sizes and morphologies, which were influenced by the operating conditions, e.g., organic solvents used, solution concentration, temperature, pressure, and nozzle geometry. Some other biopolymers, dextran, poly (hydroxypropylmethacrylamide) (HPMA) (Reverchon, et al., 2000), poly (β-hydroxy-butyric acid) (PHB) (Breitenbach, et al., 2000), and polysaccharide (HYAFF-11) (Benedetti, et al., 1997), were successfully micronized by the SAS process.

In addition to the micronizaiton of organic substances for pharmaceutical applications, the SAS process was also extended to produce nanoparticles for material science applications. Reverchon, et al., 1998 studied the production of nanoparticles of superconductor precursors using the SAS process. In this study, yttrium acetate (AcY), samarium acetate (AcSm), and neodymium acetate (AcNd) were dissolved in DMSO and were sprayed into SC CO_2. Nanoparticles, down to 100 nm of AcY, AcSm, and AcNd were successfully produced with a narrow particle size distribution. The nanoparticles of these precursors could then be applied to produce high temperature superconductors. Similar research was performed by Reverchon, et al., 1999 to produce nanoparticles of zinc oxide precursor.

To better understand the SAS process, Bristow, et al., 2001 performed a fundamental study of the SAS process using acetaminophen as a model drug. In this carefully designed study, an on-line dynamic solubility measurement was used to monitor

the solution supersaturation in the nozzle, S_m, and in the residual organic effluent, S_e. It was found the magnitude of S_m had a direct effect on the mean particle size, and the analysis of supersaturation provided a simple and effective way for optimization of the SAS process. Also, they investigated the SAS process under two different operating conditions of partial and complete miscibility, and proposed that above the mixture critical pressure, crystallization was determined by mixing and primary nucleation. Below the mixture critical pressure, droplets with very low surface tension were produced due to hydrodynamic effect and jet break-up. The solute underwent nucleation and immediate post-nucleation growth was confined within the droplets.

In another fundamental research study carried out by Lengsford, et al., 2000, it was shown that complete miscibility of the solvent and the SC CO_2, above the critical point of the mixture occurred; no distinct droplets formed and the polymer solute would nucleate and grow within the expanding gas plume. This finding supported the conclusion reached by Bristow, et al., 2001. These fundamental research studies were very helpful to elucidate the SAS process.

In the SAS process, the particle size, size distribution and morphology were thought to be strongly dependent on the mass transfer as described above. However, it was not quite understood quantitatively and qualitatively. Werling and Debenedetti, 1999; 2000 attempted to simulate the mass transfer behavior in the SAS process. In their simulation, mathematic models were set up to calculate the mass transfer between toluene and SC CO_2 at conditions below and above the mixture critical point. Calculated results showed that the interfacial flux was always into the droplet, resulting in the swelling of the droplet. This was attributed to the fact that the solubility of CO_2 was very high in

toluene. It was suggested that supercritical conditions resulted in faster mass transfer so that supercritical operation would cause a higher degree of droplet supersaturation in the presence of a solute, resulting in higher nucleation rates and smaller particles. This simulation work allowed for a better understanding of the SAS process and could provide a theoretic basis for choosing operating conditions.

Lora, et al., 2000 proposed an even more comprehensive model. Thermodynamics, hydrodynamics, and mass-transfer were all considered in this model so that it could be utilized to calculate the composition and flow-rate profiles of the vapor and liquid phases and the amount of solid product along the precipitator. The antisolvent was found to dissolve in the liquid phase faster than the evaporation of the solvent. This was consistent with the calculated result by Werling and Debenedetti, 1999. In addition, it was found that two solutes might behave completely in different ways at the same conditions and it was possible to selectively precipitate a solute from a ternary system of solute-solute-solvent using the SAS process. The proposed model was very useful for simulation of the SAS process if a suitable thermodynamic model representing the phase equilibrium of the system was available.

2.1.2.3 Precipitation from Gas Saturated Solutions/Suspensions (PGSS). In addition to the supercritical processes discussed above, there is another process, precipitation from gas saturated solutions/suspensions (PGSS), used for particle generation. This process takes advantage of the fact that the solubility of the compressed gas in liquid solutions or melt solids is much higher than the solubility of solids in the compressed gas. In this process, supercritical CO_2 is dissolved in solid melts or liquid solutions/suspensions. The

gas-saturated solutions or suspensions are then expanded through a nozzle, leading to the formation of solid particles. A few publications (Xu, et al., 1997, Sievers, et al., 1999, Xu, et al. 1998) described this process for particle formation; however, PGSS is much less popular than either GAS or SAS.

2.2 Previous Particle Coating or Encapsulation Work Using Supercritical Processes

Particle coating, encapsulation or dispersion in microspheres using SC CO_2 is of great interest for controlled drug delivery, and for food, agriculture, material science, and cosmetics applications. Coating/encapsulation of pharmaceutical substrates for drug controlled or sustained release using compressed or SC CO_2 has been a fast growing field. Various processes using SC CO_2 have been developed, such as RESS, SAS/GAS/ASES, and thermal decomposition processes.

2.2.1 Particle Coating or Encapsulation Using RESS

In a RESS coating or encapsulation process, the coating material is dissolved in SC CO_2 with or without cosolvent involved. A sudden decompression causes a significant loss of solvent strength of SC CO_2, resulting in nucleation and precipitation of the solute (coating material). The coating material either deposits onto the surface of any host particles that are present in the precipitation vessel or coprecipitates along with the host particles. Tom, et al., 1994 initiated a study of coprecipitation of PLA and pyrene in a RESS process for controlled drug delivery applications. In their work two streams of solutions of pyrene in SC CO_2 and PLA in SC CO_2 with $CHClF_2$ as the cosolvent were not mixed until they reach the precipitation unit. When the supercritical solutions flowed

through expansion device, it underwent a rapid decompression, resulting in coprecipitation of PLA and pyrene. It was shown that the morphology and particle size were strongly dependent on the expansion device (orifices or capillaries). Using fluorescence and transmission microscopy, pyrene was found to be uniformly incorporated in polymer microspheres after the RESS coprecipitation .

In another RESS work, Kim, et al., 1996 investigated the microencapsulation of naproxen with PLA. In their study, a model system of naproxen and PLA was packed in the same extraction unit instead of using two different units (Tom, et al., 1994) and extracted with supercritical CO_2. The supercritical solution was then expanded through a capillary tube. Composite particles with a naproxen core encapsulated by a PLA coating were reported. Microparticles and agglomerates were observed as the dominant morphology. Mishima, et al., 2000 studied the microencapsulation of proteins with poly (ethylene glycol) (PEG) by RESS. In this research, ethanol (about 38.5 wt. %) was employed as a co-solvent to enhance the solubility of PEG in SC CO_2 even though PEG was not soluble in ethanol. In their experiments protein particles were suspended in SC CO_2, in which polymers were dissolved with the assistance of ethanol. The resulting suspension was sprayed through a nozzle and microspheres were produced without agglomeration. The results indicated that lipase and lysozyme particles were completely encapsulated by PEG.

Tsutsumi, et al, 2001 combined the RESS process with fluidized bed technology to achieve particle coating. In this research, catalyst particles in a fluidized bed were fluidized by air, and a solution of paraffin in supercritical CO_2 was sprayed into the bed through a nozzle. Coating material was directly deposited onto the surface of the catalyst

particles with no binder or solvent involved, resulting in no significant agglomeration. A more recent study of particle coating granulation using the RESS process in a fluidized bed was carried out by Wang, et al., 2001.

However, the main drawback of the RESS technique is that SC CO_2 has a limited solvent strength for many polymers of interest, which greatly restricts its application. There is another disadvantage in that it is very difficult to control the coating or encapsulation because nucleation and precipitation of the coating material take place very rapidly (less than 10^{-5} seconds) during RESS (Matson, et al., 1987).

2.2.2 Particle Coating or Encapsulation Using SAS/GAS/ASES/SEDS

The use of SC CO_2 as an antisolvent for coating or encapsulation of particles received considerable attention recently because of its flexibility in choosing a suitable solvent. For example, coprecipitation of a drug substance and a polymer using antisolvent processes is of great interest for drug delivery system design. In this approach, a homogeneous solution containing the drug and polymer is sprayed into SC CO_2 through a nozzle and nucleation and coprecipitation of the drug and polymer occurs due to the extraction of the solvent by SC CO_2. The drug-loaded microspheres are produced as a matrix structure of drug particles dispersed in the polymer.

Bleich and Müller, 1996 reported an ASES process for drug loaded particle preparation. The drugs and carrier polymer PLA were dissolved in methylene chloride and the solution was atomized into SC CO_2. The extraction of the organic solvent results in the formation of drug loaded microparticles. Polar drugs were successfully encapsulated in their ASES process. However, less polar drugs failed to be encapsulated

because they were extracted by the SC CO_2 with the organic solvent acting as the cosolvent.

Falk, et al., 1997 investigated composite microparticle production using the SAS process. In their research a homogeneous solution of solutes (gentamycin, naloxone, and naltrexone) and PLA, which was prepared by the hydrophobic ion-pairing (HIP) method, was sprayed into SC CO_2 as an antisolvent. Co-precipitation of the solutes and polymer took place and composite microspheres or drug-loaded microcapsules were formed. Spherical composite particles were successfully produced with sizes in the range of 0.2 to 1.0 μm. The gentamycin loaded microspheres showed a 25 % (w/w) loading rate and exhibited diffusion controlled release behavior. Naloxne and naltrexone were found to be less efficiently encapsulated because these two drugs were more lipophilic and could be dissolved in SC CO_2, causing the drug to be bound on the surface of microspheres.

Ghaderi, et al., 2000 described the preparation of microparticles containing hydrocortisone in DL-PLA polymer by the SEDS process using a combination of SC N_2 and CO_2. Results showed that microparticles with a mean size less than 10 μm were produced. Hydrocortisone was successfully entrapped in DL-PLA microparticles with an entrapment efficiency of 22 %. It was found that the combination of SC N_2 and CO_2 favored a more efficient dispersion of the polymer solutions than SC CO_2 alone.

In a recent study of the coprecipitation of solute and polymer using the SAS process, Elvassore, et al., 2001 studied the production of protein loaded polymeric microcapsules. Insulin and PLA, as a model system, were dissolved in a mixed solvent of DMSO and dichloromethane. This homogeneous solution was then sprayed into SC CO_2

through a 50 μm fused silica nozzle. It was shown that 0.5 to 2 μm insulin loaded microspheres were produced with an incorporation efficiency of up to 80 %.

Recently Moneghini, et al., 2001 produced a Carbamazepine-PEG solid dispersion using SC CO_2. In this GAS coprecipitation study, the carbamazepine and PEG were dissolved in acetone in a high-pressure chamber. The SC CO_2 was injected from the bottom of the chamber. The dissolution of SC CO_2 in the solution induced nucleation and precipitation of the carbamazepine and PEG. Therefore, microparticles of the solid dispersion of carbamazepine-PEG were produced and the dissolution rate was considerably improved compared with the slow dissolution rate of pure carbamazepine.

However, coprecipitation of drug and polymer requires that both be dissolved in a suitable solvent which is a challenge for proteins since many proteins are insoluble in organic solvents. Moreover, some organic solvents might cause the protein to lose its bioactivity. In addition, the coprecipitation of two different solutes is difficult to achieve unless the two solutes have similar thermodynamic properties and undergo a similar precipitation pathway.

An alternative particle coating or encapsulation antisolvent process to those described above involves suspending the host particles in a coating polymer solution. The suspension is either sprayed into SC CO_2 or SC CO_2 is injected into the suspension. Due to the mutual diffusion between SC CO_2 and the organic solvent, the polymer precipitates out and is deposited onto the surface of host particles, forming a film coating.

Bertucco and Vaccaro, 1997 did a preliminary study of particle encapsulation by polymers using compressed CO_2 as an antisolvent (GAS). In their study, particles of KCl were suspended in a solution of various polymers (hydroxypropyl methylcellulose

phthalate, Eudragit E 100, ethylcellulose) in various organic solvents (toluene, acetone, 1,4-dioxane, ethylacetate). Compressed CO_2 was introduced into the high-pressure vessel as an anti-solvent to precipitate the polymer on the surface of suspended KCl particles and partial polymer encapsulation was achieved. It was found that processing conditions, such as, pressure, temperature, solute concentration, and polymer-to-drug ratio, strongly influenced the polymer coating on the surface of the particles.

Young, et al., 1999 studied the encapsulation of lysozyme in a biodegradable polymer by precipitation with a vapor-over-liquid antisolvent, which is simply a modified precipitation with a compressed anti-solvent (PCA) process. In this work, a suspension of 1-10 micron lysozyme particles in a polymer solution was sprayed into CO_2 vapor over a CO_2 liquid phase (below supercritical conditions) through a nozzle. By delayed precipitation, particles were allowed to grow large enough to encapsulate lysozyme. The experiments were operated at a temperature of –20 °C so that the precipitated particles were sufficiently hard and agglomeration was remarkably reduced compared with higher temperatures. The process offered an effective encapsulation approach with high encapsulation efficiency and less agglomeration.

2.2.3 Other SC CO_2 Processes for Particle Coating or Encapsulation

Some other SC CO2 processes were developed for particle coating or encapsulation. Ribeiro Dos Santos, et al., 2002 studied the microencapsulation of protein (bovine serum albumin, BSA) particles with lipids (Dynasan® 114 and Gelucire® 50-02). The BSA particles and lipids were charged into a high-pressure chamber, which was equipped with an agitator. The Dynasan® 114 and Gelucire® 50-02 were dissolved in SC CO_2 at 45 °C

and 200 bars and 35 °C and 200 bars, respectively. The subsequent cooling of the pressure chamber induced a phase change from the supercritical to the liquid state, leading to the precipitation of the coating materials onto the surface of the BSA particles. Thus, microencapsulation of protein particles was successfully achieved.

Pessey, et al., 2000; 2001 described a thermal decomposition process for particle coating in a supercritical fluid. In their research, an organic metallic precursor and host particles were loaded in a high-pressure chamber. The chamber was then filled with SC CO_2 with ethanol as a co-solvent. When the operating temperature was raised to 200 °C, higher than the deposition temperature of the precursor, 195 °C, the precursor underwent decomposition and copper was released and deposited onto the surface of core particles at a pressure up to 190 bars. However, their methods are less attractive from the point of view of safety and cost and probably cannot be applied to the pharmaceutical industry since the high temperature could adversely effect or even destroy most drug powders.

Schreiber, et al., 2002 developed a supercritical fluidized bed for particle coating. In this research silica particles or glass beads were fluidized with SC CO_2 at a pressure up to 300 bars and temperature from 40 to 80 °C. The coating material of paraffin was first dissolved in SC CO_2 in an autoclave and then the solution was sprayed into the fluidized bed. The difference in operating conditions between the fluidized bed and the autoclave made the paraffin precipitate and adhere to the surface of particles in the fluidized bed, forming a film coating.

Liu and Yates, 2002 took the advantage of the exceptional transport properties of compressed CO_2, such as high diffusivity and very low viscosity and developed a microencapsulation technique for polymer latexes using compressed CO_2. In this work,

CO_2 was emulsified in water and ethanol latexes with the assistance of a surfactant, poly (propylene oxide)-(ethylene oxide)-(propylene oxide) (PPO-PEO-PPO), Pluronic F108. The compressed CO_2 was used to plasticize the synthesized monodisperse polystyrene particles and dyes were impregnated into the polymer particles. The surfactant accelerated the transport of dye into the polymer phase.

Although the various supercritical fluid processes for particle formation, coating and/or encapsulation have been comprehensively reviewed in this chapter, some of this material will be repeated in Chapters 3, 4, 5, and 6 so that the research described in each of these chapters can stand on its own as a publishable research paper.

CHAPTER 3

EXTRACTION AND PRECIPITATION PARTICLE COATING USING SUPERCRITICAL CO_2

In order for the research described in this chapter to stand on its own (as a publishable research paper), some of the pertinent literature review that has already been described in Chapter 2 is repeated in the following introduction.

3.1 Introduction

Particle coating involves the application of another material onto the surface of individual particles to modify their surface properties, such as flowability, wettability, time release, flavor, taste, etc. Conventional particle coating processes usually employ wet chemistry or solutions of the coating material, requiring the use of large quantities of organic solvents, surfactants, and other chemicals. In general, these processes are environmentally unfriendly and can lead to the emissions of volatile organic compounds (VOCs) and other waste streams. Dry particle coating (Pfeffer, et al., 2001) is a good alternative because no organic solvents are employed, not even water. Moreover no drying is needed; thus these processes save energy. Coating is achieved through mechanical forces between host and much smaller guest particles, which are attached to the surface of the host particles. But it is often difficult to control the film structure on the surface of the host particles, such as the film thickness, uniformity, texture and robustness of the coating. Furthermore, some bio-active particles, for example, proteins and peptides, may lose much of their bio-activity due to the high shear and compressive forces employed and the local increase in temperature produced in dry coating processes.

A supercritical fluid (SCF) is a fluid above its critical temperature (T_c) and critical pressure (P_c) and has many advantages over conventional fluids. Its gas-like viscosity and high diffusivity is advantageous for mass transfer applications. Its density and related solvent strength can be tuned by controlling the temperature and pressure. Carbon dioxide is the most widely used SCF because of its low critical temperature (31.1 °C) and mild critical pressure (73.8 bars), non-toxicity, non-flamability, and low price. During the past two decades, SCF technologies have developed very rapidly. Originally, SCF processes were developed and widely used in extraction and separation because of the good solvent properties of SCFs. Since the mid 1980s, however, particle synthesis and engineering using supercritical CO_2 has emerged as a fast-growing field. The rapid expansion of supercritical solution (RESS) process to form fine particles was first suggested by Krukonis, 1984. In RESS (Chang and Randolph, 1989; Matson, et al., 1987; Tom and Debenedetti, 1991 and 1994) a SCF solution is expanded through a nozzle or capillary tube, resulting in a very high pressure drop and a high degree of supersaturation. The solute will nucleate and grow, forming very small particles.

Another technique, using a SCF as an anti-solvent, for particle engineering has been developed in a variety of forms. These include the supercritical anti-solvent (SAS) technique (Cai, et al., 1997; Yeo, et al., 1993; Dillow, et al. 1997; Reverchon, et al., 1998 and 2000) gas anti-solvent (GAS) (Gallagher, et al., 1992; Lim, et al., 1998; Dixon, et al., 1993; Winter, et al., 1999), aerosol solvent extraction system (ASES) (Reverchon, et al., 1999; Chou and Tamasko, 1997; Thies and Müller, 1998), and solution enhanced dispersion by SCFs (SEDS) (Hanna, et al., 1994). However, all of these techniques and the investigators who used them, focused on single component powder formation.

Multi-component particle formation, such as particle composites or encapsulation of particles with polymer using SCFs is of great interest for controlled drug delivery, food, agriculture, and cosmetics applications. Recently, Kim, et al., 1996 reported the microencapsulation of naproxen with poly L-lactic acid (PLA) using RESS. Naproxen and PLA were packed in an extraction unit and extracted with supercritical CO_2. The supercritical solution was then expanded through a capillary tube. Composite particles with a naproxen core encapsulated by a polymer coating were produced. Microparticles and agglomerates were observed as the dominant morphology. Mishima, et al., 2000 investigated the microencapsulation of proteins with poly ethylene glycol (PEG) by RESS. In this research, ethanol (about 38.5 wt. %) was employed as co-solvent to enhance the solubility of PEG in supercritical CO_2 even though ethanol, by itself, is a nonsolvent for PEG. The results indicated that lipase and lysozyme particles were completely encapsulated by PEG without agglomeration.

Tsutsumi, et al., 1995 used a combination of RESS with fluidized bed technology. Catalyst particles in a fluidized bed were fluidized by air, and a solution of paraffin in supercritical CO_2 was sprayed into the bed through a nozzle. Coating material was directly deposited onto the surface of the catalyst particles with no binder or solvent involved, resulting in no significant agglomeration. A more recent study of particle coating granulation using the RESS process in a fluidized bed was carried out by Wang et al., 2001. However, the main drawback for the RESS technique is that SCFs have a limited solvent strength for many polymers of interest, which restricts its application. There is another disadvantage in that it is very difficult to control the coating or

encapsulation because the nucleation and precipitation of coating materials take place very fast (less than 10^{-5} seconds) during RESS (Matson, et al., 1987).

Bertucco and Vaccaro, 1997 used the GAS technique for particle encapsulation. In their research, particles of KCl were suspended in a solution of polymer (hydroxypropyl methylcellulose phthalate, Eudragit E 100, ethylcellulose) in various organic solvents (toluene, acetone, 1,4-dioxane, ethylacetate). Compressed CO_2 was introduced into the vessel as an anti-solvent. Preliminary results showed that partial polymer encapsulation was achieved.

A recent study of Young, et al., 1999 investigated the encapsulation of lysozyme with biodegradable polymer by precipitation with a vapor-over-liquid antisolvent, which is a modified precipitation with a compressed anti-solvent (PCA) process. A slurry of 1-10 micron lysozyme particles suspended in a polymer solution was sprayed into CO_2 vapor over CO_2 liquid (below supercritical conditions) through a nozzle. By delayed precipitation, particles were allowed to grow large enough to encapsulate lysozyme. The polymer particles entraining lysozyme vitrified after falling into the CO_2 liquid phase and agglomeration was avoided.

There are also some studies (Falk, et al., 1997; Elvassore, et al., 2001) dealing with composite microsphere production by the SAS process. A homogeneous solution of interesting solutes and polymer, which was prepared by the hydrophobic ion-pairing (HIP) method (Falk, et al., 1997) or by mixed solvents (Elvassore, et al., 2001), was sprayed into supercritical CO_2 antisolvent. Co-precipitation of the solutes and polymer was expected and composite microspheres or microcapsules were formed. However, co-precipitation of two different solutes is difficult to achieve even when the precipitation

pressures of the solutes are close to each other (Bertucco and Vaccaro, 1997). In addition, exposure of proteins to solvents required for SAS leads to denaturing of the proteins probably due to a change in conformation (Yeo, et al., 1994), although some denaturation is partially reversible (Yeo, et al., 1994; Winter, et al., 1996).

In this research a modified RESS technique was used to explore the coating of host particles with polymer using supercritical CO_2 and a small amount of co-solvent to increase the solubility of the polymer in supercritical CO_2. The modified RESS technique involves extracting the polymer with supercritical CO_2, with or without a co-solvent in an extraction vessel, and then precipitating the polymer onto the surface of host particles in a second precipitation vessel by adjusting the pressure and temperature inside the precipitator to lower its solubility in supercritical CO_2.

Spherical glass beads (315 and 500 μm) were chosen as host particles for the reason that glass beads are spherical and nearly monodisperse and therefore the coatings obtained could be more easily characterized. Two different polymers were tested in the coating experiments. The coating of much finer powders with biodegradable polymers using supercritical processing for drug delivery purposes will be reported in a future paper.

3.2 Materials, Methods, and Characterization

3.2.1 Materials

CO_2 was obtained from Air Liquide Company (France); purity is 99.995 %. Two polymers, poly vinyl chloride-co-vinyl acetate (PVCVA) (Aldrich, USA) and hydroxypropyl cellulose (HPC), which is soluble in water, were used. The properties of

the two polymers are listed in Table 3.1. Unfortunately, no solubility data for these two polymers in supercritical CO_2 could be found in the literature, but it was assumed that their solubility was extremely limited. Therefore, acetone (99.5%, Fisher, France) was chosen as a co-solvent since it is widely used to increase polymer solubility by improving dispersion, inducing dipolar interactions and by increasing the solvent density [35]. Monodisperse spherical glass beads with diameters of 315 and 500 μm (Potters-Ballotini S.A., France) were chosen as host particles.

Table 3.1 Polymer Properties

Polymers	Molecular Weight	Glass Transition Temperature (Tg, °C)	Content (% wt.)
PVCVA	27,000 (Mn*)	72	86% poly vinyl chloride
HPC	100,000	-	100%

* Mn, number average molecular weight.

3.2.2 Methods

The coating experiments using supercritical CO_2 were performed on a pilot-scale apparatus (Separex, France), which is shown schematically in Figure 3.1. Liquid CO_2 was delivered by a Lewa metering pump from a CO_2 tank and was cooled down to around 0 °C before entering the pump head. Co-solvent was introduced using a Gilson piston pump. The polymer substrate was packed in a stainless steel vessel having a volume of 1.5 liter, which served as the extraction unit. Another vessel with the same capacity was used as a precipitator and held the glass beads. The temperature of each of the two vessels was maintained relatively constant by an electrical heating mantle. CO_2, with or

without co-solvent, was charged from the bottom of the extraction unit to extract the packed polymer. The supercritical solution of polymer was then introduced into the bottom of the precipitator. By adjusting the pressure and temperature inside the precipitator, the solute would precipitate and deposit on the surface of the host particles. After a certain amount of running time, the co-solvent supply was stopped and pure CO_2 was continued to flush the precipitator for some time under the same conditions to remove the co-solvent. Then the CO_2 supply was shut off and the precipitator was slowly depressurized. The coated glass beads were recovered from the precipitator for characterization and further analysis. The operating parameters are given in Table 3.2.

Table 3.2 Experimental Conditions

Coating Experiments	PVCVA - 1	PVCVA - 2	HPC
Size of glass beads (μm)	315	500	500
Weight of glass beads (g)	3.1558	2.8224	4.0268
Weight of polymer (g)	1.1789	0.5036	0.9336
Extraction T and P (^{o}C, bars)	80, 127	84, 130	80, 106
Precipitation T and P (^{o}C, bars)	30, 118	48, 115	30, 80
Running time (minutes)	25	12	20
Flushing time (minutes)	10	0	10
Flow rate of CO_2 (kg/hour)	15-20	15-20	15-20
Co-solvent used	Acetone	None	Acetone

3.2.3 Characterization

In this study a Leo 982 Scanning Electron Microscope (SEM) was employed for the morphological analysis. Samples were sputtered by palladium (SPI Sputter). Energy dispersive X-ray spectrometry (EDS) was used to analyze the elements on the surface of the uncoated and coated glass beads. The energy dispersive X-ray mapping technique was used to image the spatial distribution of elements on the surface of the particles. A TGA7 Thermo-gravimetric Analyzer (TGA) was used to estimate the thickness of the coating.

3.3 Results and Discussion

3.3.1 Coating with PVCVA

In the experiment of coating glass beads (315 μm) with PVCVA the temperature of the extraction unit was maintained around 80 °C and the pressure up to 127 bars. Acetone as co-solvent was delivered at a rate of 2 ml/min, to improve the solubility. The temperature of the precipitator was kept at 30 °C and the pressure of the precipitator was kept around 118 bars by the back pressure regulator. These conditions of temperature and pressure were chosen because it was assumed that any inherent solubility of the polymer in supercritical CO_2 would decrease rapidly as the pressure and temperature approaches the critical point (Debenedetti and Kumar, 1986), and because they allow for a single-phase mixture after depressurization. Furthermore, O'Neill, et al., 1998 stated: "Polymers in general have very limited solubility in supercritical fluid (SF) CO_2 at temperatures below 80 °C, although solubilities can increase significantly at higher temperature." Thus, in

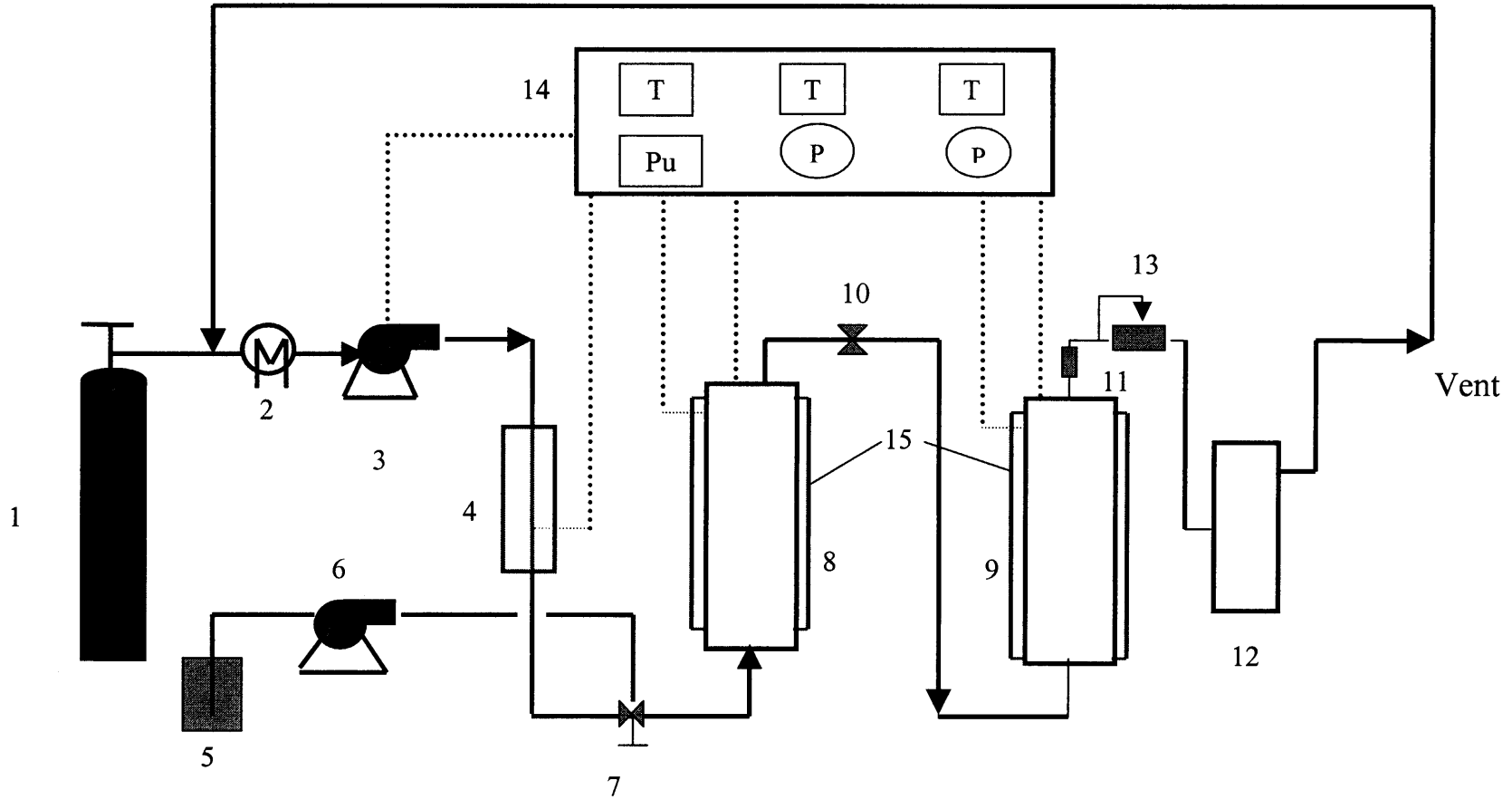

Figure 3.1 Diagram of coating process using supercritical CO_2.

Key: 1. CO_2 cylinder, 2. Cooling, 3. Pump, 4. Preheating, 5. Co-solvent, 6. HPLC pump, 7. 3-way valve
8. Extraction unit, 9. Precipitator, 10. On-off valve, 11. Filter, 12. Separator, 13. Back pressure regulator
14. Control panel 15. Heating mantle

Thus, in spite of a marked increase in the density of supercritical CO_2 (e.g., using the Peng-Robinson equation of state (Peng and Robinson, 1976), the density of pure CO_2 is 0.321 at 127 bars and 80 °C and 0.770 at 118 bars and 30 °C), polymers appear to be much less soluble at lower temperatures (Tom and Debenedetti, 1991). This was also verified by the experiments since polymer-coated glass beads could be harvested by decreasing both the pressure and the temperature in the precipitation vessel.

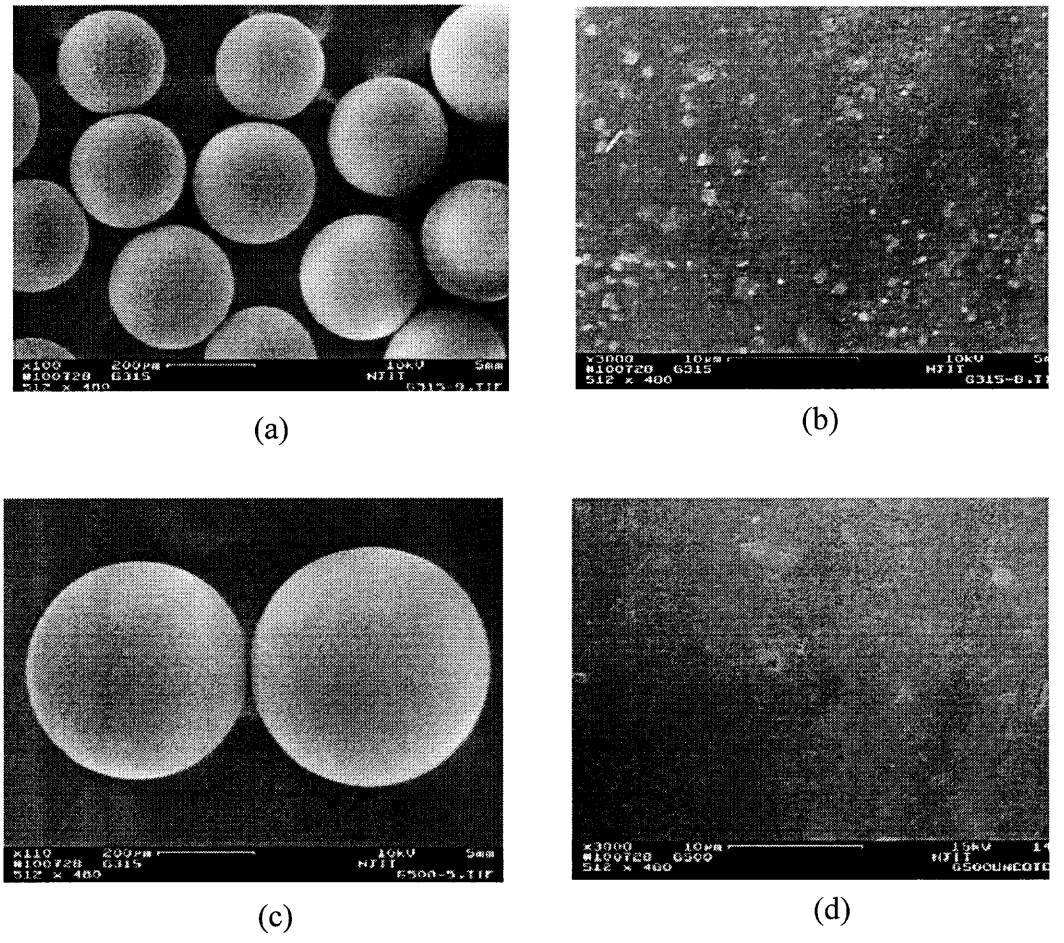

(a) (b)

(c) (d)

Figure 3.2 SEM photographs of unprocessed glass beads at different magnifications: (a) 315 μm × 100; (b) 315 μm × 3,000; (c) 500 μm × 110; (d) 500 μm × 3,000.

After 25 minutes of operation and 10 minutes of flushing (See Table 3.2, PVCVA - 1), the sample was collected from the precipitator for characterization. Figure 3.2 shows SEM photographs at two different magnifications of both the unprocessed 315 μm and 500 μm glass beads, which were used as host particles. As can be seen in the Figure 3.2 the unprocessed glass beads are monodisperse and are quite smooth and clean on the surface with some small defects. SEM photographs of the 315 μm glass beads coated with PVCVA are shown in Figure 3.3. Compared with Figure 3.2, Figures 3.3 (a) and (b) clearly show that the glass beads are coated with polymer, although the coating is not uniform, nor is it continuously distributed over the surface.

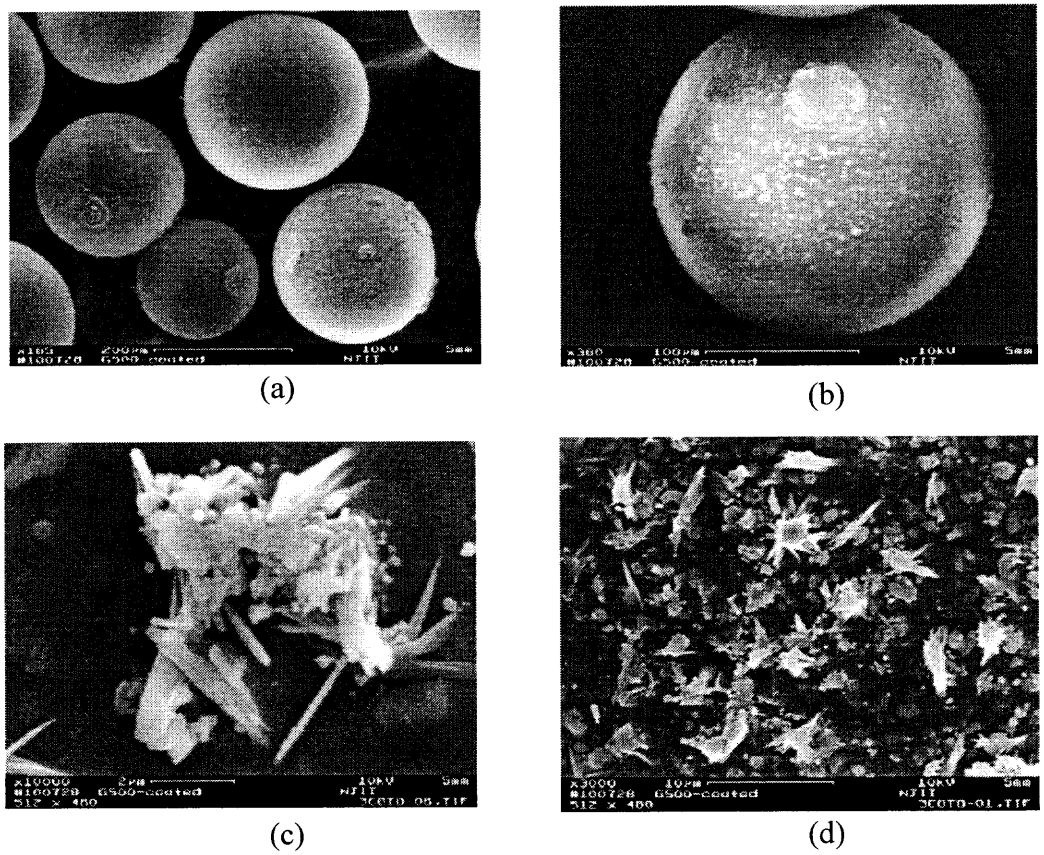

(a) (b)

(c) (d)

Figure 3.3 SEM photographs of coated glass beads (315 μm) at different magnifications: (a) × 100; (b) × 360; (c) × 10,000; (d) × 3,000.

In this coating process, due to changes in pressure and temperature (pressure from 127 to 118 bars and temperature from 80 to 30 °C), the solvent strength of the supercritical CO_2 is strongly affected, leading to a decreasing solubility of the polymer in the supercritical fluid. As the pressure and temperature decrease, the polymer nucleates. The nuclei grow into crystalline aggregates and deposit on the surface of the glass beads.

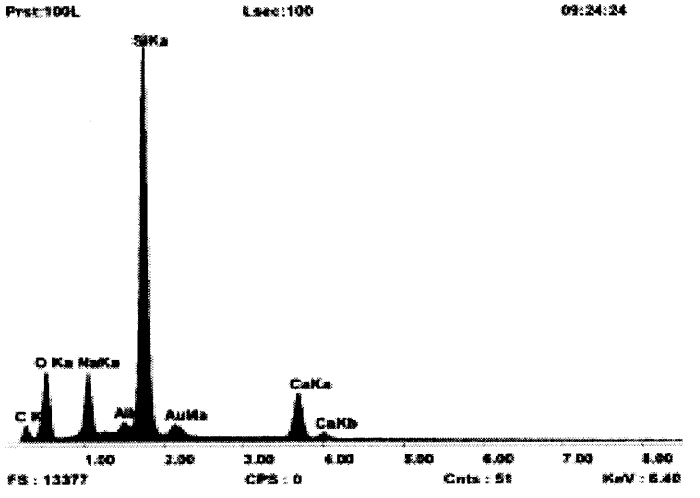

(a)

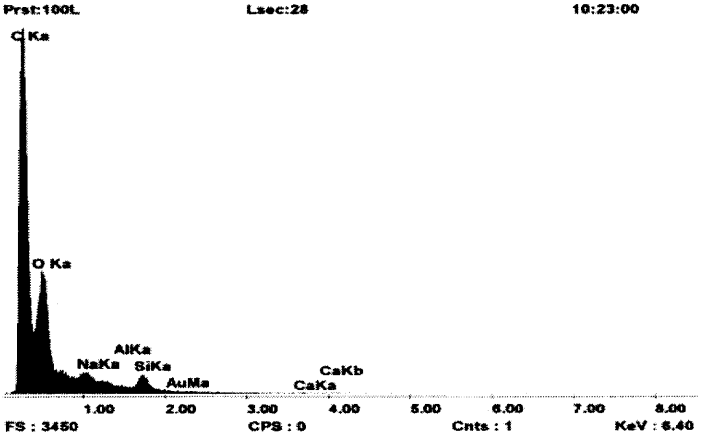

(b)

Figure 3.4 EDS of unprocessed (a) and coated (b) glass beads (315 μm).

This mechanism of polymer precipitation and coating is supported by Figure 3.3 (c), which shows a crystalline aggregate on the glass bead surface. Many discrete polymer aggregates are seen attached on the surface in Figure 3.3 (d).

Surface elemental analysis, using the EDS technique, can indicate what elements are on the surface of a particle. Figure 3.4 (a) shows the EDS pattern of unprocessed glass (315 μm) beads. Obviously, the dominant element is silicon on the surface because it is a primary component of glass. Oxygen and sodium are secondary elements contained in the glass beads. The carbon peak, however, is very small compared with that of silicon and is probably due to some impurities or contaminants attached on the surface. The EDS pattern of the processed glass beads is shown in Figure 3.4 (b). Here the carbon signal is very strong, and it is the primary element on the surface, with oxygen seen as the second dominant element on the surface of the processed glass beads. This is consistent with the polymer's composition. Moreover, the silicon signal is very weak because it is blocked by the polymer coating layer. From Figure 3.4, it is evident that the processed glass beads are coated with polymer, confirming the observation in Figure 3.3.

The processed glass beads were also examined by using the EDS mapping technique, which reflects the spatial distribution of different elements. Figure 3.5 (a) shows the SEM image of the surface of a coated glass bead. Figure 3.5 (b) is the EDS mapping pattern for the element carbon on the same glass bead. The white dots represent the signals of carbon on the surface of the glass bead; it is clear that the glass bead is not uniformly covered with PVCVA polymer. Similarly, an EDS mapping of silicon can be found in Figure 3.5 (c). A comparison of 3.5 (b) and 5 (c) shows that the carbon signal is much weaker than that of the silicon signal over most of the surface because the polymer

coating is very discrete. Also, it can be seen that where the carbon signal is strong, the silicon signal is weak. The polymer on the surface blocks the X-ray so that there is a very

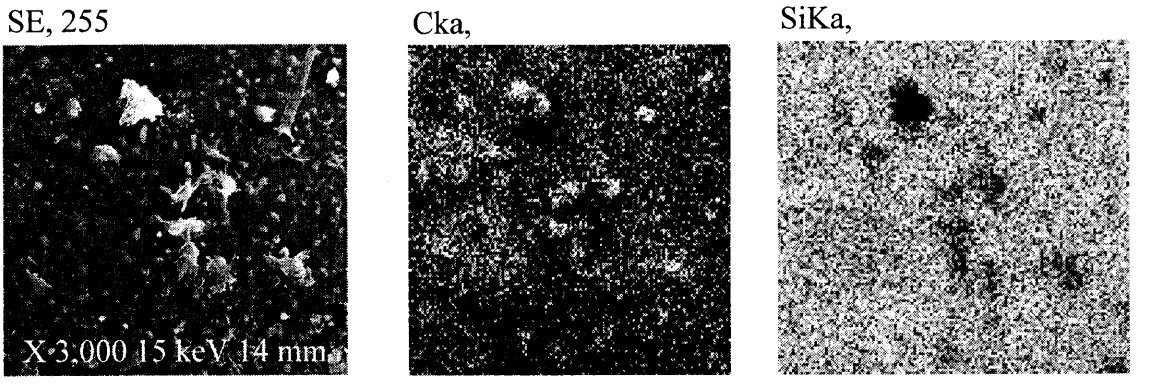

Figure 3.5 EDS mapping of coated glass beads (315 μm). (a) SEM image; (b) carbon mapping; (c) silicon mapping.

weak silicon signal in the area where the polymer deposits. The result of EDS mapping strongly supports the conclusion that the white material seen in Figure 3.5 (a) is polymer precipitated on the surface of the glass beads.

Another set of coating experiments was carried out by using 500 μm glass beads as the host particles. It should be noted that no co-solvent was added in these experiments. They were operated under the conditions that the extraction temperature and pressure were maintained at 84 °C and 130 bars and the precipitation temperature and pressure were maintained at 48 °C and 117 bars. The experiment was run for 12 minutes (See Table 3.2, PVCVA - 2) with no CO_2 flushing necessary since no co-solvent was used.

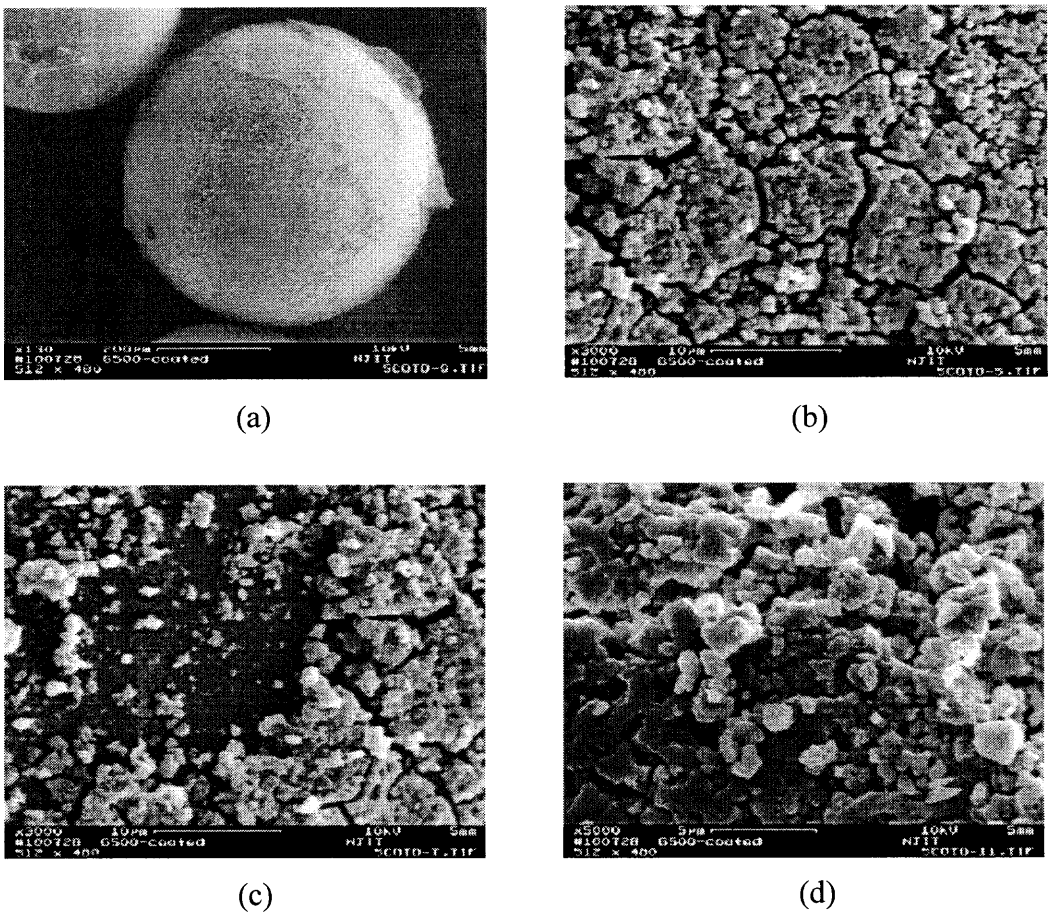

(a) (b)

(c) (d)

Figure 3.6 SEM photographs of coated glass beads (500 μm) at different magnifications: (a) × 130; (b) × 3,000; (c) × 3,000; (d) × 5,000.

SEM photographs of the coated glass beads at different magnifications are shown in Figure 3.6. When compared to the unprocessed 500 μm glass beads shown in Figure 2, it is evident that the morphology and surface texture of the coated glass beads are different from those of the uncoated glass beads. Figures 3.6 (a) clearly show that the glass beads are coated with polymer. However, it can be observed that parts of the surface are heavily covered by polymer, while a loose and discrete coating is developed on other parts of surface (Figures 3.6 (b), and (c)). The highest magnification, Figure 3.6 (d), shows that fine polymer particles (around 2μm) aggregate on the surface. The 2 μm

polymer particles were produced due to the change in the temperature and pressure of CO_2, which lowers the solubility of polymer in the supercritical CO_2 (Chang and Randolph, 1989; O'Neill, et al., 1998).

In the present coating experiments, the glass beads simply sat on the bottom of the precipitator vessel and no stirrer was used. Thus, there were many dead areas and the precipitating polymer could not deposit on all of the surfaces of the glass beads even though there was sufficient precipitant available. Consequently, uneven coating is observed. However, fluidizing or stirring the host particles to avoid dead areas so that entire glass bead surface can be exposed to the polymer precipitant may overcome this problem.

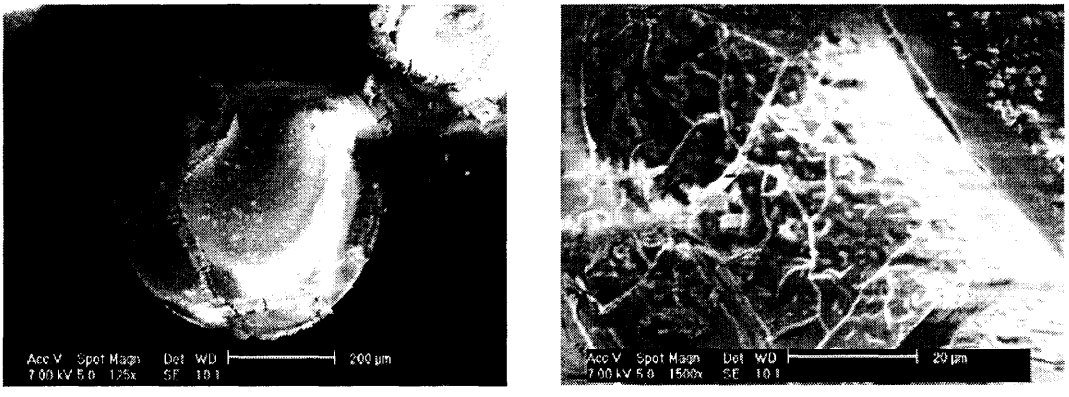

(a) (b)

Figure 3.7 SEM photograph of glass bead agglomerate (a) and polymer bridge (b).

Figure 3.7 (a) shows two glass beads "glued" together by polymer. Due to the CO_2 pressure and temperature variation, the polymer nucleates and grows, falling into the area between neighboring glass beads, forming a bridge as well as covering the surface. If enough polymer precipitant is present, it would spread between all of the neighboring

glass beads during polymer vitrification. Figure 3.7 (b) shows a high magnification of the polymer bridge between two glued glass beads.

Figure 3.8 (a) shows the EDS pattern of the unprocessed 500 μm glass beads. Again, silicon appears as one of the main component elements on the surface, and the carbon intensity is negligible compared with that of silicon, indicating that carbon shows up on the surface only as a contaminant. For the coated glass beads (Figure 3.8 (b)), carbon appears as one of the two dominant elements and silicon has a much smaller peak. These results are consistent with what was observed in Figure 3.4 when the 315 μm glass beads were coated.

It is interesting to observe that the coating of the 315 μm glass beads appears very different from that of 500 μm glass beads even though the same polymer PVCVA was employed in the experiments. The polymer coating on the surface of the315 μm glass beads (Figure 3.3) appears much more crystalline than the polymer coating on the surface of the 500 μm glass beads (Figure 3.6). These results are probably due to the use of acetone as a co-solvent in the coating of 315 μm glass beads. Acetone is a good solvent for PVCVA and thus the solubility of PVCVA in the mixture of supercritical CO_2 and acetone will increase. The mobility of the polymer chains will also increase. Therefore, the polymer chains can rearrange into a crystalline state during the precipitation (Falk and Randolph, 1998). When coating the 500 μm glass beads without acetone as co-solvent, by adjusting the temperature and pressure in the precipitation vessel, the polymer nuclei that are formed will be less inclined to rearrange into a crystalline state. Therefore, the polymer coating on the surface of the 500 μm glass beads is observed to be amorphous rather than crystalline.

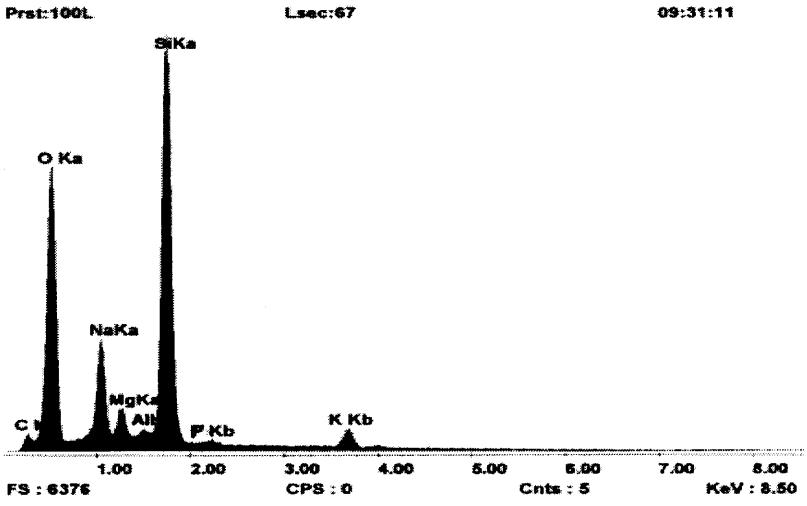

(a)

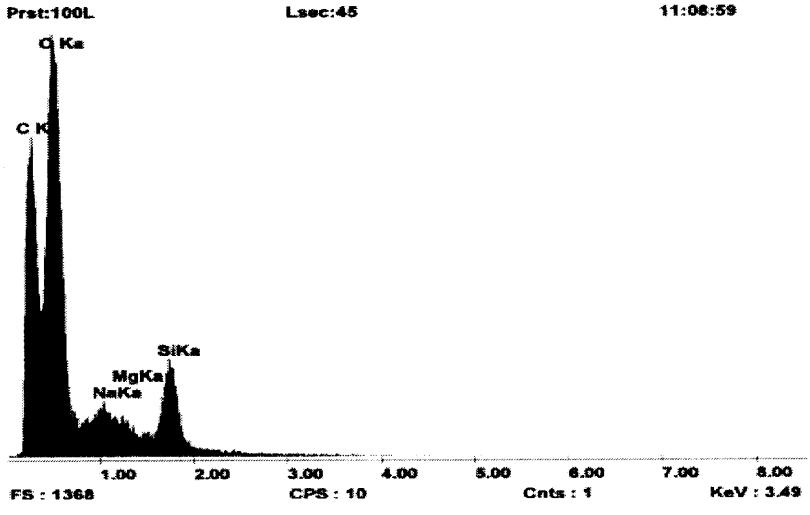

(b)

Figure 3.8 EDS of unprocessed (a) and coated (b) glass beads (500 μm).

In order to measure the average thickness of the coating, a thermo-gravimetric analyzer (TGA) was used to remove the polymer from the surface of the glass beads. The

mass of polymer can be determined by the weight loss during the heating process. The temperature of the sample was raised to 580 °C at a heating rate of 30 °C/min in air atmosphere. Figure 3.9 shows the TGA patterns of both the uncoated glass beads and the glass beads coated with PVCVA polymer. As can be seen in Figure 3.9, the weight of the uncoated glass bead sample stays constant during the experiment. For the coated glass beads, the weight loss is about 0.7 % when run under the same conditions as the uncoated glass beads. Therefore the TGA analysis results also support the conclusion that the glass beads are coated with the polymer. Assuming that the coating is continuous and

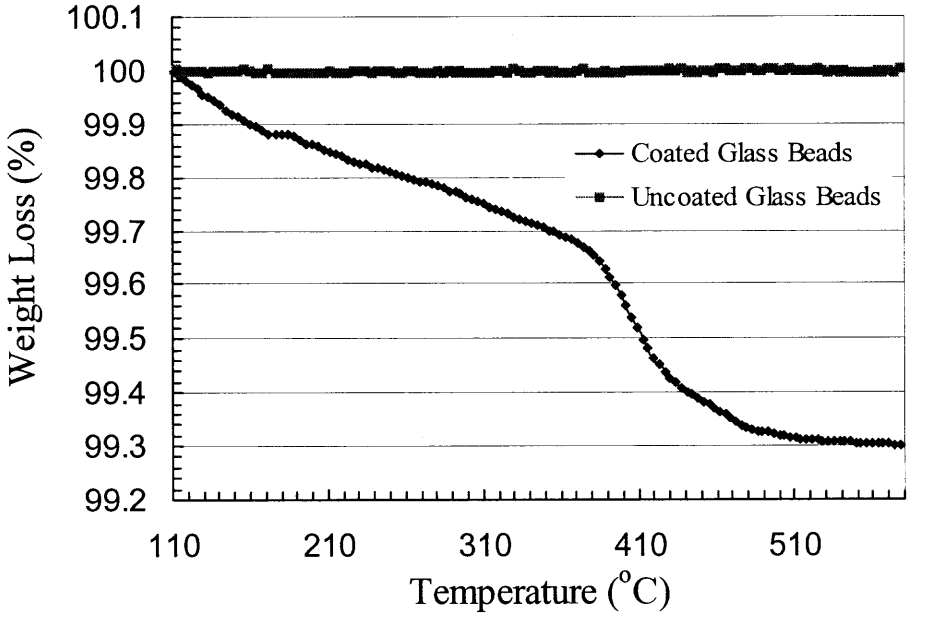

Figure 3.9 TGA pattern of uncoated and coated glass beads (500 μm) with PVCVA.

the coating thickness is negligible compared with the diameter of the host particle, the average thickness of the coating material is estimated using the formula below,

$$h = \frac{1}{6} \times \frac{m_C}{m_H} \times \frac{\rho_H}{\rho_C} \times D \qquad (1)$$

where h is coating thickness, ρ_H and ρ_C are the densities of the host particles and polymer coating, respectively and m_H and m_C are the weight of the host and polymer, respectively. D is the diameter of the host particle.

3.3.2 Coating with HPC

Hydroxypropyl cellulose (HPC) is a natural cellulose and is often used in pharmaceutical applications. However, it is hard to handle due to the lack of an appropriate solvent. Usually ethanol is used, but it will form a gel or highly viscous liquid when small amounts of ethanol are added. Moreover, other organic halide solvents are strictly prohibited in food and pharmaceutical handling because residual solvents could have ill effects on health.

As part of this research of particle coating with polymer, HPC was used for the coating of glass beads using supercritical CO_2. Although acetone is not considered to be a good solvent for HPC, it can improve the solvating power of supercritical CO_2 and was used as a co-solvent (Kiran and Pöhler, 1998).

For the coating of 500 μm glass beads with HPC, the extraction pressure and temperature were set at 106 bars and 80 °C, respectively. The precipitator was kept at 80 bars and 30 °C, very close to the critical point of CO_2 where the solubility of polymer is much lower (Debenedetti and Kumar, 1988). Acetone was delivered at 2 ml/min. The experiment was run for 20 minutes, followed by 10 minutes of flushing with CO_2 (See Table 3.2, HPC).

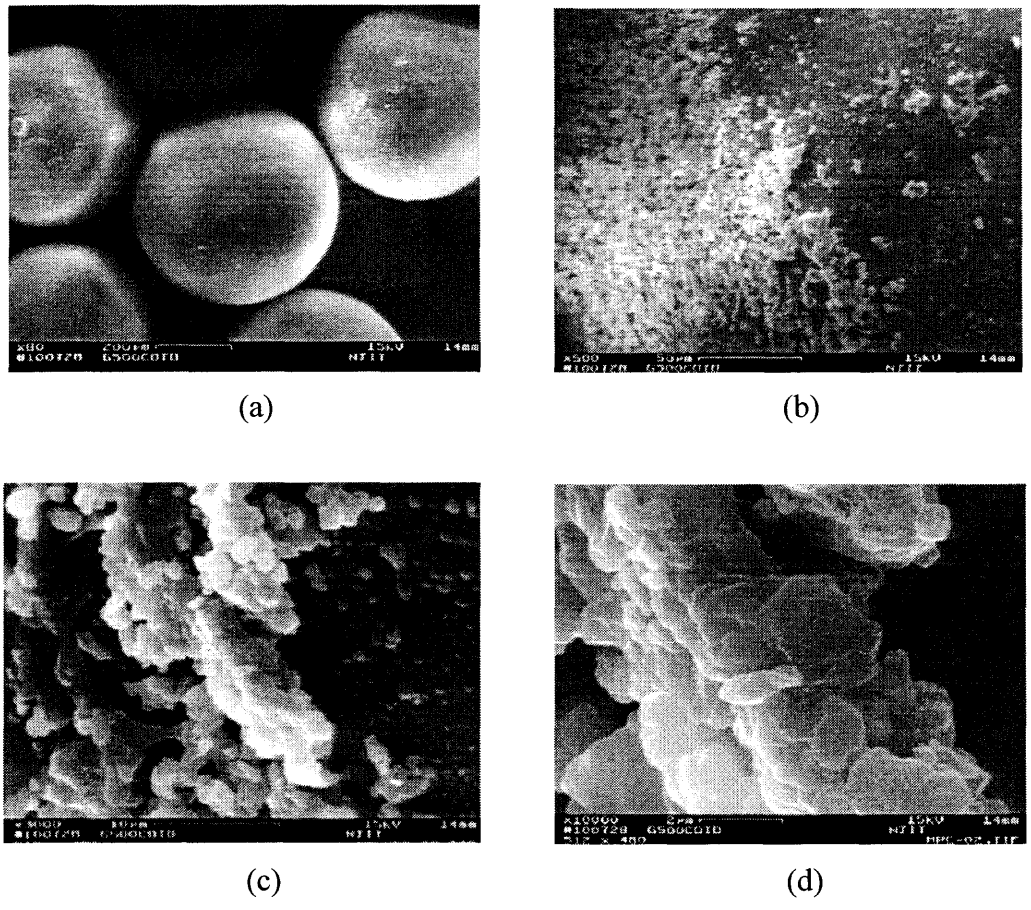

Figure 3.10 SEM photographs of coated glass beads (500 μm) with HPC at different magnifications: (a) × 90; (b) × 500; (c) × 3,000; (d) × 10,000.

Figure 3.10 shows SEM pictures of 500 μm glass beads processed with HPC. Compared with Figure 3.2, it appears that while the glass beads are coated with HPC, the coating is less than that with PVCVA. Moreover, the coating is very discrete with large areas of the surface left uncoated. When examining the SEM pictures in Figure 3.6 and Figure 3.10, it is observed that a higher degree of covering occurred with PVCVA on the

glass bead surface than with HPC. This might be due to a lower solubility of HPC as compared to PVCVA in SC CO_2. In the coating experiments with HPC, the first run was performed under the same conditions mentioned above except no co-solvent was added. Without the co-solvent, it was observed that no coating occurred on the surface of the

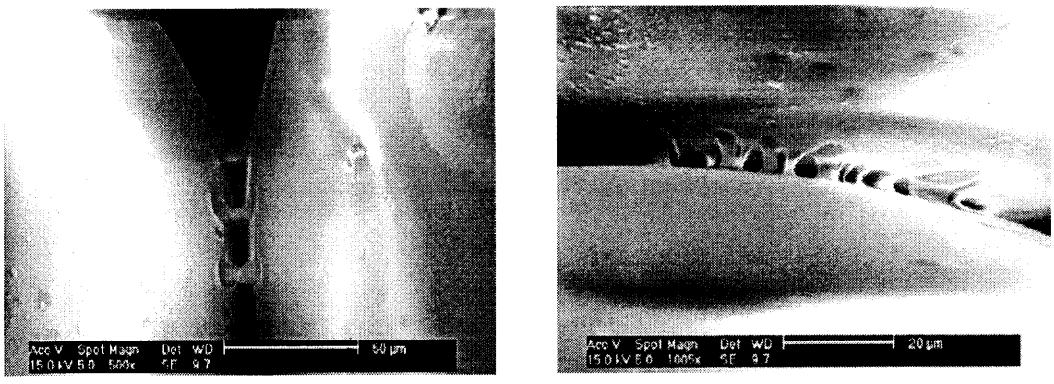

(a) (b)

Figure 3.11 SEM photographs of glass bead agglomerate.

glass beads. Since HPC is polar and a hydrophilic polymer, the solubility of HPC in supercritical CO_2 is extremely low. Acetone acts as a co-solvent and improves the solvent strength of the supercritical CO_2 considerably. The addition of organic solvents as a co-solvent to improve solvating power of supercritical fluid had been widely reported (Chang and Randolph, 1989; Tom and Debenedetti, 1991 and 1994; Mishima, et al., 2000).

Figures 3.11 (a) and (b), at different magnifications, show two glass beads stuck together with HPC. The polymer precipitant acts as binder between the glass beads and

glues them together. This is again attributed to the fact that the glass beads were not stirred or fluidized in the precipitator.

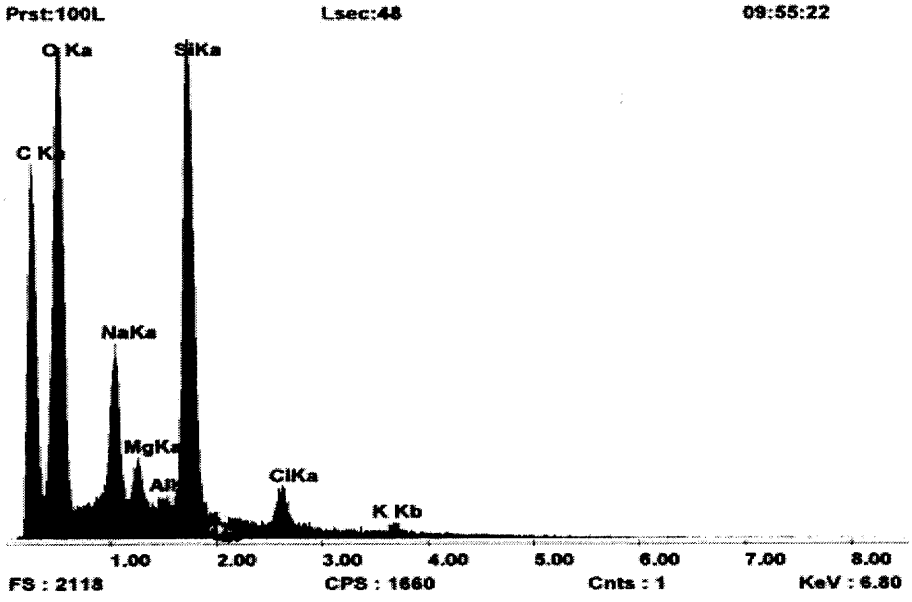

Figure 3.12 EDS pattern of coated glass beads (500 μm) with HPC.

The EDS pattern of the uncoated glass beads shows that silicon and oxygen are the two dominant elements on the surface, while carbon is negligible (Figure 3.8). However, in Figure 3.12, which shows the EDS pattern of the coated glass beads, the carbon intensity increases greatly and becomes one of three dominant elements on the surface, indicating that the surface of the glass beads was coated by HPC.

A TGA analysis of glass beads coated with HPC is shown in Figure 3.13. Compared with uncoated glass beads (Figure 3.9), the weight loss of about 0.17% confirms the conclusion that the glass beads are coated with polymer. Based on the

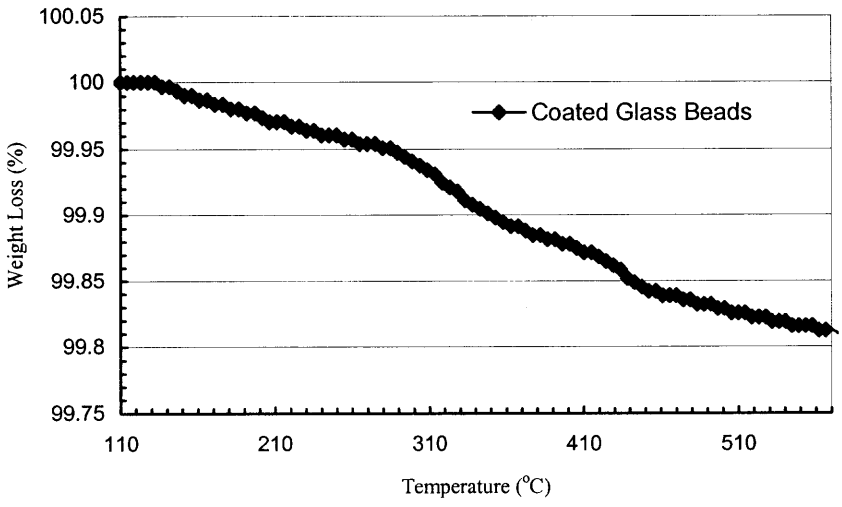

Figure 3.13 TGA pattern of coated glass beads (500 μm) with HPC.

Equation (1), the average coating thickness is about 0.24 μm, as compared to an average thickness of about 0.8 μm for PVCVA. This supports the previous observation that more coating is obtained with PVCVA as compared to HPC due to a difference in solubility.

3.4 Conclusions

A modified RESS process was developed in this study for coating particles by using a solution of polymer in supercritical CO_2. The results show that the coating of glass beads with PVCVA and HPC was successfully achieved using this technique. Solubility plays a very important part in the coating process. The use of a co-solvent can improve the solubility of polymers and will also affect the degree of crystallinity of the polymer coating on the surface of glass beads. The extraction and precipitation technique takes advantage of the properties of a supercritical solution in that the polymer would nucleate, grow and deposit on the host particle surface due to changes in its solubility caused by

adjusting the temperature and pressure. Fluidizing or stirring the host particles would probably result in a much more continuous and uniform coating than was obtained here. The process of particle coating using a supercritical solution is a promising alternative method for the coating of fine particles, with little or no organic solvents involved. It should be attractive for the pharmaceutical, food, cosmetic and other industries.

CHAPTER 4

NANOPARTICLES COATING/ENCAPSULATION WITH POLYMER USING A SUPERCRITICAL ANTISOLVENT (SAS) PROCESS

In order for the research described in this chapter to stand on its own (as a publishable research paper), some of the pertinent prior work that has already been described in Chapter 2 may be repeated here.

4.1 Introduction

The rapid development of nanotechnology and nanomaterials has led to a need for nanoparticle surface modification for a variety of applications (Ruys and Mai, 1999; Zhang and Gao, 2001; Chang, et al., 1994; Leroux, et al., 1996; Cohen, et al., 2000). The surface can be tailored to specific physical, optical, electronic, chemical, and biomedical properties by coating a thin film of material on the surface of the nanoparticles. Conventional nanoparticle coating methods include dry and wet approaches. Dry methods include: (a) physical vapor deposition (PVD) (Zhang, et al., 2000), (b) plasma treatment (Shi, et al., 2001; Vollath and Szabó, 1999), (c) chemical vapor deposition (CVD) (Takeo, et al., 1998), and (d) pyrolysis of polymeric or non-polymeric organic materials for in-situ precipitation of nanoparticles within a matrix (Sglavo, et al., 1993). Wet methods for coating nanoparticles include: (a) sol-gel processes (Ruys and Mai, 1999; Zhang and Gao, 2001) and (b) emulsification and solvent evaporation techniques (Cohen, et al., 2000; Hrkach, et al., 1997; Wang, et al., 1999).

The coating or encapsulation of nanoparticles has been found to be of particular interest for the controlled release of drugs, genes, and other bioactive agents. Controlled

release systems provide the benefits of protection from rapid degradation, targeting delivery, control of the release rate, and prolonged duration of bioactive agents. Leroux, et al., 1996 studied the surface modification of nanoparticles of poly D,L-lactic acid (D,L-PLA) loaded with drugs to improve site-specific drug delivery. The drug delivery system was prepared using the emulsion method. Results indicated that drug loaded nanoparticles of D, L-PLA, which were coated with poly ethylene glycol (PEG), provided protection from uptake by human monocytes. The findings revealed that surface modified nanoparticles with PEG could temporarily avoid the mononuclear phagocyte system and substantially prolong the circulation time of the nanoparticles.

Cohen, et al., 2000 prepared a sustained gene delivery system of DNA encapsulated in polymeric nanoparticles using a double emulsion approach. In their research the gene delivery system was found to offer increased resistance to nuclease degradation since the polymeric coating provides protection from serum nuclease. The activity of plasmid DNA administration was found to be in the sustained duration mode. The gene delivery system is a potential formulation for the application of gene therapy.

The emulsion techniques used above are associated with the following four steps: (a) preparing the solution of polymer and bioactive agent in an organic solvent, (b) dispersing the solution in another phase under vigorous stirring, (c) stabilizing under certain temperature and pH conditions, and (d) evaporating the organic solvent. However, during the emulsion preparation, the organic solvent and the strong shearing force, temperature, pH, and the interface between the oil and water phases may affect and/or alter the structure of the bioactive agents (Leong, et al., 1998; Jong, et al., 1998; Yang, et al., 1999; Fu, et al., 1999). Moreover, some severe drawbacks such as residual organic

solvent in the final product, VOC (Volatile Organic Compounds) emission, and heavy downstream processing are involved in emulsion processes.

The objective of this research is to develop a new technique for coating or encapsulation of ultrafine particles (sub-micron and nanoparticles) to modify their surface properties by using supercritical CO_2 (SC CO_2) in a SAS process. CO_2 is an ideal processing medium because of its relatively mild critical conditions (T_c=32 °C, P_c=73.8 bars). Furthermore, carbon dioxide is non-toxic, non-flammable, relatively inexpensive and recyclable.

There are a number of studies dealing with particle coating or encapsulation using SC CO_2. Kim, et al., 1996 reported the microencapsulation of naproxen using rapid expansion of supercritical solutions (RESS). The RESS process was also used to coat/encapsulate particles by Mishima, et al., 2000. In the RESS coating process the material to be coated and the coating material (polymer) are both dissolved in SC CO_2 with or without a cosolvent. The solution is then released from a nozzle (de-pressurized), generating microparticles with a polymer coating on the surface. In RESS the rapid de-pressurization of the supercritical solution causes a substantial lowering of the solvent power of CO_2 leading to very high super-saturation of solute, precipitation, nucleation and particle growth. However, the application of the RESS process is severely limited by the fact that polymers, in general, have very limited solubility in SC CO_2 at temperatures below 80 °C (O'Neill, et al., 1998). Also, the operating pressure in RESS is usually above 200 bars so that it is less attractive economically.

Tsutsumi, et al., 1995; 2001 used a combination of the RESS process and a fluidized bed for coating particles. In their research, a solution of coating material in SC

CO_2 rather than in an organic solvent is sprayed into the fluidized bed of particles to be coated. However, particles less than 30-50 μm fall into Geldart's group C particle classification and are very difficult to fluidize. Hence this method cannot be used to coat ultrafine particles

Pessey, et al., 2000; 2001 also demonstrated particle coating using a supercritical fluid process. Their research involved the thermal decomposition of an organic precursor and the deposition of copper onto the surface of core particles in SC CO_2 under conditions of temperature up to 200 ^{o}C and pressure up to 190 bars. However, their methods are less attractive from the point of view of safety and cost and probably cannot be applied to the pharmaceutical industry since high temperature could adversely effect or even destroy most drug powders.

The use of SC CO_2 as an anti-solvent (SAS process), however, can usually be performed at a pressure lower than 100 bars and at a temperature just above the critical temperature (32 ^{o}C). Also the SAS process is quite flexible in terms of solvent choice. Thus the synthesis of ultrafine particles using SAS has been reported in a number of studies (Reverchon, et al., 2000; Dixon, et al., 1993; Falk, et al., 1997; Young, et al., 1999).

Falk, et al., 1997 investigated the production of composite microspheres by the SAS process. In their research a homogeneous solution of various solutes and polymer was sprayed into SC CO_2 antisolvent. Co-precipitation of the solutes and polymer occurred and composite microspheres or microcapsules were formed. Recently, Young, et al., 1999 investigated the encapsulation of lysozyme with a biodegradable polymer by precipitation with a vapor-over-liquid antisolvent, which is a modified precipitation with

a compressed anti-solvent (PCA) process. In their research, the vapor-over-liquid antisolvent coating process was used to encapsulate 1-10 μm lysozyme particles.

The SAS process is based on the principle of SC CO_2 induced phase separation in which the solute precipitates due to a high super-saturation produced by the mutual diffusion of organic solvent into SC CO_2 and *vice versa* when an organic liquid solution comes into contact with SC CO_2. An important feature of the SAS process is that the organic solvent can be almost completely removed by simply flushing with pure CO_2. Thus, dry particles are produced after a CO_2 extraction step (flushing) following feeding of the organic solution (Randolph, et al., 1993).

4.2 Experimental

4.2.1 Materials

To evaluate the efficiency of the SAS coating process, both hydrophobic and hydrophilic silica nanoparticles of different sizes (Table 4.1) from Degussa, USA and Catalysts & Chemicals Ind. Co., Japan were chosen as host particles. Eudragit® RL 100 (Rohm America LLC, USA), a copolymer of acrylate and methacrylate, with an average molecular weight of 150,000, was chosen as the coating material. The chemical structure of Eudragit® RL 100 is shown in Figure 4.1. Bone-dry grade liquid CO_2 was supplied by Matheson Gas, USA. HPLC grade acetone was purchased from Fisher, USA. All of the materials were used as received without further treatment.

Table 4.1 Silica Nanoparticles Used in the Experiments

Suppliers	Catalysts & Chemicals Ind. Co. (Japan)	Degussa (USA)	
Trade Name	COSMO 55	Aerosil® 90	Aerosil® R 972
Particle Size (nm)	600	20	16
Surface Property	Hydrophilic	Hydrophilic	Hydrophobic

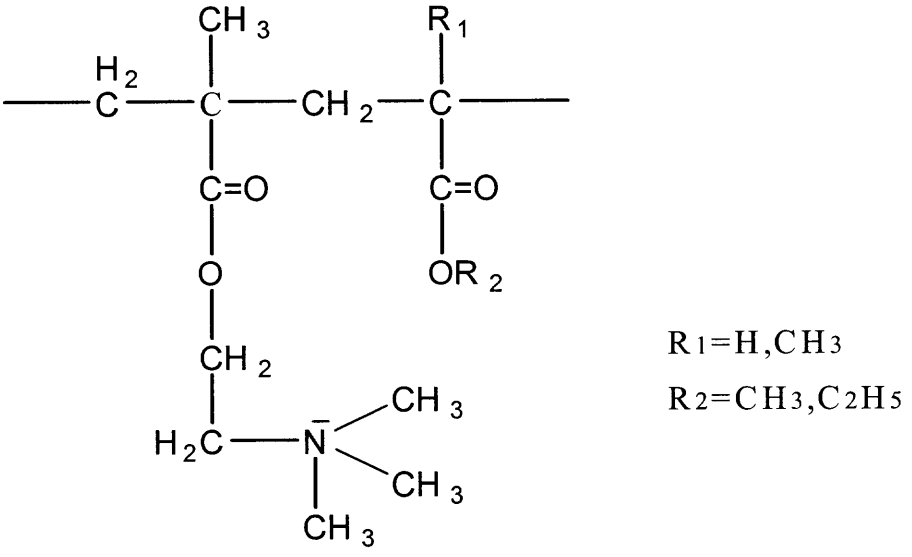

Figure 4.1 Chemical structure of Eudragit®.

4.2.2 Methods

The experimental set-up, schematically shown in Figure 4.2, consists of a CO_2 supply system, solution delivery system, and a high-pressure vessel (Parr Instruments, USA) having a capacity of one liter. The high-pressure vessel is immersed in a water-bath to keep the temperature constant during an experiment. A metering pump (Model EL-1A, AMERICAN LEWA®, USA) was used to deliver liquefied CO_2 from a CO_2 cylinder to

the high-pressure vessel. However, before entering the pump head the liquefied CO_2 was cooled down to around zero degrees Centigrade by using a refrigerator (NESLAB, RTE-111) to minimize cavitation. After leaving the pump head, liquefied CO_2 was pre-heated using a heating tape (Berstead Thermolyne, BIH 171-100).

A polymer solution was prepared by dissolving Eudragit in acetone. Silica nanoparticles were suspended in the polymer solution to produce the desired ratio of surface area than 16-20 nm silica, less polymer is required to coat the 16-20 nm silica

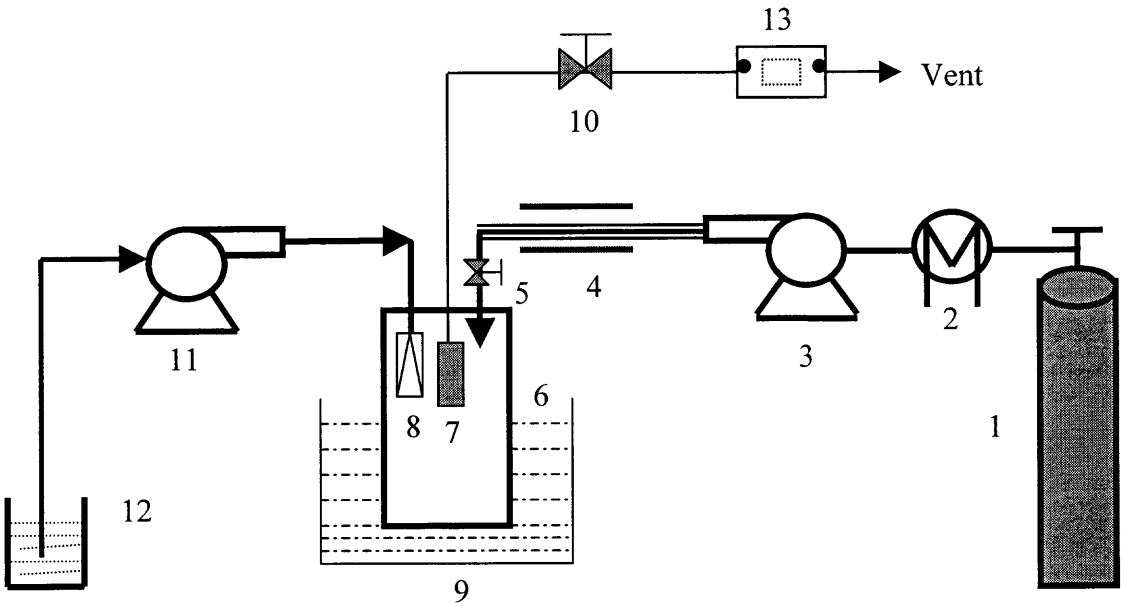

Figure 4.2 Schematic diagram of nanoparticle coating process using SAS.

Key: 1. CO_2 Cylinder, 2. Cooling, 3. CO_2 pump, 4. Pre-heating, 5. On-off valve, 6. High-pressure vessel, 7. Filter, 8. Capillary tube, 9. Water bath, 10. Needle valve, 11 High-pressure pump, 12. Slurry, 13. Mass flow meter.

polymer to silica particles by weight. Since the 600 nm silica particles possess less nanoparticles. Therefore, 14 %-20 % by weight of polymer was used for coating the 600

nm silica as compared with 33 %-50 % for coating the 16-20 nm silica. An ultrasonicator was used to break up the nanoparticle agglomerates in the silica-acetone suspension. During the experiments the temperature and pressure were kept at 32.5 °C and 82.7 bars, respectively. When steady state conditions were reached in the high pressure vessel, i.e., the pressure and temperature of the CO_2 became stable, the suspension was delivered by a high pressure pump (Beckman, 110B) at a rate of 0.7 ml/min and was sprayed through a stainless steel capilliary nozzle (125 μm ID) into the high pressure vessel. The spraying lasted about 20 minutes followed by another 30 minutes for settling. Thereafter, CO_2 was supplied at a rate of less than 3.0 standard l/min to remove any residual organic solvent. The cleaning step continued for about 3 hours (e.g., at a CO_2 flow rate of 1.8 standard l/min) depending on the CO_2 flow rate and the temperature. The higher the flushing velocity and higher the temperature, the less flushing time is required. When the cleaning step was completed, the high pressure vessel was slowly depressurized and samples were collected for characterization. The experimental parameters are given in Table 4.2.

4.2.3 Characterization

In this study it is necessary to use a high-resolution field emission scanning electron microscope (FE-SEM) (Jeol, JSM-6700F) for morphological observations since the primary particles are less than 100 nm. Specimens were sputter coated with palladium (SPI Sputter) for 20 seconds to make the surface conductive without compromising fine surface microstructure. A nonconductive surface would produce a severe surface charge problem under the high intensity electron beam and accumulated surface charge would cause abnormal contrast, image deformation and distortion. A Leo 922 Omega

Transmission Electron Microscope (TEM) was also used to examine the structure of the encapsulated nanoparticles.

Table 4.2 Experimental Parameters in SAS Coating Process

Parameters / Experiments	Polymer Concentration (g/ml)	Ratio of polymer to nanoparticles (g/g)
Coating of 16 nm hydrophobic silica	0.8	1:2
Coating of 20 nm hydrophilic silica	0.8	1:1
Coating of 600 nm Hydrophilic silica	0.4	1:4
		1:5
		1:6

FT-IR spectroscopy measurements were carried out using a Spectrum One FT-IR Spectrometer (PerkinElmer Instruments) with PerkinElmer V3.02 Software Spectrum for control of the instrument, data acquisition and analysis. The spectra were taken in the range of 400-4000 cm^{-1} using a resolution of 8 cm^{-1} and 25 scans. The spectra of the polymer, uncoated and coated silica nanoparticles were measured as pellets. The pellets of uncoated and coated silica nanoparticles were made by mixing them with ground KBr at a ratio of 0.85% (w/w) and were pressed by a press kit (International Crystal Laboratories) and a 12-ton hydraulic Carver Laboratory Press (Fred S. Carver Inc.). KBr has no absorbance in the IR range, and served as a diluent for the solid samples. In preparing the polymer specimen, Eudragit pellets were ground into powder using a

mortar and pestle. The ground Eudragit was then mixed with ground KBr at a ratio of 0.5% (w/w). Afterward, the mixture was made into a pellet for characterization.

4.3 Results and Discussion

4.3.1 Fundamentals of the SAS Process

In the SAS process, SC CO_2 acts as an anti-solvent, which is dissolved in the organic solvent, reducing the solvent strength significantly (Chang and Randolph, 1990) leading to a high degree of super-saturation and nucleation of the solute. While the actual SAS process is complicated due to the interplay of thermodynamics, mass transfer, and

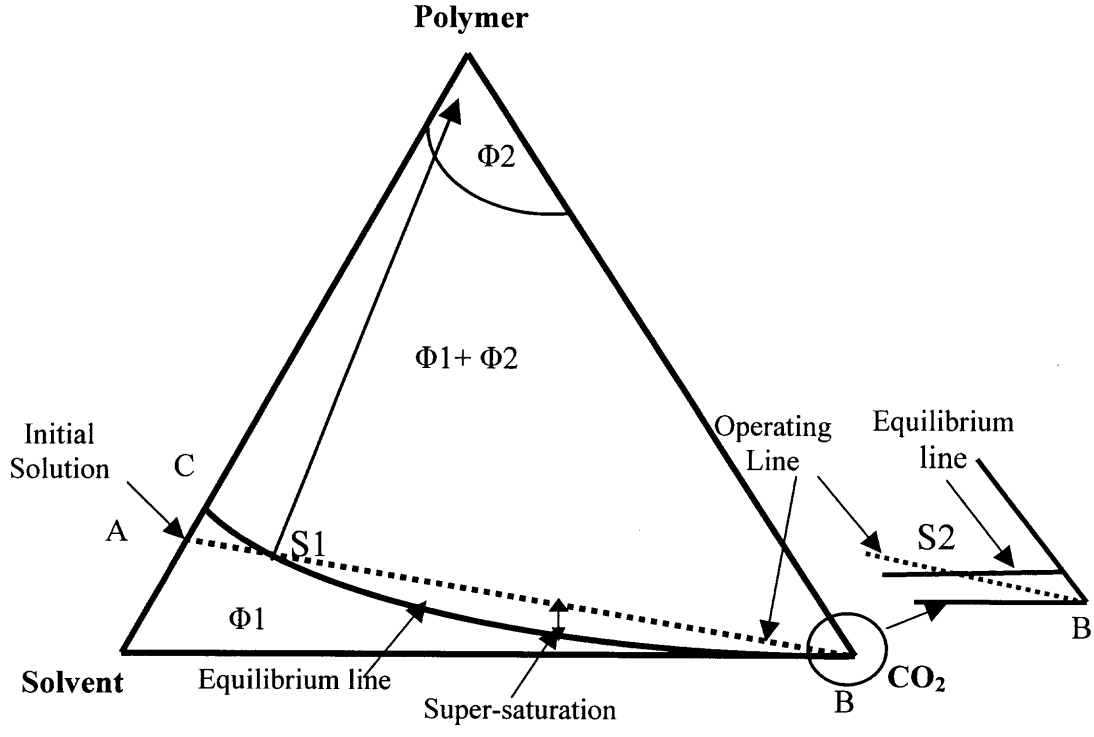

Figure 4.3 Example of ternary phase diagram for Solvent-Polymer-CO_2 at constant P and T.

hydrodynamic effects (Dixon, et al., 1993), a schematic phase diagram of SC CO_2, solvent and solute at constant temperature and pressure is useful to understand the SAS process and is shown in Figure 4.3. In this example, SC CO_2 is completely miscible with the solvent, while the polymer and SC CO_2 are partially miscible. The solubility of polymer in SC CO_2 is very limited. Generally, almost all polymers have very low solubility even at 50 °C and 300 bars (Dixon, et al., 1993). In this diagram, the one-phase region Φ1 represents the polymer dissolved in solvent, forming a polymer solution with some CO_2 dissolved in the solution. Region Φ2 is glassy region, a polymer-rich phase, with a small amount of CO_2 and solvent absorbed in the polymer. In the two-phase region, solvent-rich phase Φ1 and polymer-rich phase Φ2 coexist and are in equilibrium.

The bold line (from C to B, Figure 4.3) represents the polymer solubility in the mixture of solvent and SC CO_2. The dotted straight line is an operating line that represents the addition of polymer solution into SC CO_2 (from A to B). During the addition of polymer solution into SC CO_2, an initial very small amount of solute will be dissolved in SC CO_2 with the solvent acting as co-solvent (Φ1 region) until the saturation of polymer in the mixture of SC CO_2 and the solvent is reached (S1, saturation point). Continued feeding of the solution into SC CO_2 results in crossing over the equilibrium boundary and super-saturation of the polymer in the mixture of SC CO_2 and solvent. Subsequently, a phase transition will take place, depending on the starting conditions. The phase transition will occur initially either by nucleation, an activated process in which a free energy barrier must be surmounted, or by spinodal decomposition, a spontaneous process in which no free energy barrier must be overcome (Kiran, et al., 2000). In either case nucleation and precipitation of polymer induced by the phase

transition will take place on the surface of the nanoparticles, forming a thin layer of polymer coating.

In the present work of nanoparticle coating or encapsulation with polymer using the SAS coating process, the polymer solution with suspended nanoparticles is sprayed through a nozzle. If the solvent and the SC CO_2 are completely miscible and the operating conditions are above the critical point of the mixture, distinct droplets will never form as reported by Lengsford, et al., 2000 and Bristow, et al., 2001 and the polymer will nucleate and grow within the expanding gas plume. However, the present experiments were operated at a temperature of 32.5 ^{o}C and a pressure of 82.7 bars, which is in the partially miscible region since the mixture's critical point is 35.0 ^{o}C and 73.2 bars. Furthermore, Luo, et al., 2002 has recently submitted for publication a new experimental paper which shows that a transient jet and jet-induced droplets exist even when the pressure is slightly above the mixture critical pressure. It was observed that only when the pressure is somewhat above the mixture critical pressure does the flow behave like a single-phase gaseous jet without any definable interfacial boundaries or the formation of droplets. Therefore, it can be assumed that in this study, droplets of polymer solution with entrapped nanoparticles were generated due to jet break-up.

When a droplet contacts the SC CO_2, since acetone is highly miscible with SC CO_2, a very fast mutual diffusion into and out of the droplet occurs. The polymer solution in the droplet approachs saturation very rapidly due to the extraction of solvent from the droplet. The subsequent crossing over the equilibrium boundary initiates the gelation of the polymer. Meanwhile, the SC CO_2 continuously diffuses into the droplet and is

dissolved in the acetone solution. This process leads to swelling of the droplet (Randolph, et al., 1993).

When the solvent expansion is high, Reverchon, 1999 proposed that an empty shell or balloon structure is formed due to the interplay of mass transfer and the phase transition. This empty shell structure was clearly observed in experiments using the SC CO_2 SAS process for particle formation (see figure 6, Reverchon, 1999). The stability of the balloon structure depends mainly on the expansion of the solvent by SC CO_2, which depends on the miscibility of the solvent and SC CO_2. In this study acetone, which is highly miscible with SC CO_2, was used as the solvent for the polymer. Thus it is highly probable that a balloon structure was formed which then burst into very fine viscous droplets containing nanoparticles and polymer as shown in the cartoon in Figure 4.4.

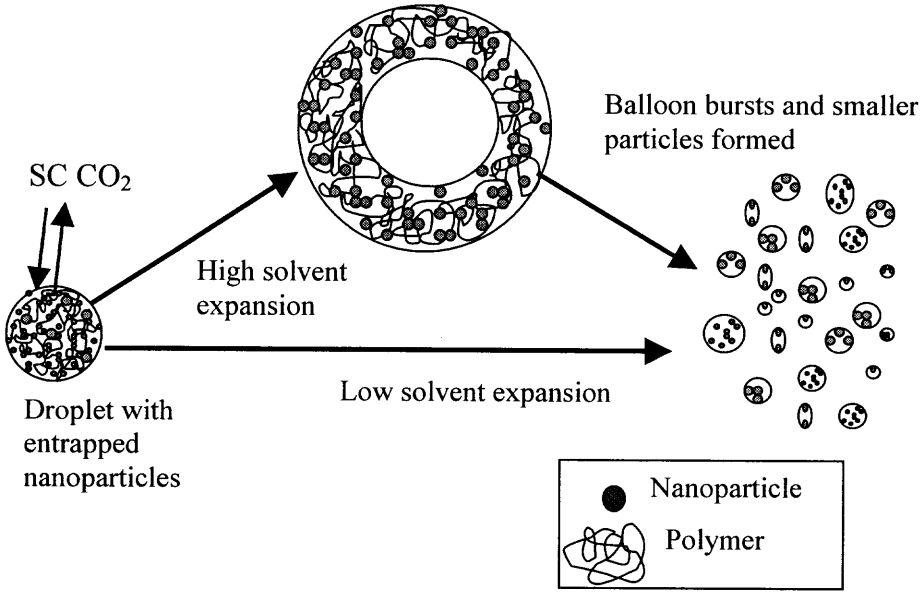

Figure 4.4 Mechanism of fine particle encapsulation using SAS process.

Further extraction of the solvent by SC CO_2 from the gelled droplets containing nanoparticles induced the glass transition of the polymer. Therefore, the nanoparticles were encapsulated within a polymer film attributed to the nucleation and precipitation of polymer on the surface of the nanoparticles. However, the encapsulated nanoparticles within the polymer film were aggregated and agglomeration took place. Thus, a nanocomposite with a matrix structure was formed with the nanoparticles as the host particles and the polymer as a coating.

4.3.2 Coating of Hydrophobic Silica Nanoparticles

Hydrophobic silica nanoparticles R972 (See Table 4.1) were chosen to evaluate the coating of nanoparticles with a hydrophobic surface. Figure 4.5 shows the morphology and size of the hydrophobic silica nanoparticles at two different magnifications. As can be observed, the hydrophobic silica nanoparticles exhibit the typical chained structure. From the scale bar of the higher magnification micrograph the primary particle size is estimated to be about 16-30 nm.

Figure 4.6 shows the SEM micrographs of the hydrophobic silica nanoparticles coated with Eudragit at two different magnifications. When compared with Figure 4.5, the morphology of the coated nanoparticles is quite different from that of uncoated nanoparticles. Furthermore, the primary particle size of coated hydrophobic silica nanoparticles is found to be increased to 50-100 nm. The morphological change and size enlargement is attributed to polymer nucleation and subsequent growth on the surface of the nanoparticles during the SAS coating process, forming a thin film encapsulation. The thickness of the polymer film is estimated to be around 10-40 nm.

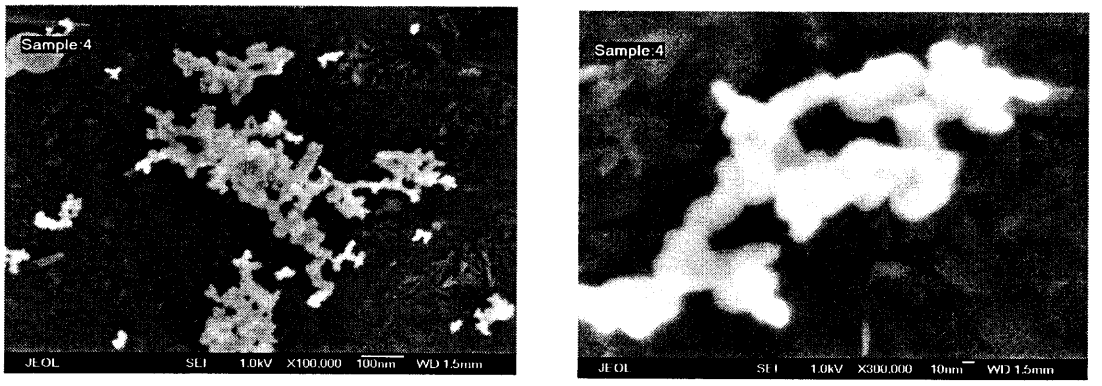

(a) (b)

Figure 4.5 SEM micrographs of uncoated hydrophobic silica nanoparticles. (a) x 100,000; (b) x 300,000.

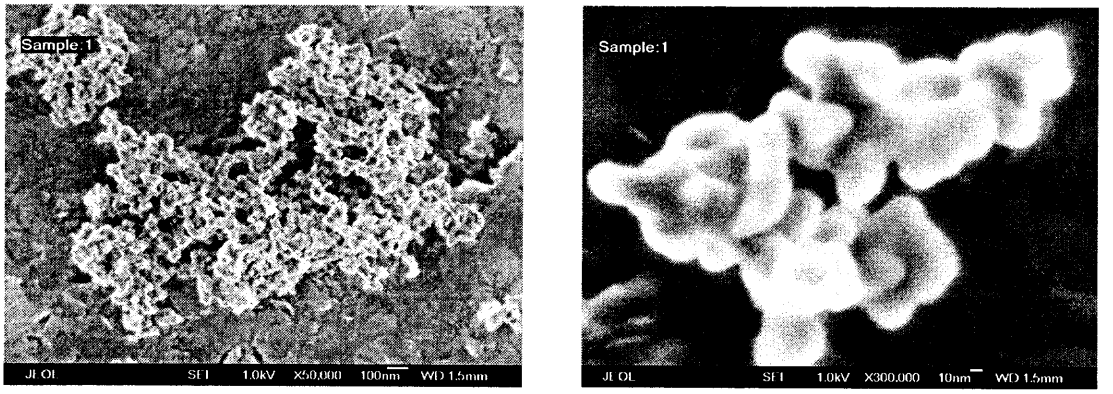

(a) (b)

Figure 4.6 SEM micrographs of hydrophobic silica nanoparticles coated with Eudragit. (a) x 50,000; (b) x 300,000.

TEM-EELS, which is a powerful tool in multi-component material characterization, was used to characterize the encapsulation of the nanoparticles. In TEM-EELS specimen preparation, a wet method was employed to achieve a good dispersion. The encapsulated samples were dispersed in very dilute alcohol, and then

were spread over an extremely thin carbon film (3 nm) supported by a copper grid. Zero-loss micrographs of uncoated and coated silica nanoparticles are shown in Figures 4.7 (a) and 4.8 (a), respectively. Compared with Figure 4.7 (a), the coated primary particle size (Figure 4.8 (a)) is estimated to be about 50 nm from the scale bar. The silicon mapping (Figure 4.8 (b)) exhibits the same shape and morphology of the silica nanoparticle agglomerate as the TEM Zero-Loss micrograph (Figure 4.8 (a)). As one of the major component of the polymer, carbon shows up in a carbon mapping micrograph (Figure 4.8 (c)). The carbon signal is generally weaker than the silicon signal because the amount of carbon is much less than that of silicon. Furthermore, carbon is number six in the periodical table, while silicon is number fourteen, and the higher the atomic number, the stronger the signal response to electrons.

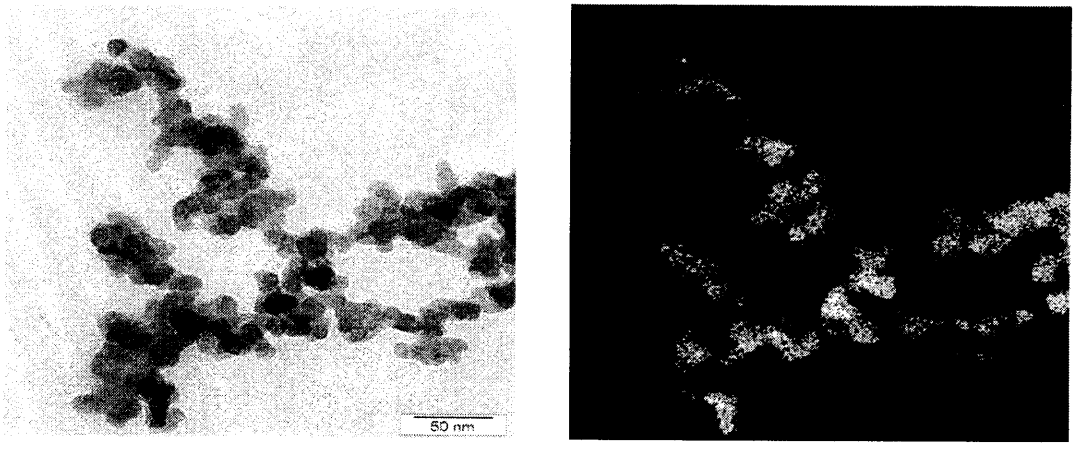

(a) (b)

Figure 4.7 TEM-EELS micrographs of uncoated hydrophobic silica nanoparticles. (a) Zero loss; (b) Silicon mapping.

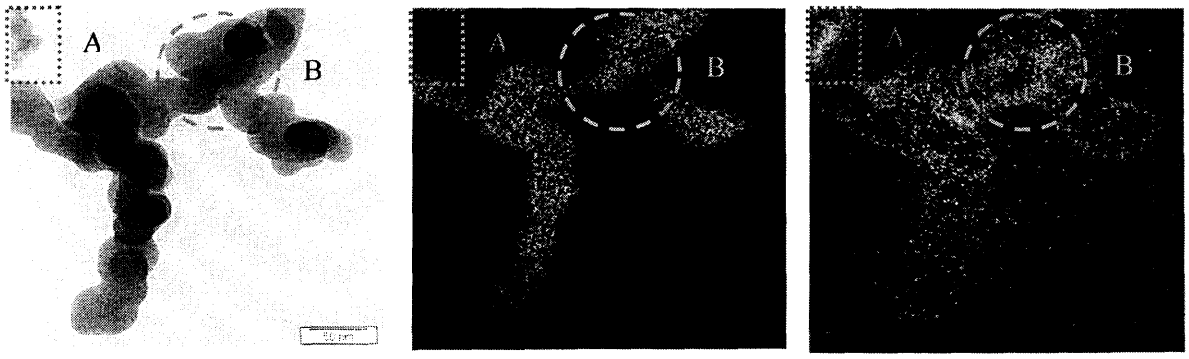

(a) (b) (c)

Figure 4.8 TEM-EELS micrographs of coated hydrophobic silica nanoparticles. (a) Zero loss; (b) Silicon mapping; (c) Carbon mapping.

From the carbon mapping, it is clear that the silica nanoparticles are coated with a thin layer of polymer. Interestingly, the coating layer looks like a shell encapsulating the nanoparticle agglomerate. However, from the carbon mapping, it also appears that the polymer is not uniformly distributed on the surface of the silica nanoparticles. In general, the stronger the carbon signal, the more the polymer has precipitated on the surface of the silica nanoparticles. In region B, it appears that more polymer coating occurs. Another feature in the carbon mapping micrograph is seen at the upper-left corner where an amorphous region appears (A in Figure 4.8 (a)). The corresponding carbon signal is strong (Figure 4.8 (c)), whereas there is practically no silicon signal in that region (Figure 4.8 (b)). Therefore, it can be concluded that the amorphous region is heavily coated with polymer.

FT-IR spectrometry is a valuable characterization tool to determine the chemical composition before and after the coating process. Three sets of FT-IR spectra of silica nanoparticles coated with polymer, uncoated silica nanoparticles, and of the Eudragit

powder are shown in Figure 4.9. The spectrum of Eudragit, which is a copolymer of acrylate and methacrylate, is shown in Figure 4.9 (c). The peaks at 2992.61 cm^{-1} and 2954.18 cm^{-1} are the absorbances of the alkyl groups ($-CH_3$ and $-CH_2$) stretching vibrations. The corresponding absorbances of bending vibrations occur at 1480.47, 1448.6, and 1388.0 cm^{-1}. A major peak at 1732.27 cm^{-1} is attributed to the stretching vibration from the carbonyl group. The band between 1300 cm^{-1} and 1000 cm^{-1} is assigned to the polymer's C-O double bond stretching mode. The peaks before 1000 cm^{-1} is the fingerprint region of the polymer. The spectrum of silica nanoparticles in Figure 4.9 (b) shows a major peak at 1104.38 cm^{-1}, this is assigned to the Si-O stretching vibration.

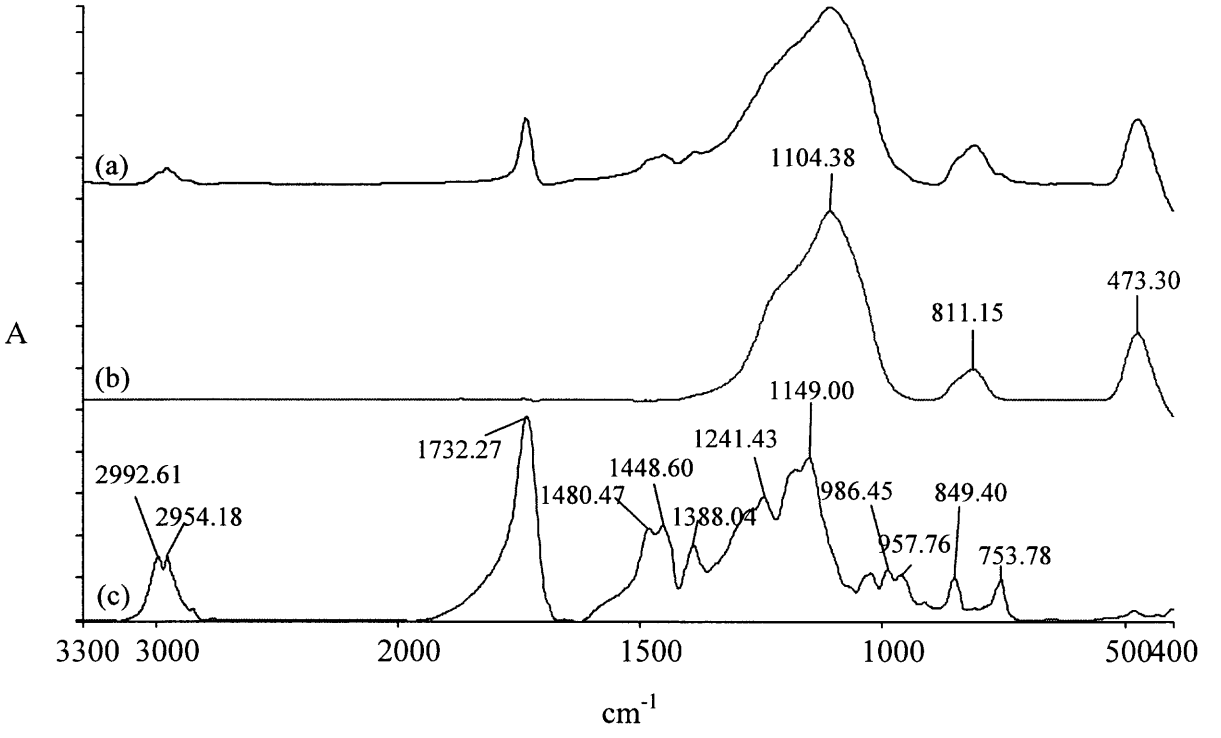

Figure 4.9 FT-IR spectra for hydrophobic silica nanoparticles. (a) Coated nanoparticles; (b) Uncoated nanoparticles (R972); (c) Eudragit.

When compared with Figure 4.9 (c), it can be observed in the spectrum of coated silica nanoparticles in Figure 4.9 (a) that the peaks at 2992.61 cm^{-1} and 2954.18 cm^{-1} associated with alkyl groups' stretching modes and peaks at 1480.47, 1448.6, and 1388.0 cm^{-1} associated with their bending vibrations show up. At exactly the same position as in the spectrum of polymer, the absorbance at 1732.27 cm^{-1} assigned to carbonyl group stretching vibration can be found in Figure 4.9 (a). However, the Si-O stretching vibration and the C-O double bond stretching vibration have almost the same absorbance region from 1300 cm^{-1} to 1000 cm^{-1}. The absorbance of the Si-O stretching mode is much stronger than that of the C-O, hiding the peaks attributed to C-O. Therefore, C-O double bond peaks do not show up in the spectrum of coated silica nanoparticles. From the FT-IR chemical analysis above, a conclusion can be reached that the surface of silica nanoparticles is coated with polymer. This strongly supports the TEM-EELS observations.

However, it is observed that no new peak shows up in the spectrum of silica nanoparticles coated with Eudragit, indicating that there is no chemical bond between the polymer and the surface of the silica nanoparticles during the process of nanoparticle coating with polymer using the SAS coating process. The SAS coating process is a process of polymer nucleation and subsequent growth on the surface of a particle, typically a physical process. Thus, it is desirable for pharmaceutical applications since any chemical interaction between the coating and the substrate may result in a change in the properties of the pharmaceutical component, which could change the effectiveness of the drug.

4.3.3 Coating of Hydrophilic Silica Nanoparticles

Hydrophilic silica nanoparticles (See Table 4.1) were also studied to determine the effect of the hydrophilic surface (if any) on coating with polymer. The uncoated and coated samples were examined using the FE-SEM. Figure 4.10 shows micrographs of hydrophilic silica nanoparticles before and after coating. It is clear that a morphological change occurred indicating that the hydrophilic silica nanoparticles were coated with polymer.

The coated hydrophilic silica nanoparticles were also characterized using TEM. The TEM micrographs of hydrophilic silica nanoparticles before and after SAS coating can be seen in Figure 4.11 (a) and (b), respectively. The most important feature of Figure 4.11 (b) is that an amorphous region shows up in the right-upper corner of Figure 4.11 (b), indicating the polymer phase formed with a matrix structure of embedded silica nanoparticles.

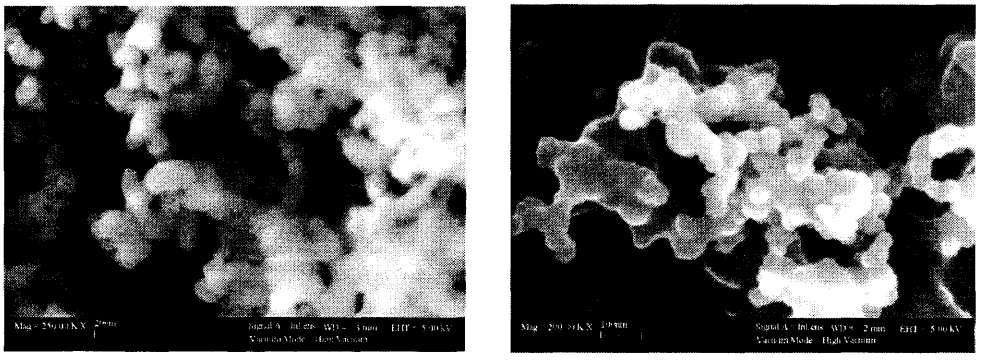

(a) (b)

Figure 4.10 SEM micrographs of hydrophilic silica nanoparticles. (a) Uncoated x 250,000; (b) Coated x 200,000.

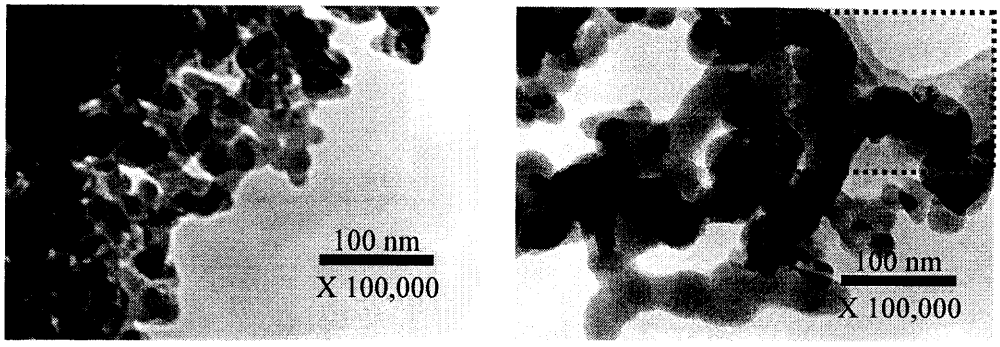

(a) (b)

Figure 4.11 TEM micrographs of hydrophilic silica nanoparticles. (a) Uncoated x 100,000; (b) Coated x 100,000.

The TEM-EELS technique was used to distinguish between the thin layer of polymer coating and the hydrophilic silica nanoparticles. Although the wet method used for the coated hydrophobic nanoparticles produced a good dispersion of agglomerated nanoparticles as shown in Figure 4.8, a dry method was used for the analysis of the encapsulated hydrophilic silica nanoparticles. In the dry method, a copper grid held by tweezers was ploughed through the coated silica nanoparticles. The very fine agglomerates of nanoparticles become attached to the copper grid due to Van der Waals and electrostatic forces. This sampling method was used to better preserve the integrity of the coated silica nanoparticles.

The Zero-loss micrograph of the agglomerate of coated hydrophilic silica nanoparticles is shown in Figure 4.12 (a) and the micrographs of silicon and carbon mapping can be found in Figure 4.12 (b) and Figure 4.12 (c), respectively. When comparing the regions A and B in Figure 4.12 (b) and Figure 4.12 (c), it can be seen that

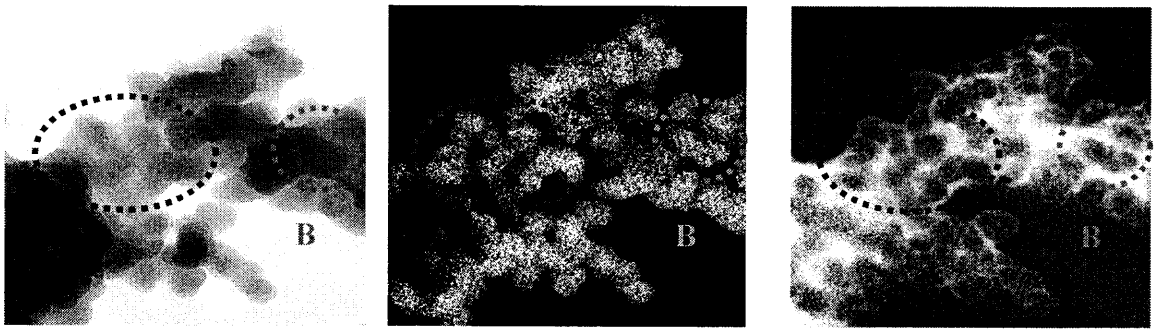

(a) (b) (c)

Figure 4.12 TEM-EELS micrographs of coated hydrophilic nanoparticles. (a) Zero-Loss; (b) Silicon mapping; (c) Carbon mapping.

the carbon signal in the carbon mapping micrograph exactly outlines the configuration of the silica nanoparticles shown in the silicon mapping micrograph. From the carbon mapping micrograph, it appears that the hydrophilic silica nanoparticles were also completely encapsulated in a polymer matrix structure.

The hydrophilic silica nanoparticles were also tested using FT-IR, to identify any chemical changes after being coated with the polymer. Figure 4.13 shows the spectra of uncoated silica nanoparticles, coated silica particles, and pure polymer powder, repectively. The results are practically the same as those found for the hydrophobic silica particles, again supporting the observations in the SEM and TEM micrographs (Figures 4.11 and 4.12) that the surface of the hydrophilic silica nanoparticles is coated with polymer in a matrix structure.

The Degussa hydrophobic silica (Aerosil® R972) was manufactured by modifying the surface with dimethyldichlorsilane so that it exhibits a hydrophobic (water-repelling) property. It was a surprise to find that the FT-IR spectra of the uncoated hydrophobic silica (Figure 4.9 (b)) appeared to be exactly the same as that of the uncoated hydrophilic

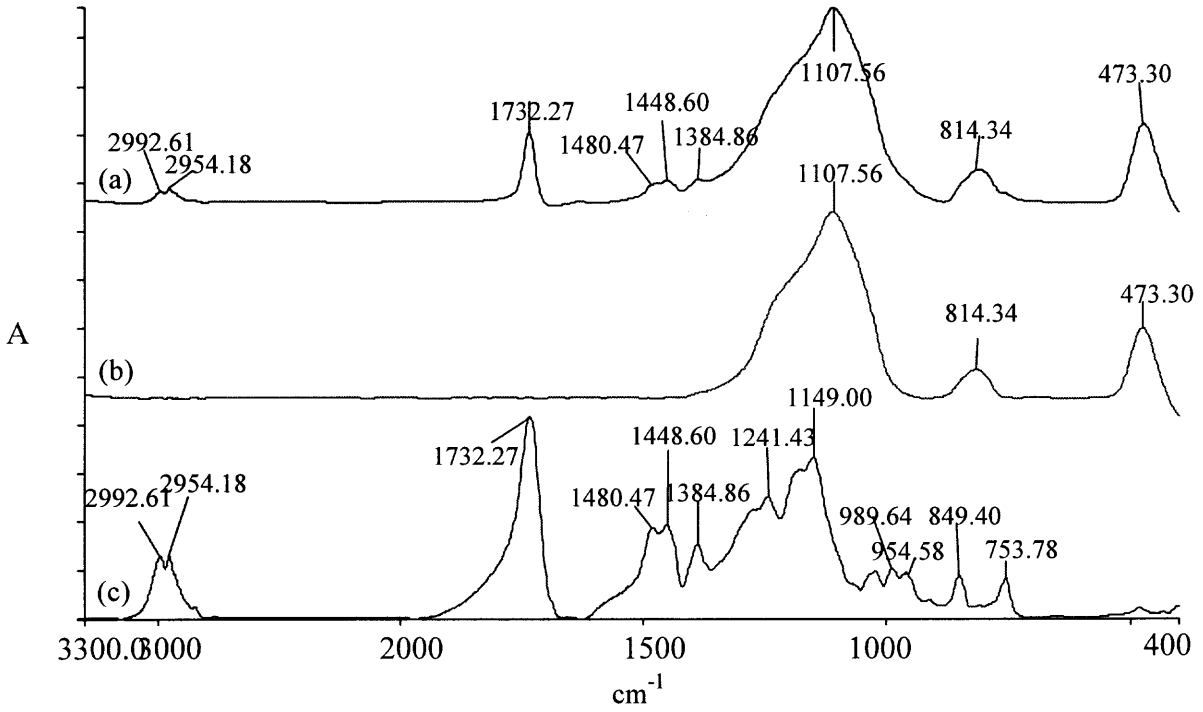

Figure 4.13 FT-IR spectra for hydrophilic silica nanoparticles. (a) Coated nanoparticles; (b) Uncoated nanoparticles; (c) Eudragit.

silica (Figure 4.13 (b)). The peaks from the methyl groups and from the C-Si bond were not observed in the Figure 4.9 (b). This is attributed to the very low concentration of methyl groups on the hydrophobic silica, which is below the detection limit of the Spectrum One FT-IR (0.1 % weight percent). As observed in Figure 4.9 (a) and Figure 4.13 (a), the spectra of the coated hydrophobic and hydrophilic silica also appear to be the same. This result indicates that the SAS coating process is a purely physical deposition of precipitated polymer on the surface of particles and is therefore independent of the hydrophilicity or hydrophobicity of the surface of the silica nanoparticles

However, the surface coverage of polymer on the hydrophobic silica particles appears to be somewhat less than that of the hydrophilic silica particles when comparing Figure 4.8 (c) to Figure 4.12 (c). This is due to the fact that a somewhat larger polymer to silica ratio was used in the hydrophilic coating experiments (see Table 4.2)

4.3.4 Coating of 600 nm Silica Nanoparticles

To further evaluate the SAS coating process, experiments to encapsulate 600 nm silica hydrophilic nanoparticles were conducted. The SEM microphotograph in Figure 4.14 (a) shows the uncoated monodisperse spherical silica particles with a size of about 600 nm from the scale bar. After the SAS coating process, it is observed that silica particles were coated with a polymer film on their surface (Figure 4.14 (b), (c), (d)) for all three weight ratios of polymer to silica investigated. When a ratio of polymer to nanoparticles (1:4 weight) is used, a composite particle (agglomerate), containing many primary particles, of about 4 μm was formed (Figure 4.14 (b)). The formation of these large agglomerates could be due to the plasticization of the polymer by CO_2 (O'Neill, et al., 1998) under high-pressure conditions since the glass transition temperature of the polymer is depressed by SC CO_2 (Condo, et al., 1994). The agglomerates are also formed when using a lower ratio of polymer to nanoparticles by weight (Figure 4.14 (c) and figure 4.14 (d)). However, it appears that less agglomeration occurs when less polymer is used.

To estimate the thickness of the coating layer on the surface of the 600 nm particles the Eugragit coated nanoparticles (1:4 weight) were heated in a Perkin Elmer thermo gravimetric analyzer (TGA) to 800 ^{o}C to burn off the polymer coating. If it is assumed that the coating forms a spherical layer of constant thickness, h, then

$$h = R(1 + \rho_H m_c / \rho_c m_H)^{1/3} - R \qquad (1)$$

where R is the radius of the uncoated nanoparticle, ρ_H and ρ_C are the densities of the host nanoparticles and polymer coating, respectively and m_H and m_C are the weight of the host and polymer, respectively. From Figure 4.15 and Equation (1), h is estimated to be 75 nanometers.

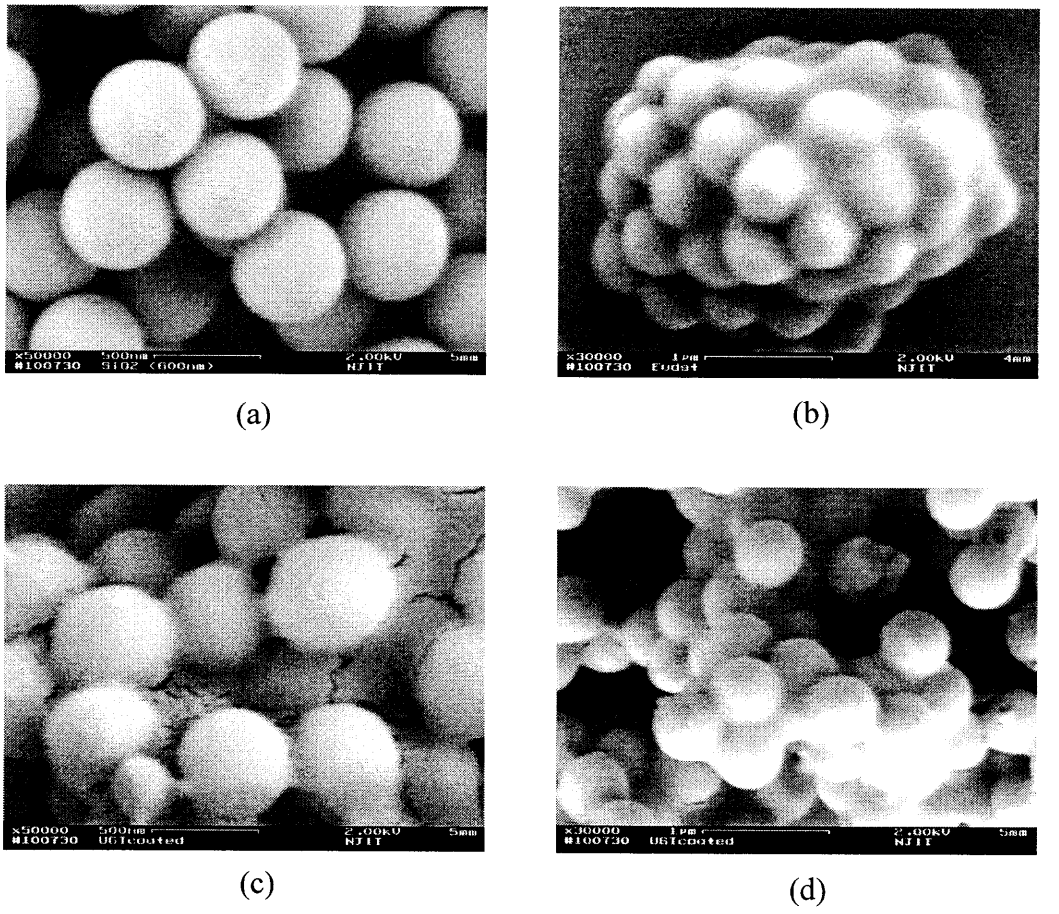

Figure 4.14 SEM microphotographs. (a) Uncoated 600 nm particles; (b) Coated (polymer to silica, 1:4, w/w) particles; (c) Coated (1:5) particles; (d) Coated (1:6) particles.

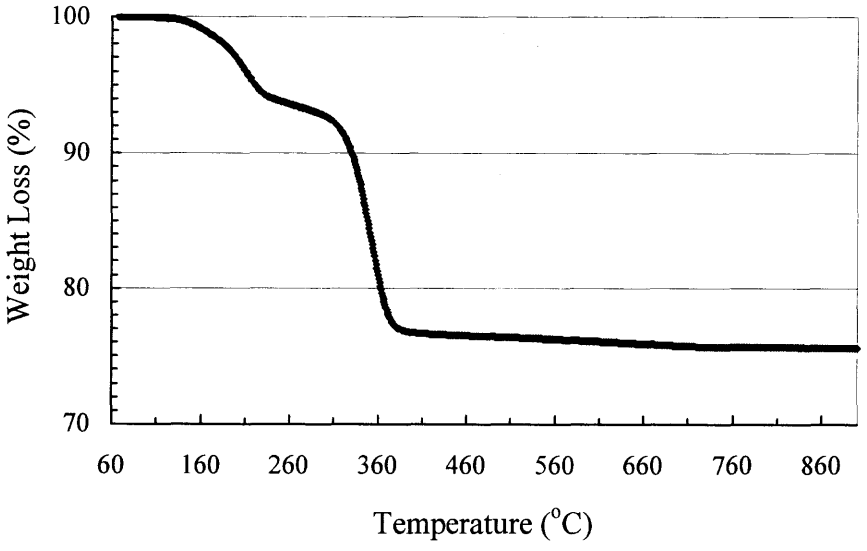

Figure 4.15 TGA experiment to estimate the thickness of the coating layer on the surface of 600 nm silica particles coated with Eugragit (1:4 weight ratio).

4.4 Concluding Remarks

Nanoparticle coating or encapsulation with polymer using the SC CO_2 SAS coating process was investigated in this research. The results revealed that 16-20 nm nanoparticles were successfully coated or encapsulated in polymer by the SAS coating process. The coating or encapsulation of nanoparticles using SC CO_2 SAS coating process appears to be independent of surface hydrophilicity. The mechanism of the SC CO_2 SAS coating process appears to be a heterogeneous polymer nucleation with nanoparticles serving as nuclei with a subsequent growth of polymer on the surface of the nanoparticles induced by mass transfer and phase transition. A polymer matrix structure of encapsulated nanoparticles was formed by agglomeration of the coated nanoparticles. For larger 600nm particles the thickness of the polymer coating can be controlled by adjusting the ratio of polymer to host particles.

TEM-EELS was found to be the best approach for the characterization of the coated nanoparticles since different elements can be detected at the nanoscale. FT-IR analysis is another valuable qualitative analysis method for material characterization.

The SAS coating process is a promising environmentally friendly technique for nanoparticle coating/encapsulation with polymer with applications to pharmaceuticals and other products where chemical interactions must be avoided.

CHAPTER 5

ENCAPSULATION OF FINE PARTICLES WITHIN POLYMER BY A SUPERCRITICAL ANTISOLVENT (SAS) PROCESS

In order for the research described in this chapter to stand on its own (as a publishable research paper), some of the pertinent literature review that has already been described in Chapter 2 is repeated in the following introduction.

5.1 Introduction

Coating or encapsulation of fine particles to produce tailored surface properties is of great interest in the pharmaceutical, cosmetic, food and agrochemical industries. The particle surface can be engineered to specific physical, chemical, and biochemical properties by spreading a thin film of material on the surface of the particles. Consequently, the flowability, dissolution rate, dispersability, chemical reactivity, bio-efficacy, and hydrophilicity of particles can be modified for a variety of applications (Davis, et al., 1998; Wang, et al., 1999; Soppimath, et al., 2001).

As discussed in Chapter 1, the conventional techniques for the encapsulation of fine particles, such as emulsion evaporation, phase separation, spray-drying, freeze-drying, etc., require large amount of organic solvents, surfactants, and other additives, leading to volatile organic compound (VOC) emissions and other waste streams. Other drawbacks include low encapsulation efficiency and further processing of the products such as down-stream drying, milling and sieving, which are usually necessary. In addition, residual toxic solvent in the end products, temperature and pH requirements,

and strong shear forces are big challenges for maintaining the fragile protein structure in the encapsulation of pharmaceutical ingredients.

During the past decade, supercritical fluid processes such as RESS, SAS and GAS have attracted increasing attention for particle engineering, including fine particle formation, coating and encapsulation. Supercritical carbon dioxide (SC CO_2), in particular, is an ideal processing medium for particle encapsulation for its relatively mild critical conditions (T_c=31.1 ^{o}C, P_c=73.8 bars). Furthermore, SC CO_2 is non-toxic, non-flammable, relatively inexpensive, readily available, and chemically stable.

A number of supercritical processes for the encapsulation of particles with polymer or composite particle formation for the controlled release of drugs have been reported. Tom, et al., 1994 studied the co-precipitation of poly (L-lactide) (PLA)-pyrene composite particles by a RESS. In their research, PLA and pyrene were extracted by SC CO_2 in two separate extraction columns. The two supercritical solutions were subsequently co-introduced through a nozzle into a precipitation vessel. A sudden depressurization results in the loss of solvent strength of the SC CO_2, leading to a high degree of supersaturation of the solute and the formation of composite particles of pyrene distributed in a polymer matrix of PLA. Similar research involving the microencapsulation of naproxen with polymer using RESS was done by Kim, et al., 1996. Mishima, et al., 2000 reported the microencapsulation of proteins with poly ethylene glycol (PEG) by RESS. Ethanol (about 38.5 wt. %) was used as a co-solvent to enhance the solubility of PEG in SC CO_2. The results indicated that core particles of lipase and lysozyme were completely encapsulated by PEG without agglomeration.

Recently, Wang et al., 2002 used a modified RESS process of extraction and precipitation to coat particles with polymer. The coating polymer and particles to be coated (host particles) were placed in two different high-pressure vessels, respectively. The coating polymer was first extracted by SC CO_2. The resulting supercritical polymer solution was then introduced into the host particle vessel. By adjusting the temperature and pressure, the polymer solubility in SC CO_2 was lowered and nucleation and precipitation of polymer took place on the surface of the host particles and a fairly uniform polymer coating was formed. However, the potential application of RESS for particle coating or encapsulation is limited because the solubility of polymers in SC CO_2 is generally very poor (O'Neill, et al., 1998).

Pessey, et al., 2000; 2001 demonstrated the deposition of copper on nickel particles and of copper on permanent magnetic $SmCo_5$ particles by the thermal decomposition of an organic precursor of bis(hexafluoroacetylacetonate) copper(II) in a supercritical fluid. They produced a core-shell structure of copper on the surface of core (host) particles in SC CO_2 under conditions of temperature up to 200 ^{o}C and pressure up to 190 bars. Clearly this encapsulation method is not attractive to the pharmaceutical industry interested in coating drug powders because the high temperature required will be harmful for most drug powders.

In comparison to RESS, the supercritical antisolvent (SAS) process offers much more flexibility in terms of choosing suitable solvents. Furthermore, SAS has advantages over RESS since SAS is usually operated under mild conditions compared with RESS, which is associated with relatively high temperature and high pressure (Chang and

Randolph, 1989; Matson, et al., 1987; Tom and Debenedetti, 1991). Therefore RESS is also less attractive from the point of view of safety and cost.

In SAS, SC CO_2 is used as an antisolvent (instead of a solvent as in RESS) to extract an organic solvent from a solution containing the solute, which is desired as the coating or encapsulation material. The solution is in the form of tiny droplets, produced by a nozzle through which the solution is sprayed into a high-pressure vessel. When the droplets contact the SC CO_2, very rapid diffusion between the droplets and the SC CO_2 take place, inducing phase separation and precipitation of the solute. SAS offers the capability of producing free flowing particles in a single step at moderate pressure and temperature.

Young, et al., 1999 studied the encapsulation of lysozyme with a biodegradable polymer by precipitation with a vapor-over-liquid antisolvent (below supercritical conditions), which is a modified SAS process. Encapsulation of 1-10 micron lysozyme particles was achieved in PLGA microspheres without agglomeration. More recently, our research group applied the SAS process for the encapsulation of nanoparticles with Eudragit (Wang, et al., 2003). A suspension of silica nanoparticles in a polymer solution was sprayed into SC CO_2 through a capillary tube. The subsequent mutual diffusion between SC CO_2 and polymer solution droplets resulted in high degree of supersaturation, causing a heterogeneous polymer nucleation induced by the phase transition, with the silica nanoparticles acting as nuclei. Thus the nanoparticles were individually encapsulated in polymer with very little agglomeration.

In the previous work, the amount of polymer used was found to affect both the coating thickness and the degree of agglomeration. The objective of this study is to

thoroughly investigate the effects of various process parameters, such as the polymer weight fraction, polymer concentration, temperature, pressure, and flow rate, on the coating of particles and the agglomeration of the coated particles in the SAS coating process. Some CO_2-soluble surfactants will also be applied to determine whether they help minimize agglomeration. A mechanism for the SAS coating process based on the experimental results was proposed.

5.2 Experimental

5.2.1 Materials

The host particles that were used in our SAS coating study were spherical silica particles (approximately 0.5 μm) which were synthesized in our laboratory using the classic Stöber process (Stöber, et al., 1968). Tetraethyl orthosilicate (TEOS) (MW 208, 98 %) was purchased from Sigma-Aldrich Co., USA. Ammonia hydroxide (28.87 %) was purchased from Fisher Scientific, USA and anhydrous ethyl alcohol from Aaper Alcohol, USA. The chemicals were used without further treatment.

The coating material was poly lactide-co-glycolide (PLGA) (Resomer® 502, MW 12,000, 50/50, T_g 40-55 °C). It was supplied from Boehringer Ingelheim Chemicals, Inc., USA. Acetone was purchased from Aldrich (Milwaukee, WI) and used as received. Liquid CO_2 was obtained from the Matheson Company, USA. Surfactants of random poly (fluoroalkylacrylate-co-styrene) (PFS) (29 mol% styrene) and poly(fluoroalkylacrylate) homopolymer (PFA) were synthesized in Professor Robert Enick's laboratory at the University of Pittsburgh. The surfactant Krytox 157 FSL, a perfluoropolyether terminated with a carboxylic acid at one end, was supplied by DuPont Chemicals (Deepwater, NJ).

These surfactants were used as received without further treatment. The chemical structures of the coating polymer and the surfactants are given in Figure 5.1. The polymer and polymeric surfactant were listed in Table 5.1.

Poly lactide-co-glycolide (PLGA)

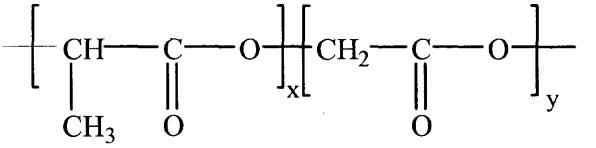

Poly fluoroacrylate-styrene (PFS)

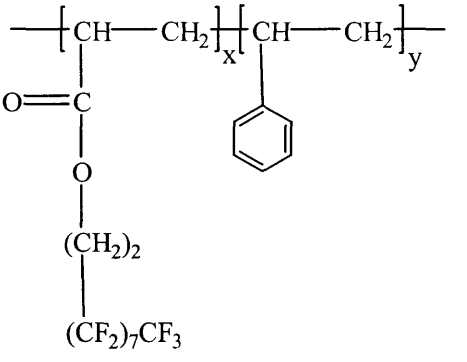

Poly fluoroacrylate (PFA)

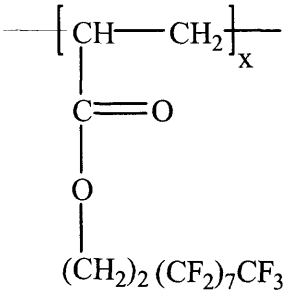

Perfluoropolyether (PFPE)

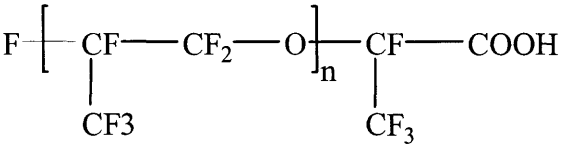

Figure 5.1 Repeat unit structure of poly lactide-co-glycolide (PLGA), poly Fluoroacrylate-styrene (PFS), poly fluoroacrylate (PFA), and perfluoropolyether (PFPE) used in this study.

Table 5.1 Polymer and Polymeric Surfactant Properties

Polymers	State	Commercial Name	Molecular Weight	Content (% mole)
PLGA	Solid	Resomer® 502 (RG 502)	12,000	50% poly glycolide
PFS	Solid	N/A	539,600	29% poly styrene
PFA	Solid	N/A	86,200	100%
PFPE	Liquid	Krytox® 157 FSL	2,500	100%

5.2.2 Methods

In the preparation of spherical silica particles, pure alcohol, ammonia hydroxide, and de-ionized water were mixed in an Erlenmeyer flask at desired concentrations. TEOS as then added into the mixture that was stirred by a magnetic bar. TEOS underwent hydrolysis in water and grew into spherical silica particles, with ammonia acting as a morphological catalyst. After 24 hours of reaction, the solution turned into a milky suspension. The resulting suspension was centrifuged at 3000 rpm for 5 minutes. The supernatant liquid was then drained and the particulate sediment was re-dispersed in pure alcohol. This washing step was needed for the removal of unreacted TEOS and water, and was repeated twice. Finally, the sediment of silica particles was re-dispersed in acetone to produce a suspension for further use in the SAS coating experiment.

Figure 5.2 shows a schematic diagram of the experimental apparatus which consists of three major components: a suspension delivery system, a CO_2 supply system, and a stainless steel precipitation chamber equipped with a pressure gauge (Parr

Instruments, USA). The precipitation chamber has a volume of 1000 ml. Its temperature was kept at the desired value using a water bath. The stainless steel capillary nozzle used to atomize the suspension, the CO_2 inlet, and the CO_2 outlet were all located on the lid of the precipitation chamber. The system pressure was controlled by a downstream metering valve (Swagelok, SS-31RS4, R.S. Crum & Company, USA) and was monitored by a pressure gauge. Liquid CO_2 was supplied from a CO_2 cylinder by a metering pump (Model EL-1A, American Lewa®, USA). A refrigerator (Neslab, RTE-111) was used to

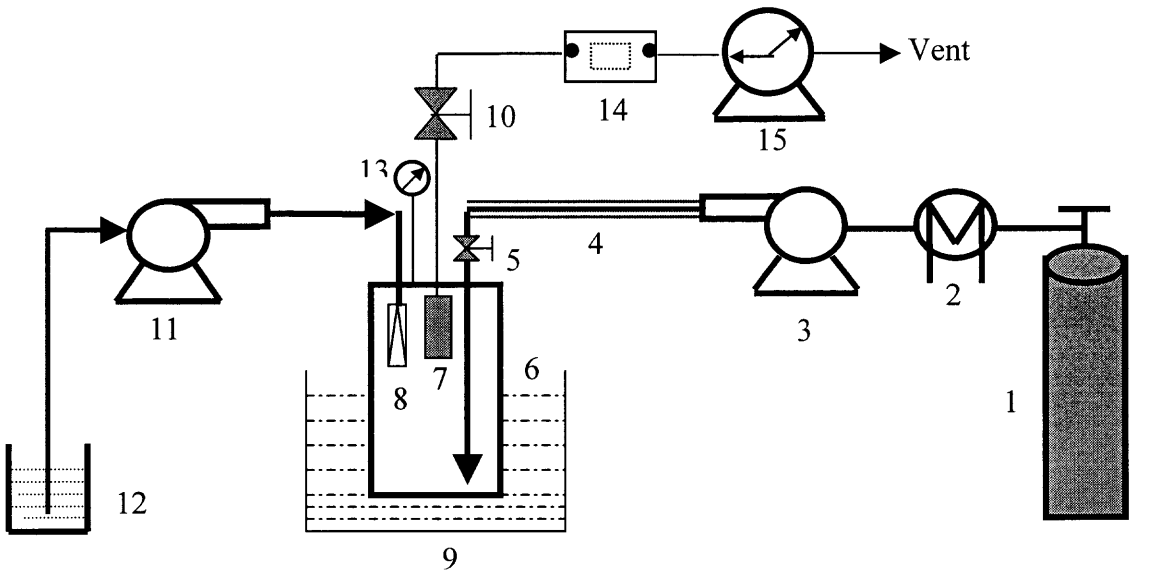

Figure 5.2 Schematic diagram of SAS coating process.

Key: CO_2 Cylinder 2. Refrigerator 3. Metering pump 4. Heating tape 5. On-off valve 6. Precipitation chamber 7. Filter 8. Nozzle 9. Water bath 10. Metering valve 11 HPLC pump 12. Suspension 13. Pressure gauge 14. Mass flow meter 15. Wet gas meter.

chill the liquefied CO_2 down to around zero degrees Centigrade to avoid cavitation. The temperature of the liquefied CO_2 was then raised up by using a heating tape (Berstead Thermolyne, BIH 171-100).

In an experiment, the precipitation chamber was first charged with SC CO_2. When the desired operating conditions (temperature and pressure) were reached, a steady flow of CO_2 was established by adjusting the metering valve and the metering pump. The flow rate of CO_2 ranged from 1.0 to 5.0 standard liters per minute (SLPM). The coating material, PLGA, was then weighed and dissolved into the acetone-silica suspension to produce the desired polymer concentration and polymer to silica ratio. The prepared suspension was delivered into the precipitation chamber through a capillary nozzle (ID 254 μm) by using an HPLC pump (Beckman, 110B) for about 15 minutes. The flow rate varied from 0.4 to 1.3 ml/min.

After spraying, fresh CO_2 continued to flush the chamber in order to get rid of the organic solvent. In this washing step, the temperature and pressure were maintained the same conditions as before. This washing step is necessary since any condensed organic solvent due to phase separation between the organic solvent and SC CO_2 would redissolve the polymer on the surface of particles during depressurization. The washing step lasted about 3 hours depending on the process conditions. After the washing process, the precipitation chamber was slowly depressurized and the coated particles were harvested for characterization. The experimental operating conditions are listed in Table 5.2.

In the SAS coating experiments using a surfactant, a predetermined amount of surfactant was charged into the precipitation chamber before the experiment began. Once

Table 5.2 Experimental Operating Conditions without Surfactant

Run No.	T (°C)	P (bars)	PLGA Conc.in acetone (mg/ml)	PLGA Weight Fraction (%) of coated particles	Flow rate (ml/min)	Observations
1	33.0	89.6	10.0	25.0	0.8	Fairly Loose agglomerates
2	33.0	89.6	10.0	16.7	0.8	Very loose agglomerates
3	33.0	89.6	10.0	12.5	0.8	Very loose agglomerates
4	33.0	110.3	10.0	25.0	0.8	Heavily agglomerated (Sintering)
5	38.0	89.6	10.0	16.7	0.8	Very loose agglomerates
6	42.5	89.6	10.0	16.7	0.8	Fairly loose agglomerates (Some sintering)
7	33.0	89.6	4.0	16.7	0.8	No agglomerates observed
8	33.0	89.6	13.0	16.7	0.8	Loose agglomerates
9	33.0	89.6	10.0	16.7	1.8	Loose agglomerates
10	33.0	89.6	10.0	16.7	2.8	Loose agglomerates

Table 5.3 Experimental Operating Conditions with Surfactants

T (°C)	P (bars)	Surfactant	Surfactant Conc. (wt.%) in SC CO_2	Observations
32.0	96.5	PFS	0.018	Dense film coating on the surface of vessel and stirrer.
32.0	96.5	PFA	0.018	Dense film coating on the surface of vessel and stirrer.
32.0	96.5	PFPE	0.018	Dense film coating on the surface of vessel and stirrer.

the pre-determined processing conditions were achieved, the magnetic stirrer was turned on (600 rpm) to assist in the dissolution of the surfactant in SC CO_2. The experiment then followed the procedure described above. Table 5.3 lists the operating conditions for the SAS coating experiments using the surfactants.

5.2.3 Characterization

The silica particles were observed under a field emission scanning electron microscope (FE-SEM) (Leo, JSM-6700F) to observe any morphological changes before and after the coating treatment. The samples were either spread on a carbon tape or on an aluminum stub support device after dispersing in alcohol and evaporating. Particle size (PS) and particle size distribution (PSD) were analyzed using a LS Particle Size Analyzer (Beckman Coulter). Before particle size analysis, the coated and uncoated particles were dispersed in ethyl alcohol, in which the PLGA was not dissolved, and the resulting suspension was sonicated for 3 minutes. The sonicated suspension was then added into the Beckman Coulter sample cell for the particle size measurement. In order to examine the true polymer amount in the coating of silica particles at different polymer weight fractions, thermogravimatric analyses were performed on a TGA machine (TA Instruments, TA Q50). In this TGA analysis, 3-5 mg coated silica particles were used. The atmosphere was air, and the flow rate was 20 ml/min. The temperature was increased from room temperature to 500 ^{o}C at a heating rate of 20 ^{o}C/min, and then held at 500 ^{o}C for 15 minutes so that the polymer on the surface of the particles would be completely burned off. The measured weight loss was assumed to consist entirely of polymer since the silica particles are inert at this temperature.

5.3 Results and Discussion

5.3.1 Theory

The solubility of the solute and solvent in SC CO_2 are important considerations in the SAS process. A successful SAS process requires good miscibility of the solvent and the SC CO_2, with the solute having negligible solubility in the SC CO_2. There is also a volumetric expansion when CO_2 is dissolved in the solvent, which is important for the precipitation of solute. The volumetric expansion $\Delta V\%$ is defined as

$$\Delta V\% = \frac{V(P,T) - V_0}{V_0} \times 100\% \qquad (1)$$

where V(P, T) is the volume of solvent expanded by CO_2 and V_0 is the volume of pure solvent.

In this system, acetone was used as the solvent and PLGA as the solute, respectively. Unfortunately, there is no experimental data available for the expansion rate and the solubility of PLGA in expanded acetone. However, the Peng-Robinson equation of state (PREoS) (Peng and Robinson, 1976) can be used to predict the expansion behavior of the binary system of CO_2-acetone. The PREoS can be written as

$$P = \frac{RT}{v-b} - \frac{a(T)}{v(v+b)+b(v-b)} \qquad (2)$$

where a and b are parameters of the mixture in the binary system. Originally, the PREoS had only one interaction coefficient, k_{ij}. However, as suggested by Kordikowski, et al., 1995, it is necessary to have a second interaction parameter l_{ij} to account for a polar compound in the binary system. In our system, k_{ij} is –0.007 and l_{ij} is –0.002, which are regressed from the experimental data reported by Katayama et al., 1975. The mixing rules are given as

$$a = \sum_i \sum_j x_i x_j a_{ij} \qquad (3)$$

$$b = \sum_i x_i x_j b_{ij} \qquad (4)$$

$$a_{ij} = (1 - k_{ij})\sqrt{a_i a_j} \qquad (5)$$

$$b_{ij} = \frac{(b_i + b_j)}{2}(1 - l_{ij}) \qquad (6)$$

where the pure component values can be determined as

$$b_{ii} = 0.07780\frac{RT_{ci}}{P_{ci}} \qquad (7)$$

$$a = 0.45724\frac{R^2 T_{ci}^{\ 2}}{P_{ci}}[1 + (0.37464 + 1.54226\omega_i - 0.26992\omega_i^{\ 2}) \times (1 - \sqrt{T/T_{ci}})]^2 \qquad (8)$$

and P_{ci}, T_{ci}, and ω_i are the critical pressure, critical temperature, and accentric factor of component *i*, respectively.

The calculated volume expansion rate as a function of the CO_2 mole fraction is shown in Figure 5.3. The volume of acetone increases slowly with CO_2 mole fraction from 0 to 0.8. However, the volume expands significantly at higher CO_2 mole fraction. When the mole fraction is greater than 0.85, the acetone is fully expanded. The expansion behavior of acetone results in a decrease in the partial molar volume of the solvent so that the solvent strength is reduced. In order to predict the solubility of PLGA in expanded acetone by CO_2, the partial molar volumes of each component $\overline{v}_i$ in the liquid phase needs to be calculated. These are obtained by differentiating the PREoS (Walas, 1985)

$$\overline{v}_i = \frac{RT}{P}(Z + (1 - x_i)(\frac{\delta Z}{\delta x_i})_{T,P}), i = 1,2 \qquad (9)$$

where Z is the compressibility factor. The solubility of a solute in the liquid phase of the expanded solvent, S_3 (T, P), is expressed as (Chang and Randolph, 1990)

$$S_3(T,P) = \frac{\bar{v}_2(T,P,x)}{\bar{v}_2(T,1,0)} S_3(T,1) \qquad (10)$$

where S_3 (T,1) is the solubility at 1 atm, $\bar{v}_2(T,P,x)$ is the partial molar volume of solvent at T, P, and x, and $\bar{v}_2(T,1,0)$ is the partial molar volume of solvent at 1 atm and at the same temperature with no CO_2 dissolved.

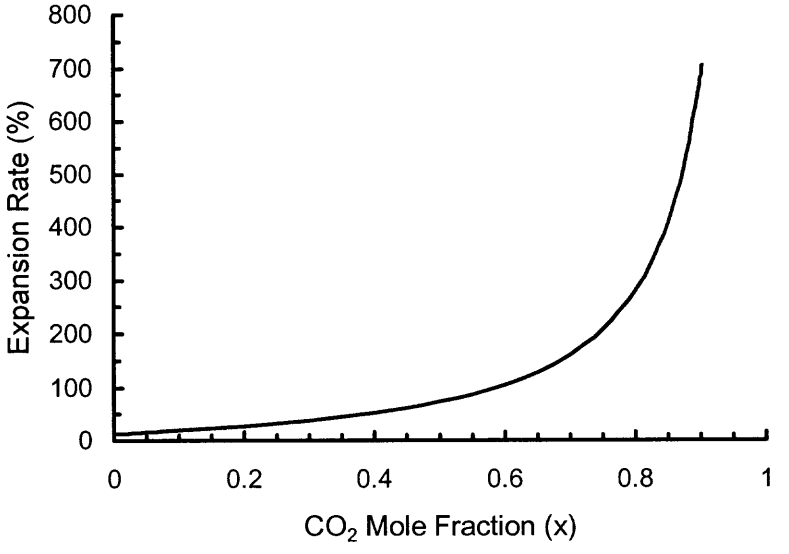

Figure 5.3 Volume expansion rate of acetone as a function of CO_2 mole fraction at 33.0 °C.

The predicted solubility of PLGA in acetone expanded by CO_2 is shown in Figure 5.4. As seen in the figure, the solubility of PLGA in the liquid phase drops as the CO_2 mole fraction is increased. When the CO_2 mole fraction is above 0.7, the solubility decreases considerably. Above 0.85, the solubility of PLGA in acetone is negligible. The CO_2 molecules tend to surround the solvent molecules and reduce the partial molar

volume of the solvent (Chang and Randolph, 1990), causing the decreased solvent strength.

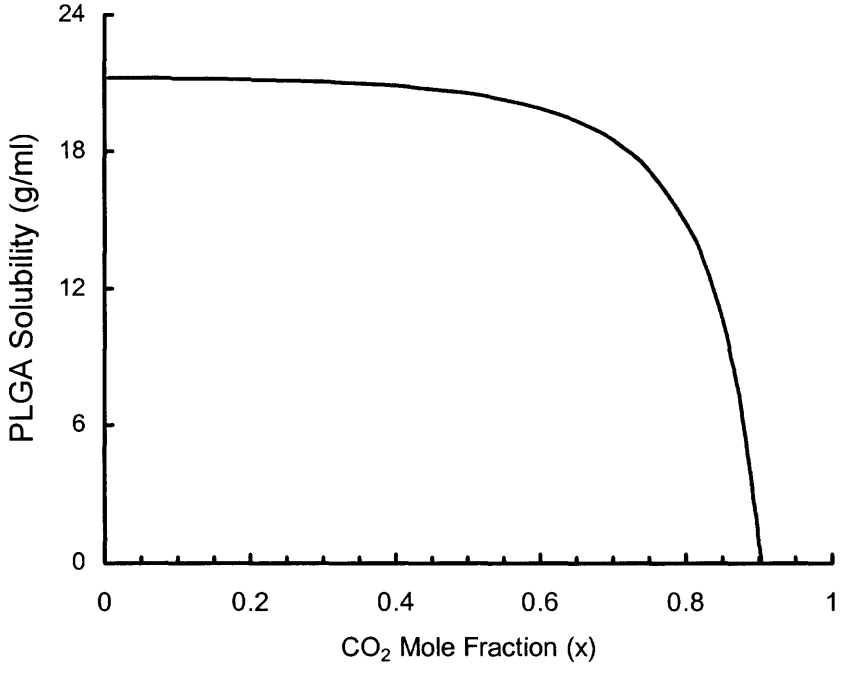

Figure 5.4 Solubility of PLGA in expanded acetone as a function of CO_2 mole fraction at 33.0 °C.

A phase diagram is helpful to explain the SAS polymer coating process although the overall process is very complicated due to the effects of hydrodynamics, kinetics, thermodynamics, and mass transfer which all need to be considered. Figure 5.5 shows a schematic ternary phase diagram for the solvent-antisolvent-polymer. The three regions (S_1), (S_2) and (S_3) in the diagram, represent a single phase region of polymer dissolved in acetone with some CO_2 absorbed, a single phase region of mostly polymer with some acetone and CO_2 absorbed, and a two-phase region made up of the polymer-rich phase and the polymer-lean phase, respectively. The bold line is the solubility curve,

representing the solubility of PLGA in the mixture of acetone and CO_2. The dotted line depicts the addition of polymer solution into SC CO_2.

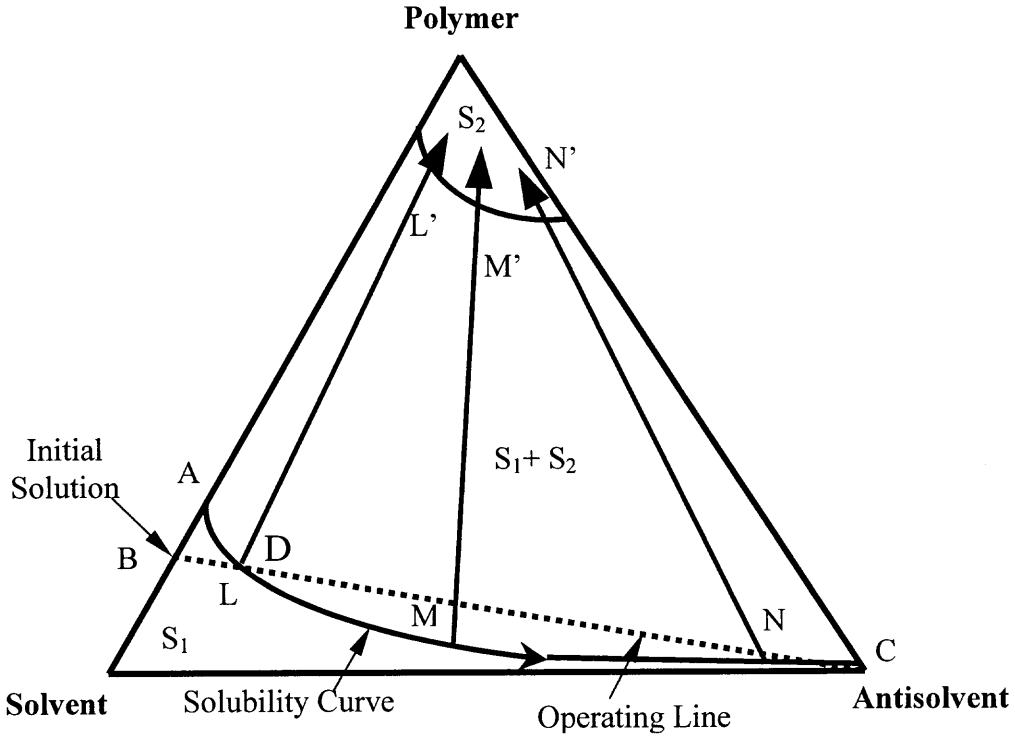

Figure 5.5 Schematic ternary phase diagram for solvent-polymer-antisolvent at constant P and T.

When the acetone-polymer solution (suspended with silica particles) is pumped through a nozzle to form small droplets and contacts SC CO_2, a mutual diffusion between the SC CO_2 and the polymer solution occurs instantaneously. The SC CO_2 is dissolved in acetone, leading to swelling of the droplets (Randolph, et al., 1993). With the continuing diffusion of SC CO_2 into polymer solution and acetone into SC CO_2, the polymer solution very quickly reaches saturation in the mixture of acetone and CO_2 as shown in Figure 5.5 (D, saturation point). Subsequently, the polymer solution forms two phases, a viscous polymer-rich phase with particles entrapped and a dilute polymer-lean phase

(From D to C). Since the solubility of most polymers is very limited, it is reasonable to assume that the polymer-lean phase composition consists mostly of acetone and SC CO_2. As the mutual diffusion continues, the polymer-rich phase becomes more concentrated and more viscous. Further removal of solvent from the polymer-rich phase induces a phase transition to the glassy region (S_2) (Lines from L to L', M to M', and N to N'). Eventually, the polymer vitrifies, forming a polymer film on the surface of particles. A cartoon illustrating the SAS process for fine particle encapsulation (as described above) is shown in Figure 5.6.

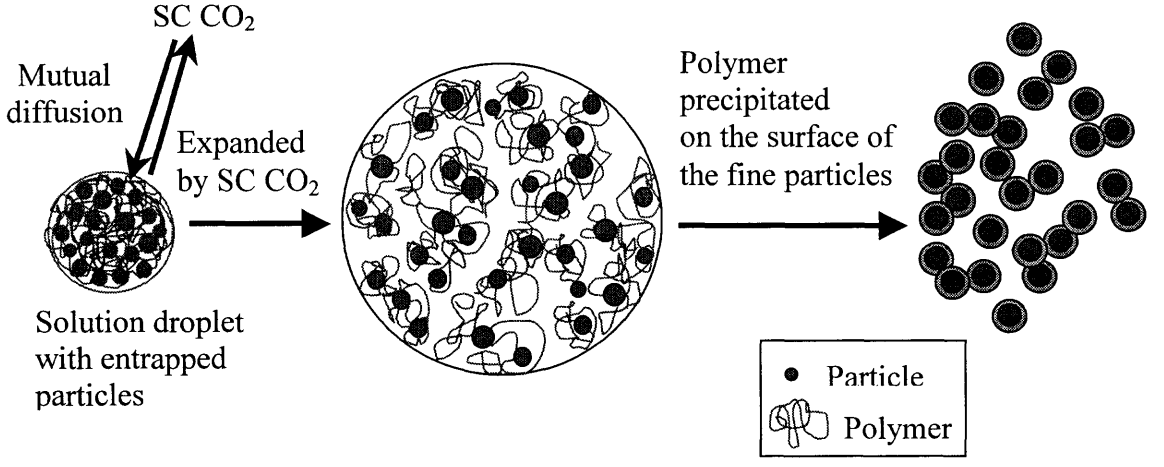

Figure 5.6 Cartoon of SAS process for fine particle encapsulation.

5.3.2 Coating of Fine Silica Particles

High resolution SEM pictures were taken to illustrate morphological changes before and after polymer coating. As seen in Figure 5.7, the synthesized silica particles are spherical and smooth on the surface. The PS and PSD of uncoated silica particles were determined

using the LS Particle Size Analyzer. From Figure 5.8, the average PS of uncoated silica particles is 0.556 micron with a standard deviation of 0.1 micron.

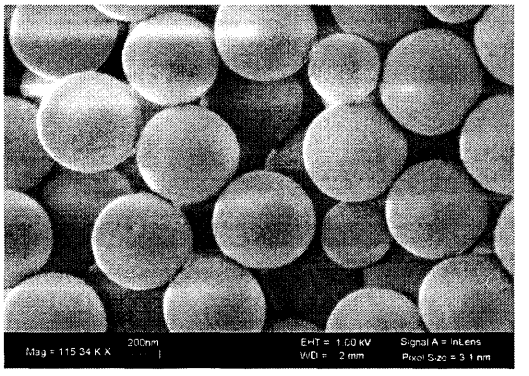

Figure 5.7 Spherical uncoated silica particles.

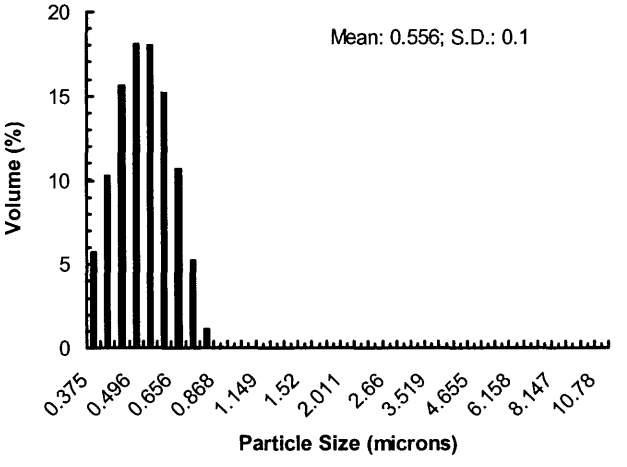

Figure 5.8 Particle size and particle size distribution of uncoated silica particles.

Figure 5.9 shows the silica particles coated with polymer at a polymer fraction of 25.0 % of the total coated particle mass. Compared with Figure 5.7, the coated silica particles (Figure 5.9a) exhibit a different morphology and surface feature. The coated particles are heavily agglomerated due to the polymer coating, which acts as a binder.

During the precipitation of the polymer, the entanglement of polymer chains between neighboring particles binds them together, forming agglomerates as shown in Figure 5.9 (a). However, after sonication in alcohol for 3 minutes, the solid polymer bridges between the coated particles appeared to be broken as shown in the outlined area in Figure 5.9 (b). In SEM, a high intensity electron beam is used to scan the surface of particle. Since some of the kinetic energy of the electron beam is absorbed by the particles, the local temperature of the area that is scanned increases. Therefore, after the coated silica particles are exposed to the high intensity electron beam for 15 minutes, the coating polymer becomes soft and spreads over the surface of particles (Figure 5.9 (c)) due to the low glass transition temperature of the polymer (40-55 ^{o}C).

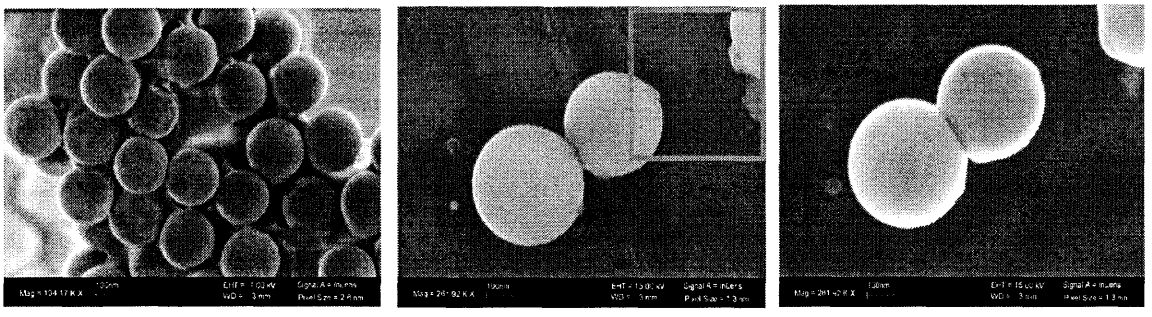

(a) (b) (c)

Figure 5.9 Coated silica particles at a polymer fraction of 25.0 % after sonication for 3 minutes. (a) Coated silica particles before sonication; (b) Coated silica particles after sonication for 3 minutes; (c) Coated particles after being bombarded for 15 minutes with the electron beam.

The quality of the coating and the degree of agglomeration were found to be affected by several operating parameters including the polymer weight fraction, polymer concentration in acetone, temperature, pressure, flow rate, and the addition of surfactants. These will be described in detail below.

5.3.3 Effect of Polymer Weight Fraction

The amount of polymer applied in the coating of particles is important in controlling the coating thickness and agglomeration of the coated particles in the SAS process. The SAS coating process was operated at 33 °C and 89.6 bars, respectively and the polymer weight fraction was varied from 12.5 % to 25.0 % (runs 1, 2 and 3). SEM photographs of the coated particles at different polymer weight fraction are shown in Figure 5.10. At a high polymer weight fraction of 25.0 %, the coated particles were seriously agglomerated (Figure 5.10 (a)). When the polymer weight fraction was lowered to 16.7 %, the agglomeration became much less pronounced (Figure 5.10 (b)). When the polymer weight fraction was lowered even further to 12.5 %, the agglomeration between the coated particles also appeared to decrease (Figure 5.10 (c)).

The coated particles were analyzed in terms of particle size and particle size distribution to determine the degree of agglomeration. In measuring the particle size and particle size distribution, the coated particles were dispersed in ethyl alcohol. The resulting suspension was sonicated for 3 minutes. Figure 5.11 shows the results of the

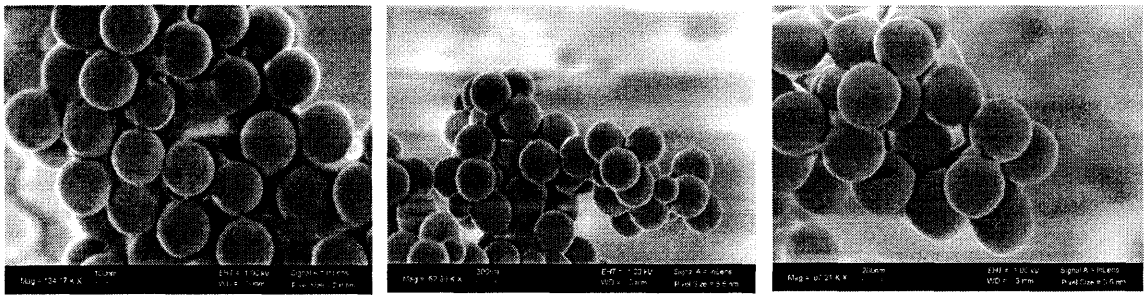

a b c

Figure 5.10 SEM photographs of coated particles at different polymer weight fractions. (a) 25.0 % (Run 1); (b) 16.7 % (Run 2); (c) 12.5 % (Run 3).

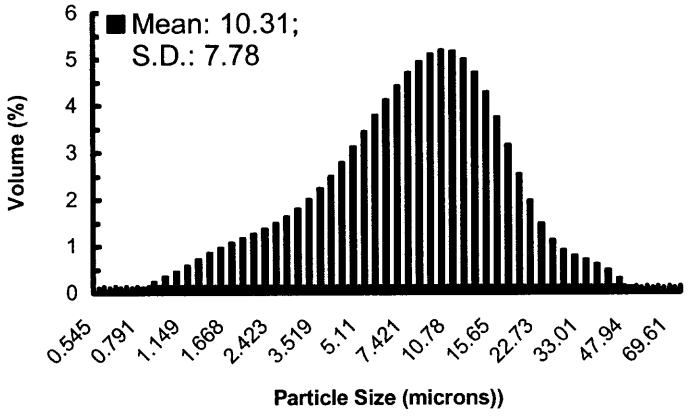

(a)

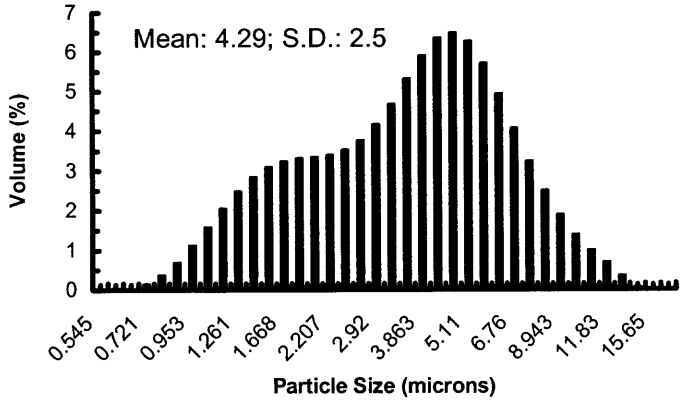

(b)

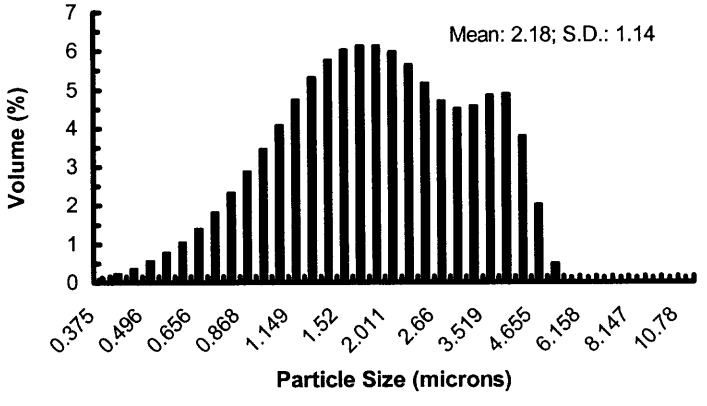

(c)

Figure 5.11 Average size and distribution of coated particles at different polymer weight fractions. (a) 25.0 % (Run 1); (b) 16.7 % (Run 2); (c) 12.5 % (Run 3).

particle size and particle size distribution at different polymer weight fractions. The average size of agglomerates of coated particles at the fraction of 25.0 % is 10.31 microns with a standard deviation of 7.78 microns as shown in Figure 5.11 (a). It is obvious that agglomeration among the coated particles occurred since the average size of the uncoated particles is 0.556 microns with a narrow size distribution of 0.1 micron. This is consistent with the observation in Figure 5.10 (a). The average size of agglomerates of coated particles decreased considerably, to 4.29 microns with a distribution of 2.5 microns when the particles were coated at the polymer weight fraction of 16.7 % (Figure 5.11 (b)). When the weight fraction was reduced to 12.5 %, the average size of agglomerates of coated particles decreased to 2.18 microns with a distribution of 1.14 microns. There is a good agreement between the SEM photographs in Figure 5.10 and the results of particle size and particle size distribution analysis using the Beckman Coulter LS Particle Size Analyzer in Figure 5.11.

The true polymer amount coated on the silica particles at different weight fractions was analyzed with TGA. The TGA curves of pure polymer and coated silica particles at different weight fractions were shown in Figure 5.12. The pure PLGA polymer started to decompose at about 200 ^{o}C from the TGA analysis. When the temperature was increased to 500 ^{o}C and held for 15 minutes, the PLGA was totally burned off and the TGA curve was leveled off. The TGA curve of coated particles at a weight fraction of 25 % showed a 24.3 % weight loss. It is very close to the theoretical polymer loading. Similarly, the TGA curves of coated samples at polymer weight fractions of 16.7 % and 12.5 % have weight losses of 18.4 % and 13.4 %, respectively. The true polymer weight fractions are consistent with the theoretical polymer loadings.

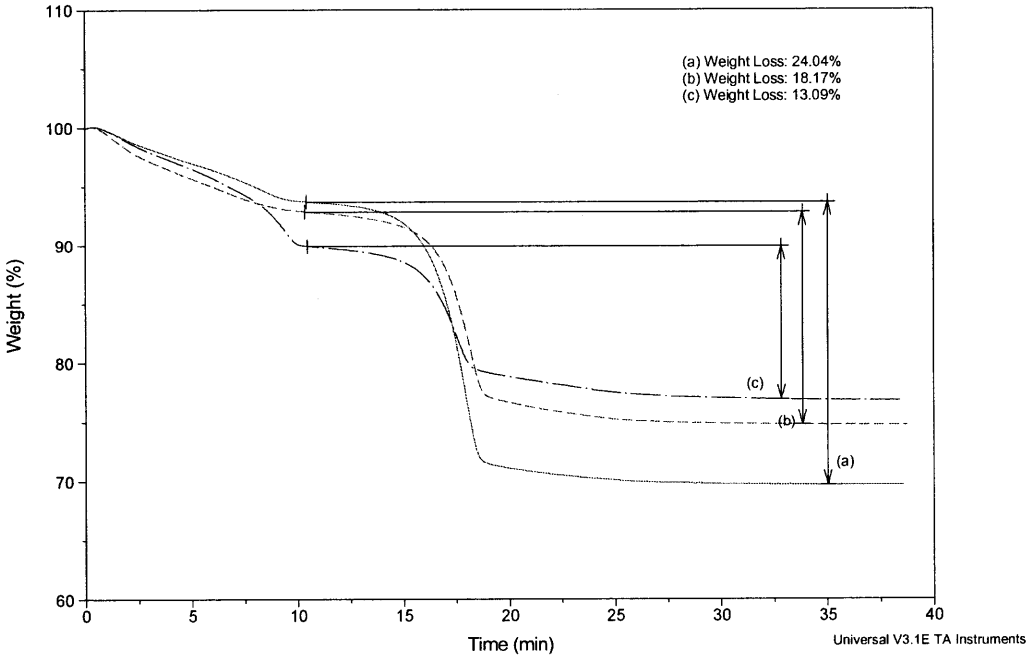

Figure 5.12 Weight loss profiles of coated silica particles at different weight fraction.

5.3.4 Effect of Polymer Concentration

Polymer concentration was found to be very important in controlling the agglomeration of coated particles in the SAS process. The polymer concentration was varied from 4.0 to 13.0 mg/ml while keeping all other operating parameters constant (runs 2, 7 and 8). SEM photographs of coated particles at different concentrations are shown in Figure 5.13. At high polymer concentration of 13 mg/ml, the coated particles were heavily agglomerated. In addition, the polymer coating on the surface of particles was found to be unevenly distributed (Figure 5.13 (a)). When the polymer concentration decreased to 10.0 mg/ml,

the polymer coating on the surface of particles appeared smoother. Nevertheless, agglomeration of coated particles can be seen in Figure 5.13 (b). A further decrease in the polymer concentration to 4.0 mg/ml showed smooth particle coating with minimal agglomeration as seen in Figure 5.13 (c).

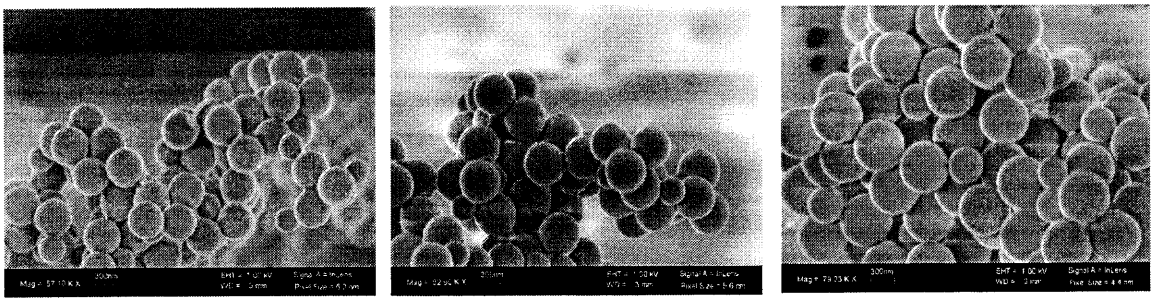

(a) (b) (c)

Figure 5.13 SEM photographs of coated particles at different polymer concentrations. (a) 13.0 mg/ml (Run 8); (b) 10.0 mg/ml (Run 2); (c) 4.0 mg/ml (Run 7).

The results of the particle size analysis of the coated particles at different polymer concentrations are shown in Figure 5.14. Although the polymer weight fraction was kept at 16.7 %, a higher polymer concentration results in larger agglomerates. When particles were coated at polymer concentration of 13.0 mg/ml, the average size of agglomerates is 7.45 microns with a distribution of 4.03 microns (Figure 5.14 (a)). However, the average size of agglomerates decreased to 4.29 microns when the polymer concentration was reduced to 10.0 mg/ml (Figure 5.14 (b)). When polymer concentration was lowered further to 4.0 mg/ml, the average size of agglomerates decreased significantly to 0.613 microns with a distribution of 0.135 microns (Figure 5.14 (c)). Hence it appears that no agglomeration occurred, and the increase in average particle size is simply due to the polymer coating on the surface of the particles. The coating thickness is estimated to be

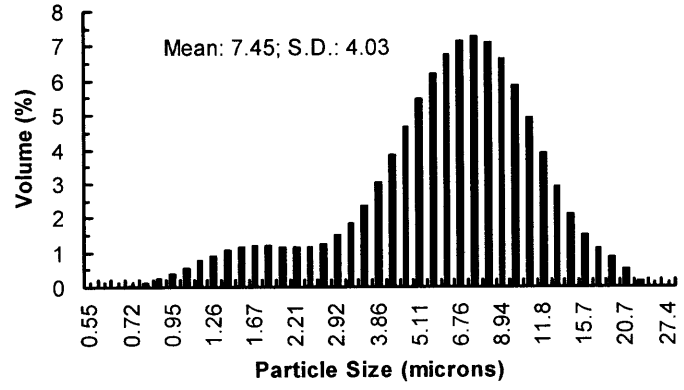

(a)

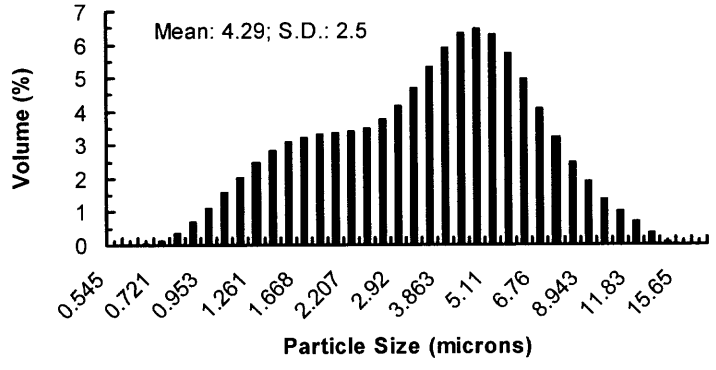

(b)

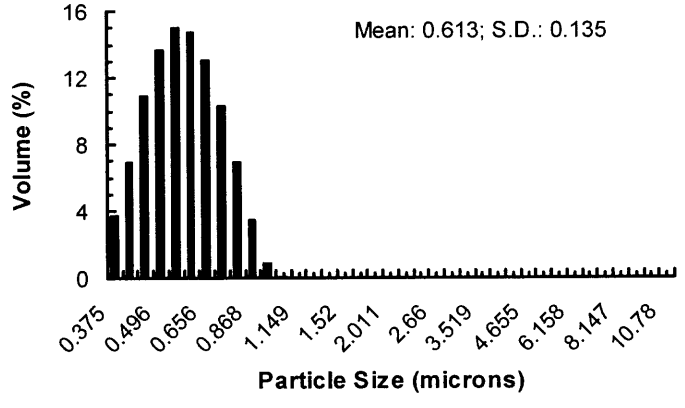

(c)

Figure 5.14 Average size and size distribution of coated particles at different polymer concentrations. (a) 13.0 mg/ml (Run 8); (b) 10.0 mg/ml (Run 2); (c) 4.0 mg/ml (Run 7).

28.5 nanometers based on the measurements of uncoated particles and coated particles at a polymer concentration of 4.0 mg/ml.

The thickness of the coating layer on the surface of the particles can also be estimated from the polymer weight fraction. If it is assumed that no agglomeration occurs, that the PLGA only coats the silica particles and the coating is uniform on the surface of a particle with a thickness, t, then

$$t = R(1+\rho_H m_c / \rho_c m_H)^{1/3} - R \qquad (11)$$

where R is the radius of the uncoated particle, ρ_H and ρ_C are the density of the host particles and PLGA, and m_H and m_c are the weight of the host particles and polymer. Knowing the polymer weight fraction and using Equation (11), t is estimated to be 29 nanometers, which is very close to the value obtained from the size measurements of the uncoated particles and coated particles. This calculation strongly supports the conclusion drawn above that no agglomeration among coated particles occurs when using a polymer concentration of 4.0 mg/ml.

5.3.5 Effect of Temperature

In previous studies using the SAS process for particle formation (Randolph, et al., 1993; Reverchon, et al., 1998; Yeo, et al., 1993), the operating temperature was found to affect both the particle size and morphology of the final product. Since the SAS process for particle formation, and that for particle coating used here, are very similar, except that for coating the host particles are suspended in the polymer solution before being delivered into SC CO_2, it is likely that temperature will have an effect on the coating and agglomeration of the coated particles. To determine the temperature effect experiments

were carried out at different temperature from 33 to 42.5 °C while the other operating parameters were kept constant (runs 2, 5, and 6). Figure 5.10 (b) and Figure 5.15

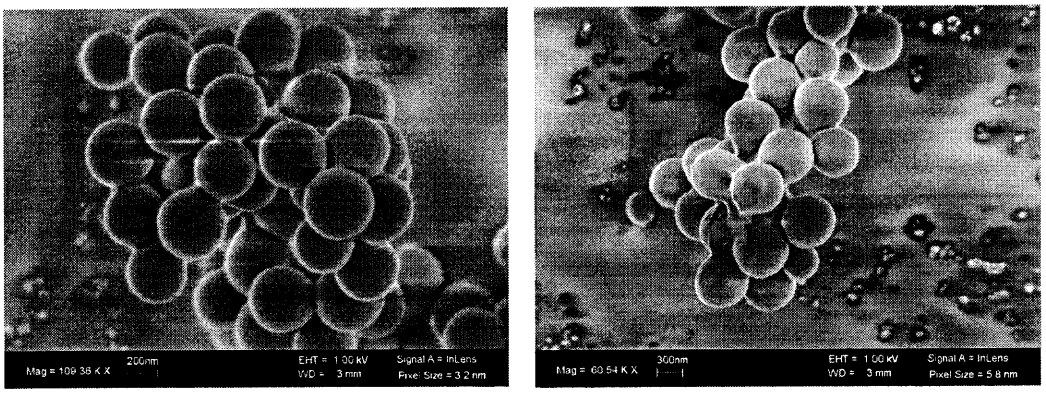

(a) (b)

Figure 5.15 SEM photographs of coated particles at different temperatures. (a). 38 °C (Run 5); (b). 42.5 °C (Run 6).

show the SEM photographs of the coated particles at different temperatures. Below the glass transition temperature of PLGA (T_g, 40~55 °C), the coated particles at 33 and 38 °C appear to be very similar. The average size of the agglomerates at 33 °C is 4.29 microns with a distribution of 2.5 microns (Figure 5.12 (b)), and at 38 °C, 4.61 microns with a distribution of 3.25 microns (Figure 5.16 (a)). There is only a very slight increase in agglomerate size with temperature. However, when the operating temperature is increased to 42.5 °C, above the glass transition temperature of PLGA, the coated particles were heavily agglomerated as seen in Figure 5.16 (b) due to sintering. In addition, the polymer coating is very unevenly distributed on the surfaces of the host particles. A particle size measurement of the coated particles at 42.5 °C shows that the average size of the agglomerates increases significantly from about 4.5 to 12.9 microns (Figure 5.16 (b)).

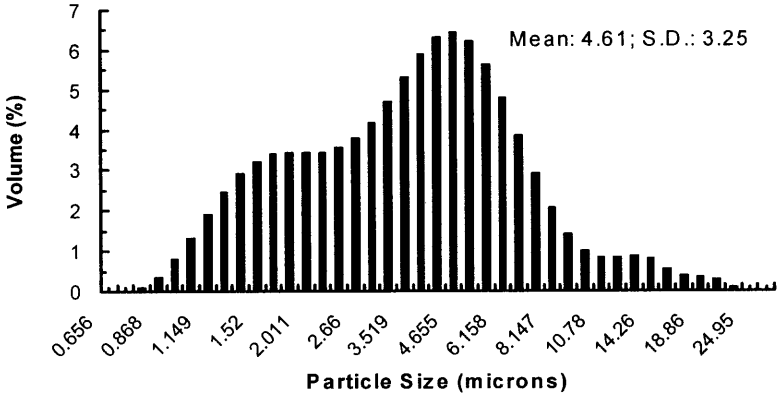

(a)

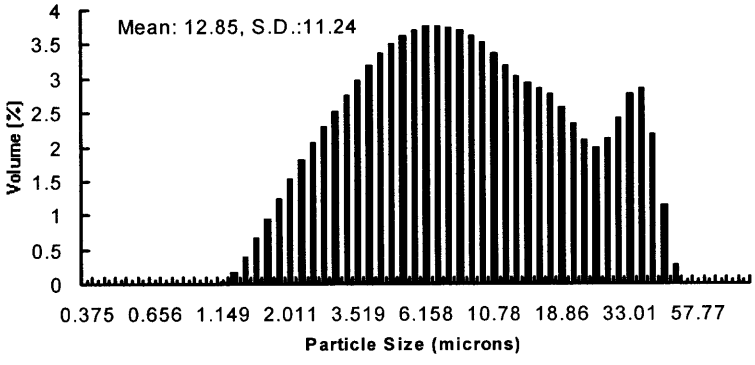

(b)

Figure 5.16 Average size and size distribution of coated particles at different temperatures. (a). 38 °C (Run 5); (b). 42.5 °C (Run 6).

5.3.6 Effect of Pressure

The pressure of the system is one of the most important variables in the SAS process since it affects the density of SC CO_2. Thus, the rate of mutual diffusion between SC CO_2 and the polymer solution will be influenced. Furthermore, Mawson, et al., 1997 and Condo, et al., 1994 found that the glass transition temperature of polymers could be depressed by compressed CO_2. In order to examine the effect of pressure, experiments were carried out at two different operating pressures of 89.6 and 110.3 bars while the

temperature was kept constant at 33 °C (runs 1 and 4). Figure 5.17 shows a SEM photograph of coated particles under a pressure of 110.3 bars. The coated particles were heavily agglomerated compared with the coated particles shown in Figure 5.10 (a) at 89.6 bars. In addition, it was found that the polymer coating was unevenly distributed. The average size of the agglomerates increased to 24.8 microns with a distribution of 18.4

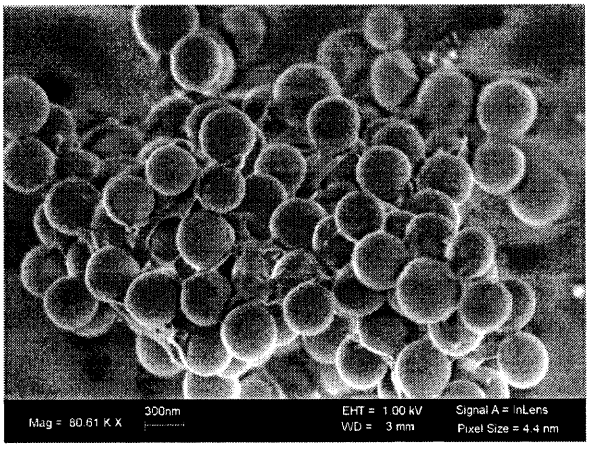

Figure 5.17 SEM photographs agglomerates of coated particles at a pressure of 110.3 bars (Run 4).

microns as shown in Figure 5.18. This may be due to a depression in T_g of the polymer in pressurized CO_2. The agglomeration of coated particles appears to be enhanced by plasticization of coating polymer under high pressure. The degree of plasticization of polymer is proportional to the amount of CO_2 absorbed into the polymer matrix, that is, proportional to the operating pressure. This explains why the agglomeration of coated particles at 110.3 bars is much worse than that at 89.6 bars. Also, T_g depression appears to favor a redistribution of polymer coating on the surface of particles as seen in Figure 5.18.

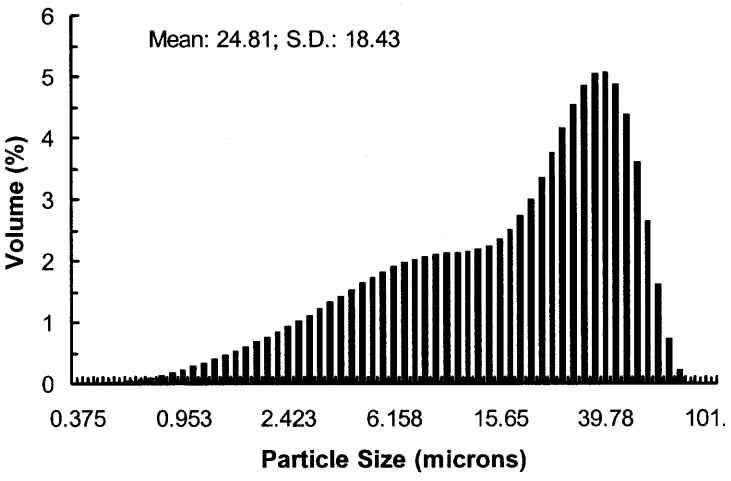

Figure 5.18 Agglomerate size and distribution of coated particles at a pressure of 110.3 bars (Run 4).

5.3.7 Effect of Flow Rate

In SAS particle formation, the flow rate of the solution has been reported to have an effect on the particle size and morphology of final products (Randolph, et al., 1993; Chattopadhyay and Gupta, 2000; Tu, et al., 2002). To study the flow rate effect in our SAS coating process, experiments were performed at different flow rates varying from 0.8 to 2.8 ml/min (runs 2, 9, and 10). The SEM photographs of the coated particles are shown in Figure 5.10 (b) and Figure 5.19. The surface of the coated particles at all three different flow rates is fairly smooth and there does not appear to be any difference in the degree of agglomeration due to changes in flow rate.

The particle size measurements are shown in Figure 5.11 (b) and Figure 20. No clearly defined trend can be observed from these figures, except that the average size of the agglomerates at a flow rate of 2.8 ml/min is slightly increased. Thus it appears that

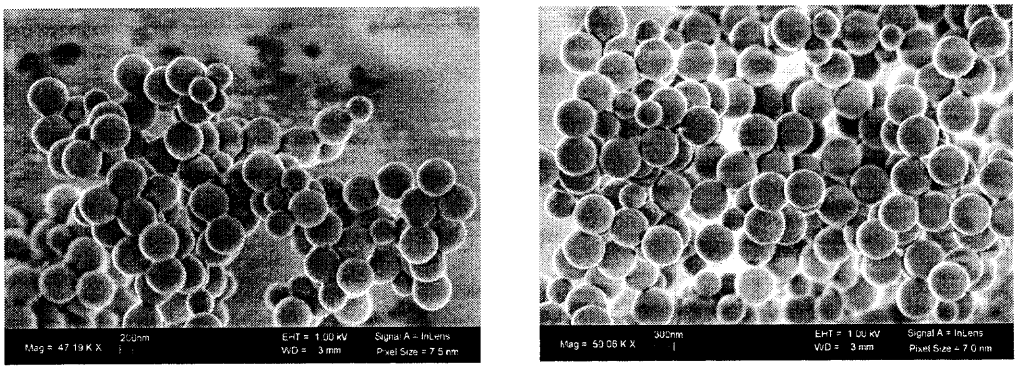

(a) (b)

Figure 5.19 SEM photographs of coated particles at different flow rates. (a). 1.8 ml/min (Run 9); (b). 2.8 ml/min (Run 10).

flow rate plays a less critical role in the coating of particles in the SAS process compared to other operating parameters, such as polymer concentration, polymer weight fraction, temperature, and pressure, which were discussed above. However, the concentration of the organic solvent in the suspension droplets extracted by SC CO_2 should be sufficiently low so that the polymer coating on the surface of the silica particles solidifies before contacting other coated particles or the surface of the vessel. Otherwise, agglomeration would take place when the viscous liquid polymer coating on the surface of particles contact each other. Therefore, the flow rate should be lower than a certain limiting value to prevent agglomeration.

5.3.8 Effect of Surfactants

To evaluate the effect of surfactants in the SAS coating process, various surfactants that are fully soluble in SC CO_2 at the concentration, temperature and pressure of interest were used. The fluoroalkyl side chains of the PFA (Blasig, et al., 2002) and PFS (Xu, et

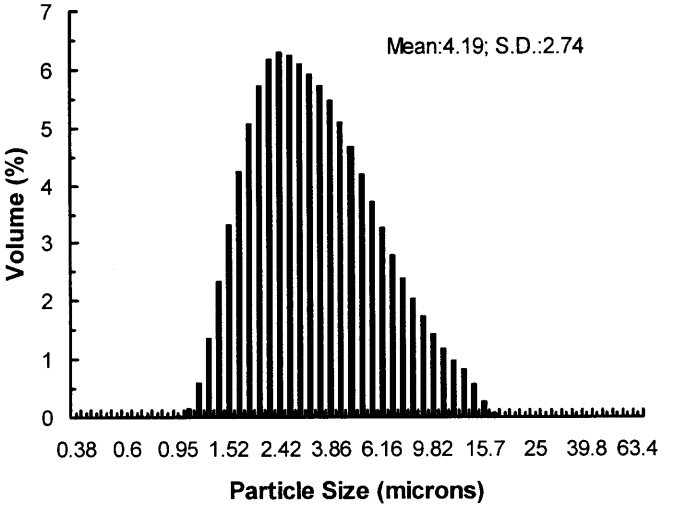

(a)

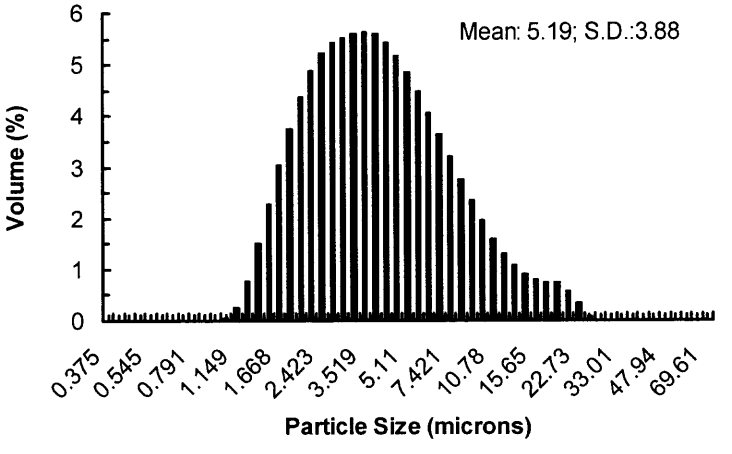

(b)

Figure 5.20 Average size and size distribution of coated particles at different flow rates. (a). 1.8 ml/min (Run 9); (b). 2.8 ml/min (Run 10).

al., 2003) polymers and the polyfluoroether tail of the Krytox 157 FS (Hoefling, et al., 1993) are known to be CO_2-philic and were expected to interact favorably with the SC CO_2. It was conjectured that the CO_2-phobic backbone of PFA, the backbone and

pendant aromatic groups of the PFS, and the carboxylic acid of the Krytox 157 FS could coat the PLGA surface.

Before starting an experiment, a known amount of surfactant was put into the high-pressure chamber. In order to compare the effect of surfactants on the reduction of agglomeration of coated particles, the operating conditions were chosen to be the same as in the coating experiments without using any surfactants. When the desired experimental conditions were reached, the magnetic stirrer was turned on (300-600 rpm) to facilitate the dissolution of the surfactant. After about 30 minutes agitation, the suspension of particles in polymer solution was then supplied by the HPLC pump through the nozzle into SC CO_2 with the surfactant presumed to be dissolved. The subsequent steps of flushing with fresh CO_2 and depressurization are same as the SAS coating experiments without surfactants.

In examining the literature of dispersion polymerization in SC CO_2, it is found that the effective concentration of surfactants used was usually in the range of 0.1 to 2.0 weight percent in CO_2 at 65 ^{o}C and over 340 bars (Shaffer, et al., 1996; Canelas, et al., 1998; Yates, et al., 1999; Shiho and DeSimone, 2000). In a recent study of dye impregnation microencapsulation for latexes using CO_2, a surfactant, Pluronic F108 was utilized to effectively disperse the dyes by emulsifying CO_2-water and CO_2-ethanol systems at concentrations from 0.1 to 1.5 % at the conditions of 25 ^{o}C and 310 bars (Liu and Yates, 2002). Since the pressure in this SAS coating process is 89.6 bars, much lower than the pressures in polymerization and impregnation work, 0.1 % of PFA surfactant in SC CO_2 was initially attempted. However, the surfactant, which was known to dissolve very slowly in SC CO_2 even when agitated (Xu, et al., 2003), was found not to have been

completely dissolved since surfactant chunks were observed inside the vessel after disassembly of the high-pressure chamber.

In a PCA microparticle formation study done by Mawson, et al., 1997, the effective surfactant concentrations to stabilize polymer microparticles were found to be in the range of 0.01 % to 0.05 % depending on which surfactants were introduced into CO_2 at the operating conditions of 23 ^{o}C and 149 bars. Therefore, the amount of surfactant was reduced to 0.0185 % and the pressure raised from 89.6 bars to 96.5 bars. However, once again the surfactants were found not to completely dissolve in SC CO_2, even at the lower concentration.

When the experiment was completed (using PFA), no free flowing particles or agglomerates were found inside the chamber. Instead, a film coating occurred on the surface of the chamber, and on the surface of the stirrer as well. The film coating was scraped from the surface and was observed underneath the SEM. Figure 5.21 (a) shows the coated particles scraped from the surface of the vessel in the SAS coating experiment with the addition of PFA. It can be seen that the coated particles are very heavily agglomerated. Furthermore, the coating is found to be very different when compared with that in Figure 5.10 (a), even though the polymer weight fraction is the same. In a separate experiment to measure the solubility of PFA in SC CO_2, it was observed that some of the PFA was dissolved and some was liquefied by SC CO_2 at these operating conditions. Therefore, it is hypothesized that the coated particles might have been glued together by the liquefied PFA. After depressurization, the PFA solidified and formed solid bridges among the coated particles, resulting in extensive agglomeration.

To further evaluate the effect of the surfactant, the SAS coating experiment using PFA at the same concentration (0.0185 %) was operated at a higher pressure of 121 bars and temperature of 32 ^{o}C, at which PFA was fully dissolved in SC CO_2. However, the result (not shown) turned out to be even worse than the coating experiment at 96.5 bars. At the higher pressure a molecular interaction between PLGA and PFA might have occurred since they both have -COO- groups. A molecular attraction may cause the backbone of PFA to stick to PLGA while the pendent CO_2-philic fluoroalkyl groups extend into the SC CO_2 phase. After depressurization, the CO_2-philic fluoroalkyl chains may intertwine and collapse, forming a network and binding the coated particles together.

The coating experiment with PFA as a surfactant was also performed at a much lower concentration of 0.00185%, one-tenth the previous value. However, the result was the same.

Two other SC CO_2 soluble surfactants, PFS and Krytox, were also used following the same experimental procedure as with PFA at the concentration of 0.0185%. Again, particle coating on the surface of the vessel and stirrer was found in both experiments. SEM photographs of the coated products from these experiments are shown in Figure 5.21 (b) and 5.21 (c), respectively. Clearly, the coated particles are very heavily agglomerated in both cases due to interactions between the surfactants and the PLGA.

Since none of the SC CO_2 soluble surfactants were effective, two other SC CO_2 soluble surfactants, poly (dimethyl-siloxane) (PDMS) (Canelas, et al., 1998) and block co-polymer poly (propylene oxide)-poly (ethylene oxide)-poly (propylene oxide) (PPO-PEO-PPO), Pluronic 25R2 (Shiho and DeSimone, 2000; Liu and Yates, 2002), which are

soluble in acetone and in SC CO_2, were tried. These two surfactants were dissolved in the coating polymer solution since they are soluble in acetone and were sprayed into SC CO_2

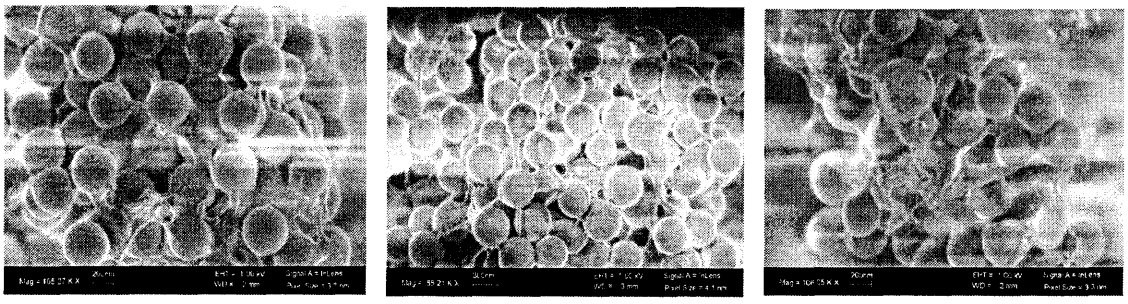

(a) (b) (c)

Figure 5.21 SEM photographs of coated particles using surfactants. (a). PFA; (b). PFS, (c). Krytox. (Polymer weight fraction 25.0 %, polymer conc. 10 mg/ml, flow-rate, 0.8 ml/min).

along with the silica particles and the coating solution. The results showed that the coatings, with or without either of these surfactants present, were similar; no effect on the minimization of agglomeration of coated particles was observed (Data not shown).

5.4 Concluding Remarks

Particle coating with polymer using the SAS process with SC CO_2 was systematically studied. Our results show that submicron silica particles were successfully coated or encapsulated by PLGA in the form of loose agglomerates. It was found that the polymer weight fraction and the polymer concentration play critical roles in the agglomeration of the coated particles. A high polymer weight fraction favors the agglomeration of the coated particles and the uneven distribution of the polymer coating. A low polymer concentration of 4.0 mg/ml appears to prevent agglomeration among the coated particles.

The operating pressure and temperature were also found to influence agglomeration. A higher pressure facilitates the agglomeration of coated particles due to sintering because the glass transition temperature of the polymer, T_g, is depressed. The operating temperature appeared to have little effect on the agglomeration of the coated particles when the temperature is below the glass transition temperature; however, when the operating temperature is above T_g, the polymer coating on the surface of particle appears to be sintered causing strong agglomeration. The flow rate of the polymer suspension was found to have little effect on the agglomeration.

Five surfactants, PFA, PFS, Krytox, PDMS, and Pluronic 25R2, all soluble in SC CO_2, were used in the hope that they would suppress agglomeration of the coated particles in the SAS process. However, the results showed that the PDMS and Pluronic 25R2 surfactants, which are also soluble in acetone, had no effect on minimizing agglomeration of the coated particles. The PFA, PFS, and Krytox surfactants, surprisingly, actually, facilitated agglomeration.

CHAPTER 6

APPLICATION OF SUPERCRITICAL ANTISOLVENT PROCESS FOR CONTROLLED DRUG DELVIERY SYSTEM

In order for the research described in this chapter to stand on its own (as a publishable research paper), some of the pertinent prior work that has already been described in Chapter 2 may be repeated here.

6.1 Introduction

The incorporation of a pharmaceutical ingredient into a polymer carrier is of great interest for controlled drug delivery systems. Polymer based drug delivery carriers are required for many reasons. Each drug has a concentration range that provides optimal therapeutic effects. When the drug concentration falls out of this range, either higher or lower, it may cause toxic effects or become therapeutically ineffective. Therefore, it is desirable to release the drug content from a polymer carrier in a sustained or a controlled manner so as to eliminate the potential of either underdosing or overdosing. A polymer carrier can also provide protection for fragile drugs, such as proteins and peptides, from hydrolysis and degradation. For highly toxic drugs, a polymer carrier for target release is required to shield them until they are released at the target tissue. In addition, a drug controlled release system can improve patient compliance by reducing the drug administration frequency.

Polymer-based microsphere controlled drug release has attracted significant attention recently because of flexibility of administration. Microspheres less than 100 μm are suitable for intravenous injection. When the particle size is less than 5 μm, the

microspheres can be administered via inhalation drug delivery. Submicron microspheres can even be injected directly into circulation system. In controlled drug release, polymer-based microspheres usually have either a matrix or a microcapsule structure. In a matrix structure, the drug is uniformly dispersed in a polymer matrix whereas a microcapsule is composed of drug particles as core particles surrendered by a polymer coating film.

For both the matrix or microcapsule structure, drug release occurs by one (or both), of two primary mechanisms: diffusion release or degradation release. Diffusion release takes place when an incorporated drug passes through the polymer pores or through polymer chains. This drug controlled release system can be designed by using a smart polymer, whose permeability is dependent on the environmental conditions, such as pH, temperature, and ionic strength, etc. (Dorski, et al., 1997). For example, pH is the stimulant for an acidic or basic hydrogel, and temperature is the stimulant for a thermo-responsive hydrogel (poly N-isopropylacrylamide). Degradation release occurs when a polymer degrades within the body as a result of natural biological processes, such as hydrolysis. In this type of controlled release system, the selection of the polymer is critical since the degradation is dependent strongly on its chemical structure and molecular weight. The most popular biodegradable polymers for drug controlled release systems include poly (lactic acid), poly (glycolic acid) and their copolymers (Brannon-Peppas, 1995).

Drug loaded microspheres can be made by emulsion evaporation, phase separation, spray-drying, freeze-drying, and interfacial polymerization techniques. All of these methods involve the dissolution of the polymer and the drug in an organic solvent, dispersion of the solution under a strong force, and stabilization under certain

temperature and pH conditions. However, problems of residual organic solvent in the final product and low encapsulation of drugs due to partitioning of the pharmaceutical components between two immiscible liquid phases are frequently encountered. Moreover, harsh conditions, such as temperatures, pH conditions, and strong shear forces, may denature some bio-active agents. Also, extensive downstream processing is usually required when using these conventional methods.

Supercritical CO_2 (SC CO_2) is the most widely used supercritical fluid because of its mild critical conditions (T_c=31.1 °C, P_c=73.8 bars), non-toxicity, non-flamability, and low price. The low critical temperature of CO_2 makes it attractive for processing heat-sensitive flavors, pharmaceuticals and labile lipids (McHugh and Krukonis, 1994). The use of SC CO_2 for microparticle preparation has been widely reported using rapid expansion of supercritical solution (RESS) (Krukonis, 1984; Matson, et al., 1987; Mohamed, et al. 1989; Charoenchaitrakool, et al. 2000; Tom and Debenedetti, 1991) and a variety of antisolvent processes (GAS/SAS/ASES/SEDS) (Yeo, et al., 1993; Dillow, et al., 1997; Reverchon, et al., 1998; Gallagher, et al., 1989; Lim, et al., 1998; Dixon, et al., 1993; Winter, et al., 1999; Thies and Müller, 1998; Hanna, et al., 1998).

The application of SC CO_2 processes to prepare drug loaded polymer microspheres for controlled drug release has become a fast growing field. Tom and Debenedetti, 1994 investigated a SC CO_2 process for the formation of drug loaded microspheres for controlled drug release. In this pioneering work, a model system of biopolymer PLA and pyrene was chosen for the composite powder formation study. PLA and pyrene were dissolved in SC CO_2 with acetone as a cosolvent in two different units. The two resulting supercritical solutions were mixed and were pumped to an expansion

device (orifices or capillaries, 25-50 μm). When the solution flowed through the expansion device, it underwent a rapid decompression, resulting in co-precipitation of the solutes. It was found that the pyrene was uniformly incorporated into the produced polymer microspheres. Kim, et al., 1996 did a similar study using the RESS co-precipitation process and produced microspheres with a naproxen core encapsulated in a PLA coating.

Mishima, et al., 2000 studied the microencapsulation of protein particles using the RESS process. In this study the protein (lysozyme and lipase) particles were suspended in a polymer solution in SC CO_2 (with ethanol as the cosolvent) instead of being dissolved as was done in the co-precipitation process (Tom and Debenedetti, 1994 and Kim, et al., 1996). The suspension was then sprayed through a capillary nozzle (280 μm). The results showed that the protein particles were successfully encapsulated in a polymer coating without agglomeration.

However, the application of RESS process is severely limited by the fact that most of the polymers and drugs of interest are not soluble in SC CO_2 at a reasonable concentration. As an alternative, antisolvent processes (GAS/SAS/ASES/SEDS) for drug delivery system design has attracted a lot of attention recently because of its flexibility in choosing a suitable solvent which is miscible with SC CO_2.

Bleich and Müller, 1996 studied drug-loaded particle formation using the ASES process. PLA was used as the carrier and several different drugs, such as hyoscine butylbromide, indomethacin, piroxicam and thymopentin, were selected as model drugs for this study. The drugs and PLA were dissolved in methylene chloride and the solution was atomized into SC CO_2 through a 400 μm nozzle at a flow rate of 6 ml/min. The

solvation of SC CO_2 in the organic solvent resulted in the formation of drug loaded microparticles. It was found that, with decreasing polarity of the incorporated drug, drug loading was lowered as a result of an increase in extraction by SC CO_2, with the organic solvent acting as a cosolvent. Polar drugs, such as proteins and peptides, were successfully encapsulated by the ASES process whereas non-polar drugs failed to be encapsulated and were completely extracted by the SC CO_2 and the organic solvent.

Falk, et al., 1997 proposed making drug loaded microspheres using the SAS process. In this study drugs of gentamycin, naloxone and naltrexone and PLA were dissolved in methylene chloride using the hydrophobic ion-pairing (HIP) complexation method, which improved the solubility of the drugs considerably, to make a homogeneous solution. The prepared solutions were sprayed into SC CO_2 through an ultrasonic nozzle vibrating at 120 kHz. The drug loaded microspheres (0.2-1.0 μm) formed due to the co-precipitation of the drugs and the PLA. Drug release tests showed that gentamycin was successfully incorporated into a PLA matrix, exhibiting diffusion controlled drug release. However, naltrexone and rifampin were found to be poorly incorporated because these two drugs were more lipophilic and somewhat soluble in SC CO_2, resulting in drug surface bonding on the microspheres.

Elvassore, et al., 2001 studied the formation of protein loaded polymeric microcapsules in the SAS process. A model system of insulin and PLA was dissolved in a mixture of DMSO and dichloromethane. The prepared solution was then sprayed into SC CO_2 through a 50 μm fused silica nozzle. The results showed that insulin loaded microspheres with particle size from 0.5 to 2 μm were produced and the incorporation efficiency was as high as 80%.

Ghaderi, et al., 2000 studied the formation of microparticles with hydrocortisone loaded in DL-PLA polymer using a combination of SC N_2 and CO_2 as the antisolvent in the SEDS process. It was shown that microparticles of size less than 10 μm were produced. Hydrocortisone was successfully entrapped in DL-PLA microparticles with a loading efficiency up to 22%. The combination of SC N_2 and CO_2 was found to facilitate a more efficient dispersion of the polymer solutions than SC CO_2 alone.

Recently Tu, et al., 2002 attempted the microencapsulation of para-hydroxybenzoic acid (β-HBA) and lysozyme with PLA using the ASES process. In this research the drug solution, polymer solution and SC CO_2 were delivered through a specially designed coaxial multiple nozzle. A higher loading efficiency of 15.6 % was achieved for lysozyme encapsulation, while the β-HBA was poorly encapsulated with an efficiency of only 9.2 %.

Most of the reported research on the formation of drug loaded microspheres for controlled drug release has focused on the co-precipitation of the solute of interest (drug) and the carrier polymer using an antisolvent process. However, since a SAS co-precipitation process requires the dissolution of both the drug and the polymer in a solvent, this creates a challenge for proteins since many proteins are insoluble in organic solvents. Also, many organic solvents can denature the protein's bioactivity. Moreover, the co-precipitation of two different solutes is difficult to achieve except when the two solutes have similar thermodynamic properties and undergo similar precipitation pathways.

Therefore an alternative antisolvent process for particle coating or encapsulation was developed for drug delivery applications. In this process the host particles of interest

are suspended in a coating polymer solution instead of being dissolved as in the co-precipitation process. The prepared suspension is either sprayed into SC CO_2, or SC CO_2 is injected into the suspension. As a result of the mutual diffusion between SC CO_2 and the organic solvent, the polymer becomes supersaturated, is driven out of solution and deposits on the surface of the host particles producing a film coating.

Bertucco and Vaccaro, 1997 did a preliminary study of particle encapsulation by polymer using a GAS process. In their study, particles of KCl were suspended in a solution of polymers (hydroxypropyl methylcellulose phthalate, Eudragit E 100, ethylcellulose) in various organic solvents (toluene, acetone, 1,4-dioxane, ethylacetate). Compressed CO_2 was introduced into a high-pressure vessel, in which the suspension was charged. The compressed CO_2 was dissolved in the organic solution, leading to the loss of solvent strength of the organic solvent. As a result, the polymer precipitated out and deposited on the surface of suspended KCl particles.

Young, et al., 1999 studied the encapsulation of lysozyme in a biodegradable polymer by precipitation with a vapor-over-liquid antisolvent, which is simply a modified precipitation with a compressed anti-solvent (PCA) process. In this work, a suspension of 1-10 micron lysozyme particles in a polymer solution was sprayed into CO_2 vapor over a CO_2 liquid phase (below supercritical conditions) through a nozzle. By delayed precipitation, particles were allowed to grow large enough to encapsulate lysozyme. The process showed a high encapsulation efficiency because the polymer precipitated onto the surface of protein particles in a small droplet.

The objective of this research is to apply the SAS process to coat or encapsulate drug particles to achieve controlled drug release. Drug particles less than 30 μm in size

were chosen as hosts and a biopolymer of PLGA (50:50) was used as the coating polymer. The SAS process requires good miscibility of the solvent and SC CO_2. Once the polymer solution containing host particles in suspension contacts SC CO_2, very rapid mass transfer from the organic solvent to the bulk SC CO_2, and vice versa, takes place so that a high degree of supersaturation is achieved. The polymer nucleates and precipitates out of solution and deposits on the surface of the host particles; a film coating can be expected if sufficient polymer is deposited on the surface of the host particles.

6.2 Experimental

6.2.1 Materials

The coating material was poly lactide-co-glycolide (PLGA) (Resomer® 502, MW 12,000, 50/50, T_g 40-55 ^oC) supplied by Boehringer Ingelheim Chemicals, Inc., USA. The structure of PLGA can be seen in Figure 5.1. Acetone was purchased from Aldrich and used as received. Bone-dry liquid CO_2 was obtained from the Matheson Company, USA. Hydrocortisone (HC) (mean size less than 30 μm) was supplied by ICN Biomedical Inc., USA. It was used as received without further treatment. The molecular structure of hydrocortisone is shown in Figure 6.1.

6.2.2 Methods

The experimental set-up is schematically shown in Figure 6.2. It consists of three major systems: a suspension delivery system, a CO_2 supply system, and a stainless steel high pressure chamber with a volume of 1000 ml (Parr Instruments, USA). A water bath

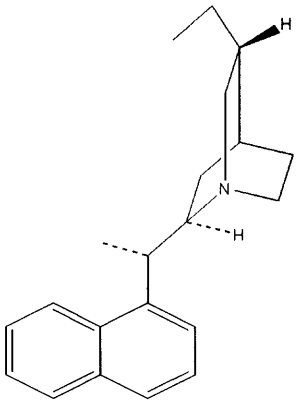

Figure 6.1 Molecular structure of hydrocortisone.

is used to keep the temperature at a desired value. A metering valve (Swagelok, SS-31RS4, R.S. Crum & Company, USA) was utilized to control the system pressure; the CO_2 inlet and outlet, and a pressure gauge are located on the lid of the high pressure chamber. A capillary nozzle (254 μm ID) is used to spray the suspension into the high pressure chamber and a metering pump (Model EL-1A, American Lewa®, USA) is used to deliver liquid CO_2 into the chamber from a CO_2 cylinder. The liquid CO_2 is chilled to around zero degrees Centigrade by a refrigerator (Neslab, RTE-111) to avoid cavitation. A heating tape (Berstead Thermolyne, BIH 171-100) is used to preheat the liquid CO_2 before it enters into the high-pressure chamber.

The experimental protocol is as follows. The precipitation chamber is first charged with SC CO_2. After the predetermined operating conditions (temperature and pressure) are reached, a steady flow of CO_2 is established by adjusting the metering valve and the metering pump. The flow rate of CO_2 was usually less than 3.0 standard liters per minute (SLPM). PLGA and hydrocortisone are then weighed and mixed into

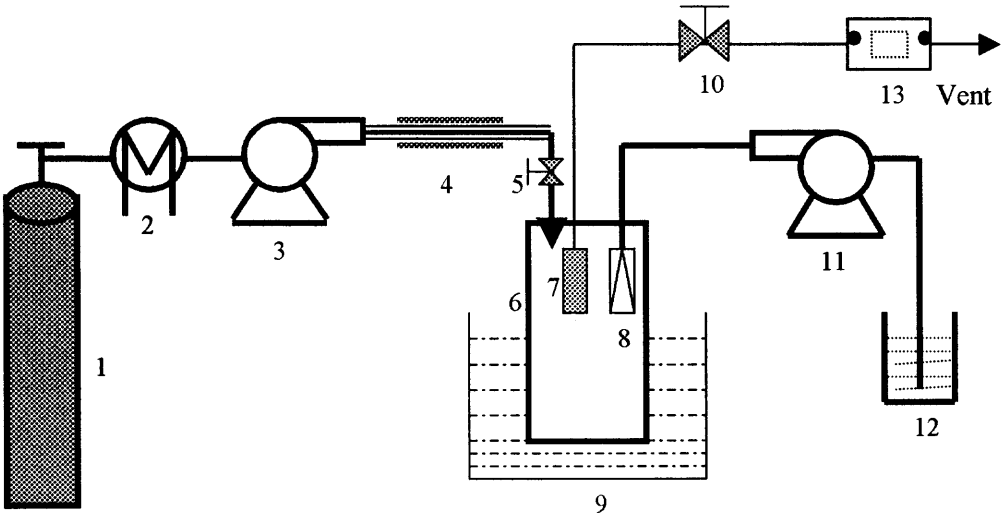

Figure 6.2 SAS coating process set-up.

Key: 1. CO_2 Cylinder, 2. Cooling, 3. CO_2 pump, 4. Pre-heating, 5. On-off valve, 6. High-pressure vessel, 7. Filter, 8. Capillary tube, 9. Water bath, 10. Needle valve, 11 High-pressure pump, 12. Slurry, 13. Mass flow meter.

dichloromethane (DCM) to produce a suspension with the desired polymer concentration and PLGA to HC ratio. The made suspension is then injected at a flow rate of 0.8 ml/min into the high pressure chamber through the capillary nozzle by using an HPLC pump (Beckman, 110B) for about 10 minutes. After spraying, fresh CO_2 is supplied continuously to purge the chamber with about 1 equivelent volume of CO_2 in order to remove any remaining dichloromethane. After purging, the precipitation chamber is slowly depressurized and the coated drug particles collected for characterization.

In addition, a parallel study of co-precipitation of hydrocortisone and PLGA was performed for comparison purposes. In the co-precipitation experiment, PLGA and hydrocortisone are dissolved in either acetone or a mixture of methanol and (volume ratio

of 1:1) to make a homogeneous solution. The solution is then sprayed into the high-pressure chamber at the same operating conditions as was used in the SAS coating process. The operating conditions of the SAS coating and the co-precipitation experiments are listed in Table 6.1.

Table 6.1 Experimental Conditions in SAS Coating and Co-precipitation Process

Parameters / Experiments	Solvent	Polymer Conc. (g/ml)	Ratio of polymer to particles (g/g)
Coating of drug particles	DCM	1.0	1:4
			1:2
			1:1
Co-precipitation of drug and PLGA	Acetone	1.0	1:1
	Methanol and DCM	1.0	1:1

6.2.3 SEM Microscopy

Field emission scanning electron microscopy (FE-SEM) (Leo, 1530VP) was used to observe any morphological changes before and after the coating treatment. The samples were simply spread on carbon tape for observation under SEM.

6.2.4 HPLC Analysis

HPLC assay analysis of hydrocortisone was performed using a Hewlett Packard 1100 equipped with a reverse phase C-18 column (Microsorb-MV 100, 150x4.6 mm, 5μm, Varian). The mobile phase was made at a composition of acetonitrile : purified water (40:60, v/v) and the injection volume was 10 μl. The flow rate was 1.0 ml/min and

hydrocortisone was detected at 242 nm by a UV detector. The run time for the assay was 4.0 minutes and the retention time for hydrocortisone was 2.9 minutes.

6.2.5 Determination of Encapsulation Efficiency (EE)

A known amount of coated drug samples was washed with ethanol, which is a good solvent for hydrocortisone but a poor solvent for PLGA, to dissolve the uncoated or partially coated drug particles. The suspension was centrifuged at 1500 rpm for 5 minutes. The supernatant fluid was sampled to determine the un-encapsulated drug content using HPLC. The sediment was then dissolved with a mixture of acetone and ethanol (50:50) and the drug content was determined using HPLC assay analysis. Each sample was analyzed in triplicate. The encapsulation efficiency (EE) was calculated using the following equation:

$$\%EE = \frac{\text{encapsulated drug}}{\text{unencapsulated drug} + \text{encapsulated drug}} \times 100\%$$

6.2.6 *In vitro* Drug Release Tests

The coated or encapsulated drug was weighed and put into a test tube along with 30 ml of pH buffer solution (PBS, pH 7.4) with 0.05% Brij 58. A small magnetic stirrer bar was used to improve the mixing. All samples were incubated at 37 ^{o}C while being agitated. At given time intervals the test tubes were centrifuged at 1500 rpm for 5 minutes and 200 µl of supernatant fluid was transferred into small vials for HPLC assay analysis, and was replaced with the same volume of fresh PBS. Dissolution tests of each sample were performed in three replicates.

6.3 Results and Discussion

SEM pictures of the original hydrocortisone particles are shown in Figure 6.3. Hydrocortisone is seen to be in crystal form with defined facets and sharp edges. The average particle size is less than 30 μm as seen from the scale bar. The coated hydrocortisone particles, at a polymer to hydrocortisone weight ratio of 1:4, are shown in Figure 6.4. The coated particles have a different shape (morphology) and no clear sharp

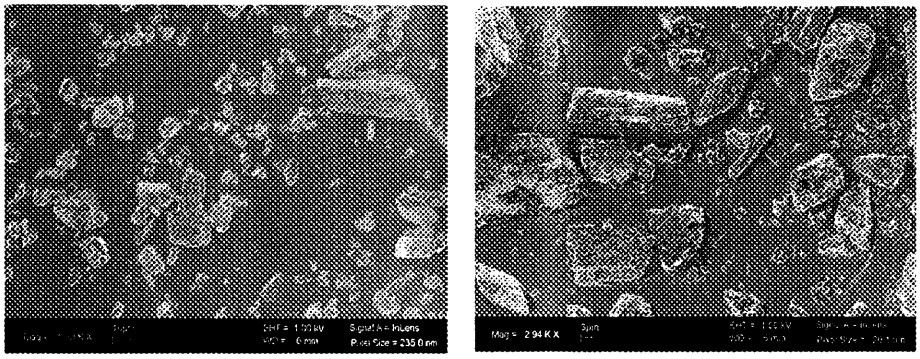

(a) (b)

Figure 6.3 Original hydrocortisone particles at different magnifications.

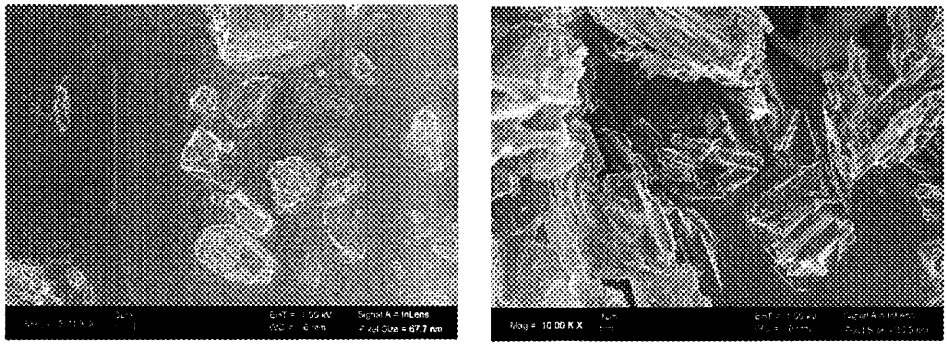

(a) (b)

Figure 6.4 Coated hydrocortisone particles at polymer to particle ratio of 1:4 at different magnifications.

edges when compared with the uncoated drug particles. This indicates that some of the drug particles were partially coated with polymer during the SAS process but no film coating or encapsulation seemed to have occurred.

The difference in shape between the coated and uncoated drug particles may be attributed to the fact that some hydrocortisone (about 17% of the total) dissolved in DCM, although DCM is not a good solvent for hydrocortisone. The dissolved drug may undergo nucleation and re-crystallization during the SAS process. Therefore, the re-crystallized drug particles formed during the SAS process may have a different shape than the original particles.

When the polymer to drug ratio was increased to 1:2, more polymer precipitated out and deposited on the surface of the drug particles as seen in Figure 6.5. The smaller drug particles seemed to be embedded or entrapped in the coating polymer. However, the larger drug particles appeared to have been left uncoated, indicating that large, irregular shaped particles may require even more polymer to encapsulate them.

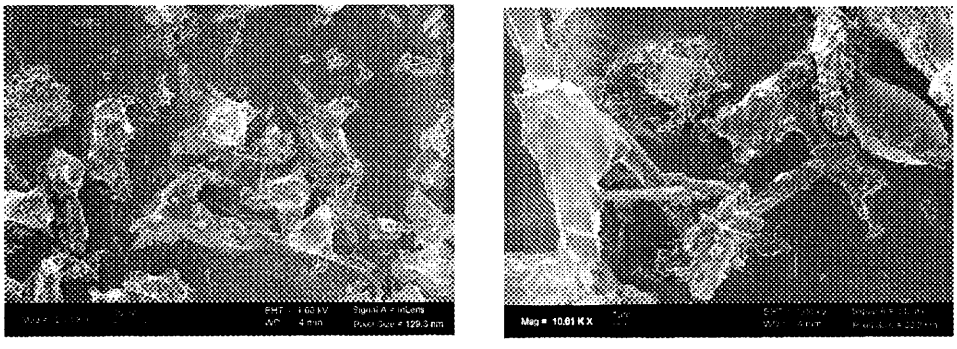

(a) (b)

Figure 6.5 Coated hydrocortisone particles at polymer to particle ratio of 1:2 at different magnifications.

In order to encapsulate the larger particles, the polymer loading was increased to a polymer to drug ratio of 1:1. SEM pictures of the coated drug particles are shown in Figure 6.6. As observed in Figure 6.6, more polymer coating took place on the surface of the drug particles as compared with drug particles coated at a 1:4 (Figure 6.4) and a 1:2 ratio (Figure 6.5). Some of the smaller drug particles were even encapsulated in polymer microspheres. However, it was found that the polymer coating on the surface of the drug particles was still unevenly distributed due to the irregularity of the drug particles. Thus it appears that uniformly coating or encapsulating irregular particles by SAS presents a major challenge.

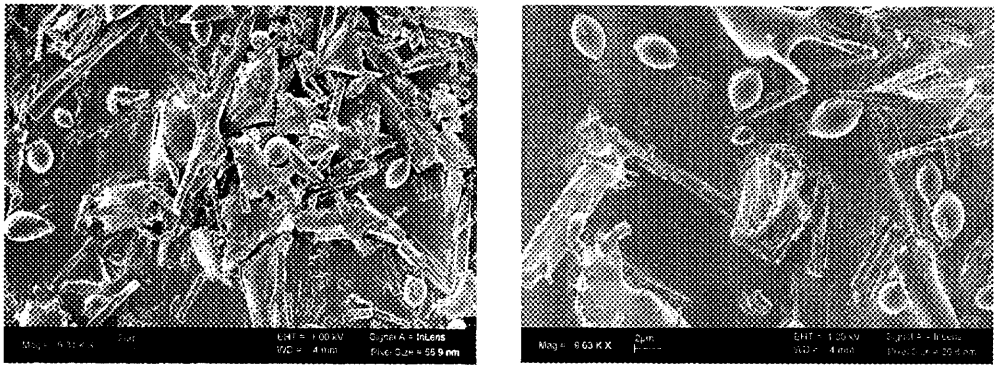

(a) (b)

Figure 6.6 Coated hydrocortisone particles at polymer to particle ratio of 1:1 at different magnifications.

A parallel study was performed to compare drug particle coating and co-precipitation using the SAS process. In the co-precipitation experiments, hydrocortisone and PLGA were dissolved in acetone or a mixture of methanol and DCM. A clear solution instead of a suspension was sprayed into SC CO_2 in the SAS process.

SEM photographs of the co-precipitated particles of drug and polymer in Figure 6.7 clearly show that the co-precipitated particles have a very different morphology and shape from the original particles. The re-crystallized drug particles have defined facets and the polymer appeared to be simply attached to (rather than coating) the surface of the re-crystallized drug particles. It was apparent that there was a phase separation during the precipitation of polymer and drug from the acetone or mixture of DCM and methanol solutions. Therefore, it appears that no coating or encapsulation occurred in the SAS co-precipitation process.

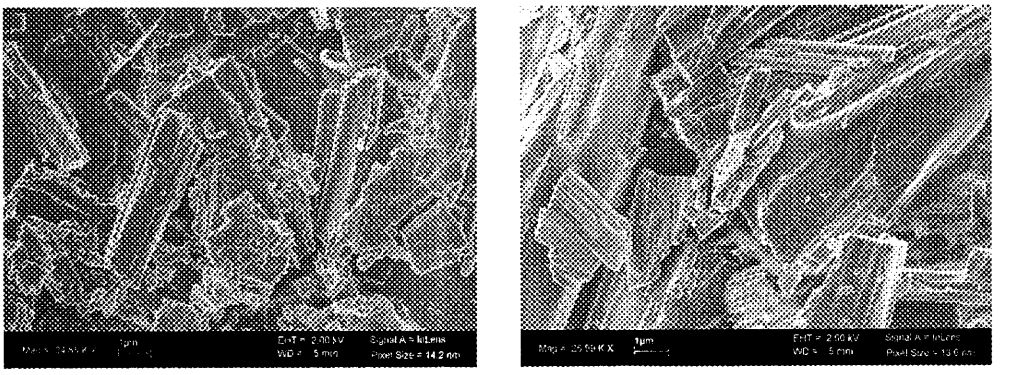

(a) (b)

Figure 6.7 Co-precipitated particles of polymer to drug ratio at 1:1. (a) Methanol and DCM; (b) Acetone.

The coated drug particles and co-precipitated drugs were analyzed to determine the encapsulation efficiency. The results are listed in Table 6.2. The coated drug particles at a polymer to drug ratio of 1:4 showed that drug particles were not encapsulated within the polymer. This supported the conclusion that the drug particles were only partially coated by polymer as shown in Figure 6.4. In the encapsulation efficiency test, if an

uncoated part of the surface of a drug particle is exposed to ethanol, the whole drug particle would be dissolved gradually. Therefore, partially coated drug particles did not show any encapsulation efficiency. When the polymer loading was increased to a ratio of 1:2, more polymer coating occurred on the surface of drug particles and the average encapsulation efficiency increased to 6.7%. When more polymer was used, the smaller drug particles were probably completely encapsulated by the polymer. Consequently,

Table 6.2 Encapsulation Efficiency (EE) of Coated and Co-precipitated Drug Particles

Ratio of PLGA to HC	SAS Process	Encapsulation Efficiency (EE) (%)	Average (%)	SD
1:4	*Coating	0	0	0
1:2	Coating	8.4	6.7	± 1.4
		6.3		
		5.4		
1:1	Coating	21.5	22.6	± 2.3
		25.2		
		21.2		
1:1	*Co-precipitation from methanol and DCM	0	0	0
1:1	*Co-precipitation from acetone	0	0	0

* Analysis was performed in three replicates on each sample.

these encapsulated drug particles were not washed away by ethanol in the encapsulation efficiency test and they contributed to the encapsulation efficiency. However, the encapsulation rate was not improved considerably even though the polymer loading was doubled. This was probably due to the fact that the larger, irregular-shaped drug particles

left some sharp edges or corners uncoated and therefore were completely dissolved by the ethanol treatment.

When the polymer to particle ratio was further raised to 1:1, more drug particles were encapsulated and the encapsulation efficiency increased to 22.6%. This supported the observation in Figure 6.6 that more of the drug particles were completely encapsulated or trapped in polymer microspheres. This suggests that the encapsulation efficiency could be further improved by either increasing the amount of polymer or reducing the size of host particles.

The co-precipitated drug and polymer particles from either acetone or a mixture of methanol and DCM showed no encapsulation of drug particles even at a polymer to drug ratio of 1:1. This is in good agreement with what was observed in Figure 6.7 that the re-crystallized drug was not encapsulated with polymer and that the polymer was simply attached on the surface of the drug particles.

In vitro drug release tests were carried out to determine the release behavior of coated drug particles at different polymer to drug ratios. The release profiles are plotted in Figure 6.8. The drug particles coated at a 1:4 ratio showed a fast release behavior; almost all of the drug content was released in about 1.5 hours. This rapid release rate was attributed to the fast dissolution of the drug particles. The release behavior confirmed the result of the encapsulation test of the coated particles at a 1:4 polymer to drug ratio that no drug particles were entirely encapsulated.

The coated particles at a 1:2 ratio showed an initial release of about 90% of the drug content in about 1.5 hours. After the initial burst, a second phase of much slower drug release (Figure 6.8) occurred. At day 9 the PLGA started to degrade and the rest of

the encapsulated drug was released in about 1 day. This suggested that about 10% of the drug particles were completely encapsulated, which was close to the encapsulation efficiency test result. The uncoated or partially coated drug particles were quickly dissolved in the release medium and this accounted for the burst release.

The drug particles coated at a 1:1 ratio showed a lower amount of fast release of drug than those coated at the 1:2 ratio. About 80% of drug was released during this phase. After this initial burst stage, a period of much slower drug release occurred before the onset of the polymer degradation stage. In about 9 days, PLGA started to degrade and the encapsulated drug was continuously released for about 3 days. This release behavior

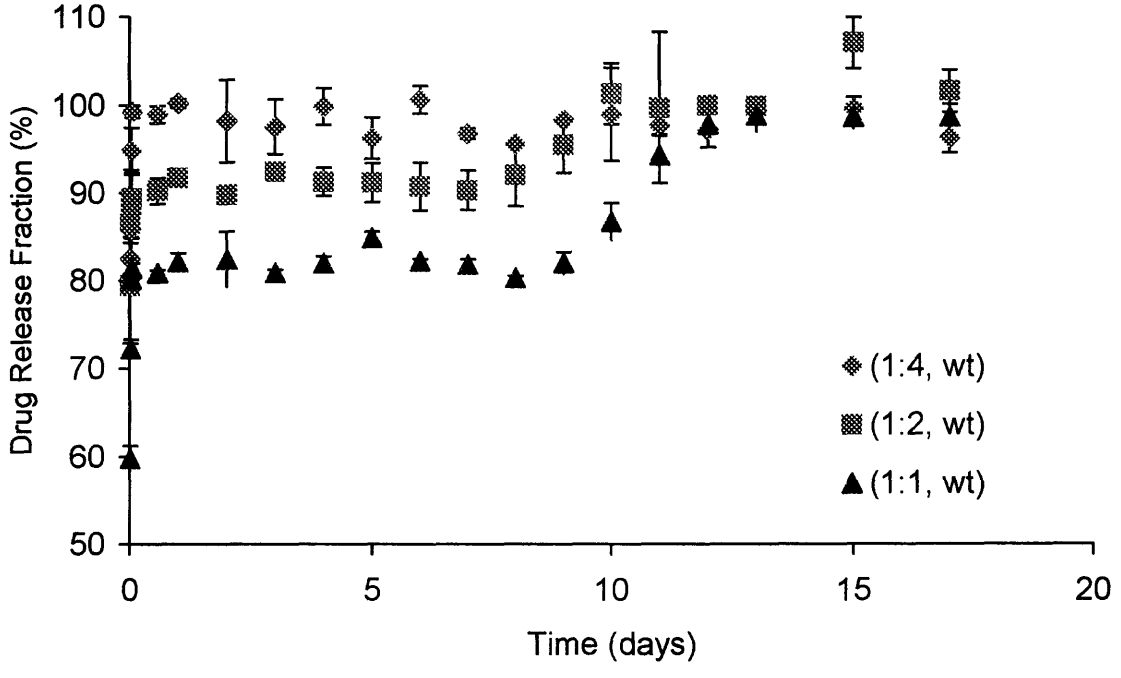

Figure 6.8 Overall hydrocortisone release profiles of coated drug particles at different polymer to drug ratios.

again supported the results of the encapsulation efficiency test on the coated drug particles at a 1:1 ratio. The sigmoidal release profile exhibited by the drug articles coated with at a 1:1 polymer to drug ratio was typical of polymer degradation controlled drug release (Fitzgerald and Corrigan, 1996; Gallagher and Corrigan, 2000). By increasing the amount of polymer used for coating or reducing the size of the drug particles, a larger fraction of drug particles would be incorporated into polymer microspheres. Thus, the initial burst release would be reduced and the release of drug would last longer.

To compare the SAS coating and co-precipitation processes, a drug release test of the co-precipitated sample from acetone was performed following the same procedure. The release profile is shown in Figure 6.9. It is clear from the figure that the re-crystallized drug and PLGA from the co-precipitation process exhibited a very fast

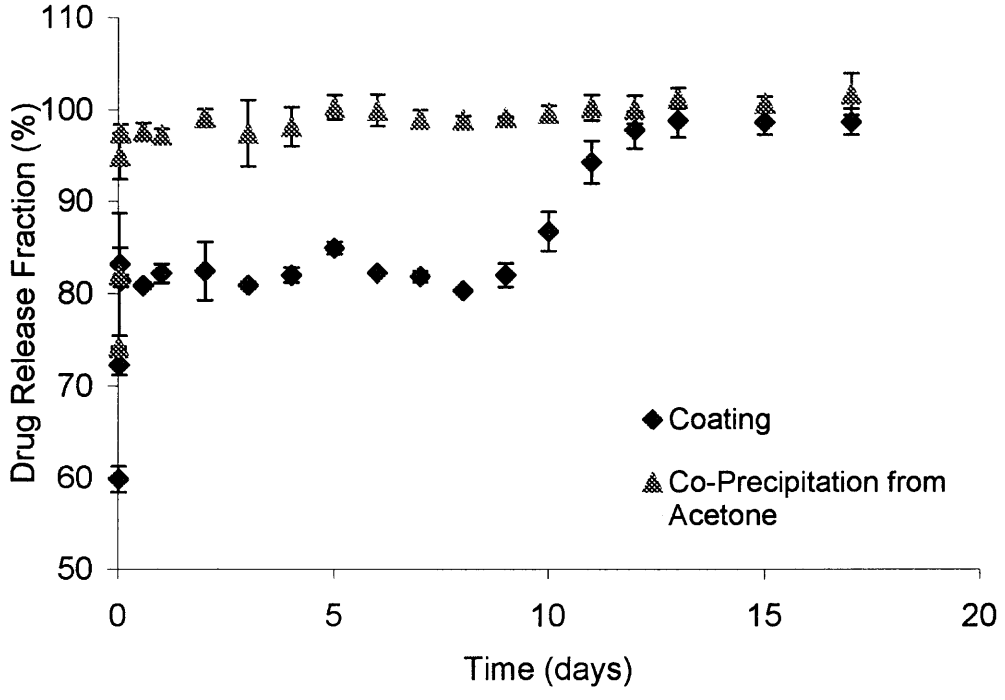

Figure 6.9 Overall hydrocortisone release profiles of coated drug particles and co-precipitated drug and PLGA from acetone.

release of the drug throughout the entire duration of the test. This suggests that no encapsulation occur ed during the co-precipitation of drug and PLGA even at a polymer to drug ratio of 1:1. This release test result confirmed the encapsulation test result.

6.4 Concluding Remarks

Hydrocortisone particles were shown to be successfully coated with PLGA in the SAS coating process. At a low 1:4 polymer to drug weight ratio the drug surface was only partially coated and no encapsulation (encapsulation efficiency of zero) occurred The encapsulation efficiency improved with an increase in polymer to drug ratio and increased to 22.6% when the polymer to drug ratio was 1:1. At polymer to drug ratios of 1:2 and 1:1, the coated drug particles exhibited a sustained release behavior. However, coprecipitations of drug and polymer (both in solution) failed to achieve encapsulation; the polymer appeared to be simply attached in chunks on to the surface of the drug particles.

Although the encapsulation efficiency achieved was low and an initial burst stage was observed, an impovement in the drug sustained release properties could probably be obtained by increasing the polymer loading or reducing the size of the drug particles because smaller particles have a greater chance to be encapsulated or entrapped. Thus the SAS coating process is a promising technique for the design of drug delivery systems and might be especially useful for inhalation drugs where the particle size cannot be larger than a few microns.

CHAPTER 7

RECOMMENDATIONS FOR FUTURE WORK

The research presented in this dissertation has focused on applying supercritical fluid processes for particle coating or encapsulation. Two main processes have been investigated: a modified RESS and a SAS coating process. An important commercial application of the SAS coating process is in the coating or encapsulation of drug particles for controlled drug release system design. The results of this research showed that supercritical CO_2 could be been successfully applied as an antisolvent for particle coating or encapsulation when using a polymer as the processing (coating) medium. The SAS coating process, in particular, because of its flexibility in choosing a solvent for dissolving the polymer and the mild operating conditions associated with supercritical CO_2, has been utilized to coat or encapsulate particles in a very broad size range from 20 nm to 30 μm. Moreover, it was found that each individual particle could be coated or encapsulated with polymer with minimum agglomeration.

The nature of the physical deposition process due to a phase separation, which is prompted by mutual mass transfer between SC CO_2 and an organic solvent, made the SAS coating process attractive for controlled drug release. A case study of hydrocortisone particle coating or encapsulation with PLGA polymer utilizing the SAS coating process revealed that the coated or encapsulated drug particles showed sustained release behavior. Thus the SAS process is very promising for coating or encapsulating those drugs, which are heat sensitive and less likely to be dissolved (e.g. peptide or proteins) in organic solvents.

Although supercritical coating processes (Modified RESS and SAS) are technically feasible alternatives for particle coating or encapsulation, they are still in their nascent stage. The results of this dissertation suggest many opportunities for future research work. Since the solubility of many substances of interest in supercritical CO_2 is very low, the application of a modified RESS particle coating process is limited. Therefore specific recommendations for future work are directed to the SAS coating process; these include a better understanding of its fundamentals, applicability, productivity enhancement, and applications for controlled drug release.

7.1 Recommendation for Future Work in the SAS Coating Process

7.1.1 Fundamental understanding of the SAS coating process

The SAS process has been extensively investigated both in the academic and industrial arena. Numerous research results have been published covering its applications for particle formation and particle coating, modeling and computer simulations, and mechanisms. The SAS process is very complicated since thermodynamics, kinetics, mass transfer, and hydrodynamics are all involved. Although many mechanisms were proposed from different point of views in many publications (Dixon, et al., 1993; Thies and Müller, 1998; Randolph et al., 1993; Bristow, et al., 2001), the fundamental understanding of SAS process remains unclear and contradictory observations were revealed (Reverchon and Porta, 1999; Moshashaée, et al., 2000). Due to the interplay of thermodynamics, kinetics, mass transfer, and hydrodynamics, an isolated consideration of one or two effects is not sufficient to address this complex issue. This is the reason why contradictory findings were reported on different systems.

To fully understand the SAS process, the thermodynamics of solvent-CO_2-solute phase behavior should be considered first. It determines the mass transfer, the degree of supersaturation of solute, and the interfacial energy of the solute and solvent, which will affect the particle size, particle size distribution, morphology and crystalline structure. Therefore, it is necessary to investigate the thermodynamic behavior before one considers a system for particle formation. In consideration of mass transfer, the diffusion coefficient between the SC CO_2 and organic solvent is important because the time scale for the solution to reach a high degree of supersaturation is strongly dependent on the mass transfer between the two miscible phases. Faster mass transfer favors primary nucleation, which results in smaller particles according to classical nucleation theory.

Kinetics is directly related to the formation of particles and should be carefully considered (see for example, Bristow, et al., 2001). Hydrodynamic considerations are also very important and influence the design of the nozzle. The effects of nozzle geometry on the final particle properties, which were reported by Thies and Müller, 1998, Reverchon, et al., 2000, Breitenbach, et al., 2000, and Mawson, et al., 1997, can be correlated to the hydrodynamic effects.

When a polymer is used as the solute, the SAS process becomes more complicated because the viscosity of the polymer solution increases considerably as the mass transfer between SC CO_2 and organic solvent proceeds (Dixon and Johnston, 1993). In addition, CO_2 is a small molecule substance and can easily diffuse into polymer chains. The dissolved or absorbed CO_2 causes a depression of the glass transition temperature (T_g) (Chiou, et al., 1985; Wissinger and Paulaitis, 1991 a, b; Condo, et al., 1994) and the subsequent plasticization of the polymer will facilitate the agglomeration

of polymer particles. Therefore an understanding of the correlation between the viscosity of the polymer solution, the mass transfer rate and a knowledge of the plasticization of the polymer by compressed CO_2 would be very helpful to better control either polymer particle formation or particle coating/encapsulation with polymer in the SAS process.

7.1.2 Enhancement of productivity and controllability of the SAS coating process

In this research the SAS coating process was operated in batch mode and in each experiment only a small amount of sample was collected for performing different characterizations. However, the SAS process has the potential to be operated in continuous mode as described by Randolph, et al., 1993. Theoretically, as long as an equilibrium is established between the inlet and outlet CO_2 flow rate, and if the extraction of organic solvent is fast enough so that the coated particles become solidified before contacting other coated particles, the spraying of a suspension of host particles in the coating polymer solution can be continued until the amount of coated particles reaches a predetermined value in the high pressure chamber. At this point in time the spraying of the suspension can be switched to another high pressure chamber and the SAS coating process can be continued. Meanwhile, the first chamber containing the coated particles can be depressurized for product collection. A multi-nozzle spraying system can also be considered to increase the throughput of product.

Process control can also be implemented as long as the critical parameters, which are based on an understanding of the mechanisms of the SAS process, are identified and found to have a direct influence on the quality of the final product. From the observations and results reported in this dissertation, parameters such as temperature, pressure, flow

rate of CO_2, flow rate of solution, solution concentration, solvent molar fraction in the chamber, should all be carefully monitored.

7.2 Recommendation for Future Work for Controlled Drug Release Using SAS

Although the SAS coating process for controlled drug release showed very promising results, the encapsulation efficiency was low, 22.6 %, at a polymer to drug ratio of 1:1. This is attributed to the large particle size and irregular shape of drug particles that were used in the experiments. Smaller particles would have a greater chance to be encapsulated or entrapped in the polymer microspheres. It is recommended that future research for the design of a controlled drug release system using SAS should focus on smaller drug particles (less than 10 μm). Moreover, smaller particles incorporated into polymer microspheres could make a matrix structure.

In this dissertation, it was found that the PLGA biopolymer used to coat the drug was a degradation controlled release biopolymer (Gallagher and Corrigan, 2000), in which the PLGA absorbed water from the medium and underwent hydrolysis. This was a very slow process. Furthermore, once the coating polymer degrades on a surface with a very thin film coating, the whole drug particle is eroded right away. This drug release behavior is undesirable. Therefore, smaller particles entrapped in polymer microspheres with a matrix structure are desirable to give a better controlled release behavior.

Usually PLGA is used to produce a long-term sustained release, sometimes as long as 30 days or more. For some drugs it is not necessary to have such a long time release, normally 1 or 2 days is sufficient. Diffusion controlled polymer release would be useful for this purpose. These polymers include Eudragit (copolymer of methacrylates

and acrylates), chitosan (cationic polysaccharide), hydrogels, etc. In terms of selecting the model drug for research purposes, the drug should have a relative easy assay analysis method available.

Another research direction should that might be useful in the design of a drug delivery system using the SAS process is the method of solid dispersion composite particle fabrication (Moneghini, et al., 2001). When drugs with low solubility are dispersed in polymer at the molecular level so that the drug is in an amorphous state instead of having a crystalline structure, the dissolution and bioavailability of the drugs can be improved. The carrier polymer, such as povidone, cyclodextrin (Chulia, et al., 1998) and PEG (Moneghini, et al., 2001), is used to stabilize the drug and to improve the bioavailability. The SAS process appears to be very attractive for a drug delivery system design for this category of drugs.

REFERENCES

Agkerman, A. and Yeo, S. "Supercritical extraction of organic components from aqueous slurries", *Supercritical Fluid Engineering Science*, eds, E. Kiran and J. F. Brennecke, *ACS Symp, Ser. 514*, American Chemical Society: Washington, D. C., 1989.

Allen, A., *US Patent 4 073 131*, 1978.

Andrews, A. T.; Ahlert, R. C.; Kosson, D. S., "Supercritical extraction of aromatic contaminants from a sandy loam soil", *Env. Prog.*, 17, 1991, 1.

Baxter, G., "Microencapsulation technology and modern business forms", *Tappi*, 60, 1977, 84.

Benita, S.; Zouai, D.; Benoit, J. P., "5-Fluorouracil: Carnauba wax microspheres for chemoembolization, an in vitro evaluation", *J. Pharmac. Sci.*, 75, 1986, 847.

Bergna, H. E., *US Patent 4 677 084*, 1987.

Berends, E. M.; Bruinsma, O. S. L.; Graauw, J. D.; Rosmalen, G. M., "Crystallization of phenanthrene from toluene with carbon dioxide by the GAS process", *AIChE J.*, 42, 1996, 431.

Bertucco, A. and Vaccaro, F., "Drugs encapsulation using a compressed gas antisolvent technique", *The Forth Italian Conference on Supercritical Fluids and their Application*, E. Reverchon (Ed.), September 7-10, Capri, 1997, 327.

Blanco-Príeto, M. J.; Fattal, E.; Gulik, A.; Dedieu, J. C.; Roques, B. P.; Couvreur, P., "Characterization and morphological analysis of a cholecystokinin derivative peptide-loaded poly(lactide-co-glycolide) microspheres prepared by a water-in-oil-in-water emulsion solvent evaporation method", *J. Control. Rel.*, 43, 1997, 81.

Blasig, A.; Shi, C.; Enick, R. M.; Thies, M. C., "Effect of concentration and degree of saturation on RESS of a CO_2-soluble fluoropolymer", *Ind. Eng. Chem. Res.*, 41, 2002, 4976.

Breitenbach, A.; Mohr, D.; Kissel, T., "Biodegradable semi-crystalline comb polyesters influence the microsphere production by means of a supercritical fluid extraction technique (ASES)", *J. Control. Rel.*, 63, 2000, 53.

Brennecke, J. F., "New applications of supercritical fluids", *Chemistry & Industry*, 4, 1996, 831.

Bristow, S.; Shekunov, T.; Shekunov, Yu. B.; York, P., "Analysis of the supersaturation and precipitation process with supercritical CO_2", *J. Supercrit. Fluids*, 21, 2001, 257.

Brannon-Peppas, L., "Recent advances on the use of biodegradable microparticles and nanoparticles in controlled drug delivery", *Intl. J. Pharm.*, 116, 1995, 1.

Cai, J. G.; Liao, X. C.; Zhou, Z. Y., "Microparticle formation and crystallization rate of HMX using supercritical dioxide anti-solvent recrystallization", *The 4th International Symposium on Supercritical Fluids*, May 11-14, Sendai, Japan, 1997 23.

Canelas, D. A.; Betts, D. E.; DeSimone, J. M., "Poly (vinyl acetate) and poly (vinyl acetate-*co*-ethylene) latexes via dispersion polymerizations in carbon dioxide", *Macromolecules,* 31, 1998, 6794.

Capan, Y.; Woo, B. H.; Gebrekidan, S.; Ahmed, S.; DeLuca, P. P., "Influence of formulation parameters on the characteristics of poly (D, L-lactide-co-glycolide) microspheres containing poly (L-lysine) complexed plasmid DNA", *J. Control. Rel.*, 60, 1999, 279.

Chang, C. J. and Randolph, A. D., "Precipitation of microsize organic particles from supercritical fluids", *AIChE J.*, 35, 1989, 1876.

Chang, C. J. and Randolph, A. D., "Solvent expansion and solute solubility predictions in gas-expanded liquids", *AIChE J.*, 36, 1990, 939.

Chang, S.-Y.; Liu, L.; Asher, A. A., "Preparation and properties of tailored morphology, monodisperse colloidal silica-cadmium sulfide nanocomposites", *J. Am. Chem. Soc.*, 116, 1994, 6739.

Charoenchaitrakool, M; Dehghani, F; Foster, N. R., "Micronization by rapid expansion of supercritical solution to enhance the dissolution rate of poorly water-soluble pharmaceuticals", *Ind. Eng. Chem. Res.*, 39, 2000, 4794.

Chattopadhyay, P. and Gupta, R. B., "Supercritical CO_2 based production of fullerence nanoparticles", *Ind. Eng. Chem. Res.*, 39, 2000, 2281.

Chattopadhyay P. and Gupta, R. B., "Protein nanoparticles formation by supercritical antisolvent with enhanced mass transfer", *AIChE J.*, 48, 2002, 235.

Chattopadhyay, P. and Gupta, R. B., "Production of antibiotic nanoparticles using supercritical CO_2 as antisolvent with enhanced mass transfer", *Ind. & Eng. Chem. Res.*, 40, 2001, 3530.

Chiannikulchi, N.; Driouich, Z.; Benoit, J. P.; Couvreur, P., "Doxorubicin-loaded nanoparticles: Increased efficiency in murine hepatic metastase", *Select. Cancer. Therap.*, 5, 1989, 1.

Chiou, J. S.; Barlow, J. W.; Paul, D. R., "Plasticization of glassy polymers by CO_2", *J. Appl. Polym. Sci.*, 30, 1985, 493.

Chou, Y. H. and Tomasko, D. L., "GAS crystallization of polymer-pharmaceutical composite particles", *The 4th International Symposium on Supercritical Fluids*, May 11-14, Sendai, Japan, 1997, 55.

Chulia, D.; Deleuil, M.; Pourcelot, Y., *Powder Technology and Pharmaceutical Processes*, Elsevier, 1998.

Cocero, M. J. and Ferrero, S., "Crystallization of β-carotene by a GAS process in a batch effect of operating conditions", *J. Supercrit. Fluids*, 22, 2002, 237.

Condo, P. D.; Paul, D. R.; Johnston, K. P., "Glass transition of polymers with compressed fluid diluents: Type II and III behavior", *Macromolecules*, 27, 1994, 365.

Cohen, H.; Levy, R. J.; Gao, J.; Kousaev, V.; Sosnowski, S.; Slomkowski, S.; Golomb, G., "Sustained delivery and expression of DNA encapsulated in polymeric nanoparticles", *Gene Therapy*, 7, 2000, 1896.

Curt, T., *Encyclopedia of polymer science and technology*, 9, 1987, 724.

Davies, R.; Schur, G. A.; Meenan, P.; Nelson, R. D.; Bergna, H. E.; Brevett, C. A. S.; Goldbaum, R. H., "Engineered Particle Surfaces", *Advanced Materials*, 10, 1998, 1264.

Debenedetti, P.G. and Kumar, S. K., "Infinite dilution fugacity coefficients and general behavior of dilute binary systems", *AIChE J.*, 32, 1986, 1253.

Department of Commerce, US Industrial Output, Washington, DC 1993.

DeSimone, J. M.; Guan, Z.; Elsbernd, C. S., "Synthesis of fluoropolymers in supercritical carbon dioxide", *Science*, 257, 1992, 945.

Dixon, D. J.; Johnston, K. P.; Bodmeier, R. A., "Polymeric materials formed by precipitation with a compressed fluid antisolvent", *AJChE J.*, 39, 1993, 127.

Dillow, A. K.; Dehghani, F.; Foster, N.; Hrkach, J.; Langer, R. S., "Production of polymeric support materials using supercritical fluid anti-solvent process", *The 4th International Symposium on Supercritical Fluids*, May 11-14, Sendai, Japan, 1997, 247.

Domingo, C.; Berends, E. M.; Van Rosmalen, G. M., "Precipitation of ultrafine benzoic acid by expansion of a supercritical carbon dioxide solution through a porous plate nozzle", *J. Crystal Growth*, 166, 1996, 989.

Dorski, C. K.; Doyle, F. J.; Pappas, N. A., "Preparation and characterization of glucose-sensitive P(MAA-g-EG) hydrogels", *Polym. Mater. Sci. Eng. Proceed.*, 76, 1997, 281.

Elvassore, N.; Bertucco, A.; Caliceti, P., "Production of protein-loaded polymeric microcapsules by compressed CO_2 in a mixed solvent", *Ind. Eng. Chem. Res.*, 40, 2001, 795.

Falk, R. F. and Randolph, T. W., "Process variable implications for residual solvent removal and polymer morphology in the formation of gentamycin-loaded poly (L-lactide) microparticles", *Pharm. Res.*, 15, 1998, 1233.

Falk, R.; Randolph, T. W.; Meyer, J. D.; Kelly, R. M.; Manning, M. C., "Controlled release of ionic compounds from poly (L-lactide) microspheres produced by precipitation with a compressed antisolvent", *J. Control. Rel.*, 44, 1997, 77.

Fattal, E.; Youssef, P.; Couvreur, P.; Andremont, A., " Treatment of experimental salmonellosis in mice with ampicillin-bound nanoparticles", *Antimicrob. Agent Chimother.*, 33, 1989, 1540.

Fitzgerald, J. F. and Corrigan, O. I., "Investion of the mechanisms governing the release of levamisole from poly-lactide-co-glycolide delivery systems", *J. Control. Rel.*, 42, 1996, 125.

Fu, K.; Griebenow, K.; Hseih, L.; Klibanov, V. M.; Langer, R., "FTIR characterization of the secondary structure of proteins encapsulated within PLGA microspheres", *J. Control. Rel.*, 58, 1999, 357.

Gallagher, P. M.; Coffey, M. P.; Krukonis, V. J., "Gas anti-solvent recrystallization of RDX: Formation of ultrafine particles of a difficult-to-comminute explosive", *J. Supercrit. Fluids*, 5, 1992, 130.

Gallagher, K. M. and Corrigan, O. I., "Mechanistic aspects of the release of levamisole hydrochloride from biodegradable polymers", *J. Control. Rel.*, 69, 2000, 261.

Gallagher-Wetmore, P., *3rd symposium on supercritical fluids*, October 1994, Strasbourg (France).

Ghaderi, R.; Artursson, P.; Carlfors, J., "A new method for preparing biodegradable microparticles and entrapment of hydrocortisone in D,L-PLG microparticles using supercritical fluids", *European J. of Pharm. Sci.*, 10, 2000, 1.

Hanna, M. and York, P., *Patent WO 95/01221*, 1994.

Hannay, J. and Hoghart, "On the solubility of solids in gases", *J. Proc. Roy. Soc.* (London), 29, 1879, 324.

Helfgen, B.; Hils, P.; Holzknecht, Ch.; Türk, M.; Schaber K., "Simulation of particle formation during the rapid expansion of supercritical solutions", *J. Areosol Sci.*, 32, 2001, 295.

Hoefling, T. A.; Beitle, R. R.; Enick, R. M.; Beckman, E. J., "Design and synthesis of highly CO_2-soluble surfactants and chelating agents, *Fluid Phase Equilibria*, 83, 1993, 203.

Hrkach, J. S.; Peracchia, M. T.; Domb, A.; Lotan, N.; Langer, R., "Nanotechnology for biomaterials engineering: Structural characterization of amphiphilic polymeric nanoparticles by ^{1}H NMR spectroscopy", *Biomaterials*, 18, 1997, 27.

Ike, O.; Shimizu, Y.; Wada, R.; Hyon, S. -H.; Ikada, Y., "Controlled cisplatin delivery system using poly (D, L-Lactic acid)," *Biomaterials,* 13, 1992, 230.

Iler, R. K., *US Patent 2 885 366,* 1959.

Ishizaka, T.; Honda, H.; Kikuchi, Y.; Katano, T.; Koishi, M., *Chem. Pharm. Bull.*, 36, 1988, 2562.

Ivy, E. E. and Pencap, M., "Improved methylparathion formulation", *J. of Economic Entomology*, 65, 1972, 473.

Jacobson, H. W., *US Patent 4 222 789,* 1980.

Jennings, D. W.; Deutsch, H. M.; Zalkow, L. H.; Teja, A. S., "Supercritical extraction of taxol from the bark of Taxus brevifolia", *J. Supercrit. Fluids*, 5, 1992, 1.

Jessop, P. G.; Ikariya, T.; Noyori, R., "Homogeneous catalysis in supercritical fluids", *Chem. Rev.*, 99, 1999, 475.

Jong, Y. S.; Jacob, J. S.; Yip, K. –P.; Gardner, G.; Seitelman, E.; Whitney, M.; Montgomery, S.; Mathiowitz, E., "Controlled release of olasmid DNA", *J. Control. Rel.*, 47, 1997, 123.

Kage, H.; Takahashi, T.; Yoshida, T.; Ogura, H.; Matsuno, Y., "Coating efficiency of seed particles in a fluidized bed by atomization of a powder suspension", *Powder Technol.*, 86, 1996, 243.

Katayama, T.; Ohgaki, K.; Maekawa, G.; Goto, M.; Nagano, T., "Isothermal vapor-liquid equilibria of acetone-carbon dioxide and methanol carbon dioxide systems at high pressures", *J. Chem. Engr. of Japan*, 8, 1975, 89.

Kazarian, S. G.; Brantley, N. H.; Eckert, C. A., "Dyeing to be clean: Use supercritical carbon dioxide", *Chemtech*, 7, 1999, 36.

Kendall, J. L.; Canelas, D. A.; Young, J. L.; DeSimone, J.M., "Polymerizations in supercritical carbon dioxide", *Chem. Rev.*, 99, 1999, 543.

Kim, J. H.; Paxton, T. E.; Tomasko, D. L., "Microencapsulation of naproxen using rapid expansion of supercritical solutions", *Biotechnol. Prog.*, 12, 1996, 650.

Kiran, E. and Pöhler, H., "Alternative solvents for cellulose derivatives: miscibility and density of cellulosic polymers in carbon dioxide + acetone and carbon dioxide + ethanol binary fluid mixtures", *J. Supercrit. Fluids*, 13, 1998, 135.

Kiran, E.; Debenedetti, P. G.; Peters, C. J., *Supercritical fluids: Fundamentals and applications*, *NATO Science Series*, E 366, Kluwer Academic Publishers, 2000.

Ko, J. A.; Park, H. J.; Hwang, S. J.; Park, J. B.; Lee, J. S., "Preparation and characterization of chitosan microparticles intended for controlled drug delivery", *Intl. J. of Pharm.*, 249, 2002, 165.

Kordikowski, A; Schenk, A. P.; Van Nielen, R. M.; Peters, C. J., "Volume expansions and vapor-liquid equilibria of binary mixtures of a variety of polar solvents and certain near-critical solvents", *J. Supercrit. Fluids*, 8, 1995, 205.

Krukonis, V, "Supercritical fluid nucleation of difficult-to-comminute solids", paper 140f, *AIChE meeting*, San Francisco, Number, 1984.

Lefebvre, A.H., *Atomisation and Sprays*, Hemisphere Publishing, New York (1989).

Lele, A. and Shine, A. D., "Effect of RESS dynamics on polymer morphology", *Ind. Eng. Chem. Res.*, 33, 1994, 1476.

Lengsfeld, C. S.; Delplangue, J. P.; Barocas, V. H.; Randolph, T. W., "Mechanism Governing Microparticle Morphology during Precipitation by a Compressed Antisolvent: Atomization vs. Nucleation and Growth. *J. Phys. Chem. B*, 104, 2000, 2725.

Leong, K. W.; Mao, H. -Q.; Truong-Le, V. L.; Roy, K.; Walsh, S. M.; August, J. T., "DNA-polycation nanospheres as non-viral gene delivery vehicles", *J. Control. Rel.*, 53, 1998, 183.

Leroux, J. C.; Allémann, E.; Jaeghere, F. D.; Doelker, E.; Gurny, R., "Biodegradable nanoparticles-from sustained release formulations to improved site specific drug delivery", *J. Control. Rel.*, 39, 1996, 339.

Lim, G. B.; Lee, S. Y.; Koo , K. K.; Park, B. S.; Kim, H. S., "Gas anti-solvent recrystallization of molecular explosives under sub-critical to supercritical conditions", *Proceedings of the 5th Meeting on Supercritical Fluids*, Tomel; ISBN 2-905-267-28-3, March 23-25, Nice, France, 1998, 271.

Liu, H. and Yates, M. Z., "Development of a carbon dioxide-based microencapsulation technique for aqueous and ethanol-based latexes", *Langmuir,* 18, 2002, 6066.

Lora, M.; Bertucco, A.; Kikic, I., "Simulation of the semicontinuous supercritical antisolvent recrystallization process", *Ind. Eng. Chem. Res.,* 39, 2000, 1487.

Lück, M.; Pistel, K.-F.; Li, Y.-X.; Blunk, T.; Müller, R. H.; Kissel, T., "Plasma protein adsorption on biodegradable microspheres consisting of poly(D, L-lactide-co-glycolide), poly(L-lactide) or ABA triblock copolymers containing poly(oxyethylene): Influence of production method and polymer composition", *J. Control. Rel.*, 55, 1998, 107.

Luna-Xavier, J.-L.; Guyot, A.; Bourgeat-Lami, E., "Synthesis and characterization of silica/poly (methyl methacrylate) nanocomposite latex particles through emulsion polymerization using a cationic azo initiator", *J. Colloid and Interface Science*, 250, 2002, 82.

Matson, D. W.; Fulton, J. L.; Petersen, R. C.; Smith, R. D., "Rapid expansion of supercritical fluid solutions: solute formation of powders, thin film, and fibers", *Ind. Eng. Chem. Res.*, 26, 1987, 2298.

Matson, D. W.; Peterson, R. C.; Smith, R. D., "Production of fine powders by the rapid expansion of supercritical fluid solutions", *Adv. Ceram.*, 21, 1987, 109.

Mawson, S.; Johnston, K. P.; Combes, J. R.; DeSimone, J. M., "Formation of poly (1,1,2,2,-tetrahydroperfluorodecyl acrylate) submicron fibers and particles from supercritical carbon dioxide solutions", *Macromolecules*, 28, 1995, 3182.

Mawson, S.; Kanakia, S.; Johnston, K. P., "Coaxial nozzle for control of particle morphology in precipitation with a compressed fluid antisolvent", *J. Appl. Polym. Sci.*, 64, 1997, 2105.

Mawson, S.; Yates, M. Z.; O'Neill, M. L.; Johnston, K. P., "Stabilized polymer microparticles by precipitation with a compressed fluid antisolvent. 2. Poly (propylene oxide)- and poly (butylene oxide)-based copolymers", *Langmuir*, 13, 1997, 1519.

McHugh, M. and Krukonis, V. J., *Supercritical Fluid Extraction: Principles and Practice*, Butterworths, Boston, 1986.

McHugh, M. and Krukonis, V. J., *Encyclopedia of Polymer Science and Engineering*, 2 nd., N. M. Bikales, C. G. Overberger, and G Menges, eds., Wiley, New York, 1988.

McHugh, M. and V. J. Krukonis, *Supercritical Fluid Extraction: Principles and Practice*, 2nd edition, Stoneham, MA: Butterworths-Heinemann, 1994.

Mishima, K.; Matsuyama, K.; Tanabe, D.; Yamauchi, S.; Young, T. J.; Johnston, K. P., "Microencapsulation of proteins by rapid expansion of supercritical solution with a nonsolvent", *AIChE J.*, 46, 2000, 857.

Mohamed, R. S.; Debenedetti, P. G.; Prud'homme, R. K., "Effects of process conditions on crystal obtained from sypercritical mixtures", *AIChE J.*, 35, 1989, 325.

Moneghini, M.; Kikic, I.; Voinovich, D.; Perissutti B.; Filipović-Grčić, J., "Processing of carbamazepine–PEG 4000 solid dispersions with supercritical carbon dioxide: preparation, characterisation, and in vitro dissolution", *Intl. J. Pharm.*, 222, 2001, 129.

Moshashaée, S.; Bisrat, M.; Forbes, R. T.; Nyqvist, H.; York, P., "Supercritical fluid processing of proteins. I: Lysozyme precipitation from organic solution", *European J. Pharm. Sci.*, 11, 2000, 239.

Moyler, D. A., *Extraction of natural products using near-critical solvents*, eds, M. B. King and T. R. Bott, Chapman & Hall, Glasgow, 1993.

Muhrer, G.; Mazzotti, M.; Müller, M., "Gas antisolvent recrystallization of an organic compound. Tailoring product PSD and scaling-up", *J. Supercrit. Fluids*, 27, 2003, 195.

Muhrer, G.; Lin, Cheng; Mazzotti, M, "Medelling the GAS antisolvent recrystallization process", *Ind. Eng. Chem. Res.*, 41, 2002, 3566.

Ogawa, Y.; Yamamoto, M.; Takada, S.; Okada, H.; Shimamoto, T., "A new technique to efficiently entrap Leuprolide acetate into microcapsules of poly (lactic acid) or copoly (lactic/glycolic acid) and Controlled release of Leuprolide acetate from poly (lactic acid) or copoly (lactic/glycolic acid) microcapsules: Influence of molecular weight and copolymer ratio of polymer", *Chem. Pharm. Bull.*, 36, 1988, 1095 and 1502.

O'Neill, M. L.; Cao, Q.; Fang, M.; Johnston, K. P.; Wilkinson, S. P.; Smith, C.; Kerschner, J. L.; Jureller, S. H., "Solubility of homopolymers and copolymers in carbon dioxide", *Ind. Eng. Chem. Res.*, 37, 1998, 3067.

Özyazici, M.; Sevgi, F.; Ertan, G., "Micromeritic studies on nicardipine hydrochloride microcapsules", *Intl. J. Pharm.*, 138, 1996, 25.

Peng, D.-Y. and Robinson, D. B., "A New Two-Constant Equation of State", *Ind. Eng. Chem. Fundam.*, 15, 1976, 59.

Pessey, V.; Mateos, D.; Weill, F.; Cansell, F.; Etourneau, J.; Chevalier, B., "$SmCo_5$/Cu particles elaboration using a supercritical fluid process", *J. Alloys and Compounds*, 323, 2001, 412.

Pessey, V.; Garriga, R.; Weill F.; Chevalier, B.; Etourneau, J.; Cansell, F., "Core-shell materials elaboration in supercritical mixture CO_2/ethanol, *Ind. Eng. Chem. Res.*, 39, 2000, 4714.

Pfeffer, R.; Dave, R. N.; Wei, D.; Ramlakhan, M., "synthesis of engineered particulates with tailored properties using dry particle coating", *Powder Technol.*, 117, 2001, 40.

Platzer, B. and Maurer, G., "A generalized equation of state for polar and nonpolar fluids", *Fluid Phase Equilibria*, 51, 1989, 223.

Randolph, T. W.; Randolph, A. D.; Mebes, M.; Yeung, S., "Sub-micrometer-sized biodegradable particles of poly (L-lactic acid) via the gas antisolvent spray precipitation process", *Biotechnol. Prog.*, 9, 1993, 429.

Reverchon, E. and Porta, G. Della, "Production of antibiotic micro- and nano-particles by supercritical antisolvent precipitation", *Powder Technol.*, 106, 1999, 23.

Reverchon, E.; Porta, G. Della; Pallado, P., "Supercritical antisolvent precipitation of salbutamol microparticles", *Powder Technol.*, 106, 1999, 17.

Reverchon, E.; Porta, G. Della; Rosa, I. D.; Subra, P.; Letourneur, D., "Supercritical antisolvent micronization of some biopolymers", *J. Supercrit. Fluids*, 18, 2000, 239.

Reverchon, E.; Porta, G. Della.; Trolio, A. Di.; Pace, P., "Supercritical antisolvent precipitation of nanoparticles of superconductor precursors", *Ind. Eng. Chem. Res.*, 37, 1998, 952.

Reverchon, E.; Porta, G. Della; Sannino, D.; Ciambelli P., "Supercritical antisolvent precipitation of nanoparticles of a zinc oxide precursor", *Powder Technol.*, 102, 1999, 127.

Reverchon, E., "Supercritical antisolvent precipitation of micro- and nano-particles", *J. Supercrit. Fluids*, 15, 1999, 1.

Riberio Dos Santos, I.; Richard, J.; Pech, B.; Thies, C.; Benoit, J. P., "Microencapsulation of protein particles within lipids using a novel supercritical fluid process", *Intl. J. Pharm.*, 242, 2002, 69.

Ruys, A. J. and Mai, Y. W., "The nanoparticle-coating process: A potential sol-gel route to homogeneous nanocomposites", *Materials Sci. and Eng., A*, 265, 1999, 202.

Schreiber, R.; Vogt, C.; Werther, J.; Brunner G., "Fluidized bed coating at supercritical fluid conditions", *J. Supercrit. Fluids*, 24, 2002, 137.

Sglavo, V. M.; Dal Maschio, R., Soraru, G. D.; Bellosi, A., "Fabrication and characterization of polymer-derived silicon nitride oxide zirconia (Si_2N_2O-ZrO_2) nanocomposite ceramics", *J. Mater. Sci.*, 28, 1993, 6437.

Shaffer, K. A.; Jones, T. A.; Canelas, D. A.; DeSimone, J. M., "Dispersion polymerizations in carbon dioxide using siloxane-Based stabilizers", *Macromolecules*, 29, 1996, 2704.

Shi, D.; Wang, S. X.; Ooij, W. J.; Wang, L. M.; Zhao, J. G.; Yu, Z., "Uniform deposition of ultrathin polymer films on the surfaces of Al_2O_3 nanoparticles by a plasma treatment", *Appl. Phys. Lett.*, 78, 2001, 1243.

Shiho, H. and DeSimone, J. M., "Dispersion polymerization of acrylonitrile in supercritical carbon dioxide", *Macromolecules,* 33, 2000, 1565.

Shim, J.-J.; Yates, M. Z.; Johnston, K. P., "Polymer coatings by rapid expansion of suspensions in supercritical carbon dioxide", *Ind. Eng. Chem. Res.*, 38, 1999, 3655.

Shim, J.-W.; Kim, J.-W.; Han, S.-H.; Chang, I.-S.; Kim, H.-K.; Kang, H.-H.; Lee, O.-S.; Suh, K.-D., "Zinc oxide/polymethylmethacrylate composite microspheres by in situ suspension polymerization and their morphological study", *Colloids and Surfaces A: Physicochemical and Engineering Aspects*, 207, 2002, 105.

Sievers, R. E.; Sellers, S. P.; Kusek, K. D.; Clark, G. S.; Korte, B. J., "CO_2-activated nebulization and `bubble' spray drying to form fine (1–5 μm) particles of proteins and small molecules for inhalation drug therapy", *Conference on Drug Delivery*, Breckenbridge, July, 1999.

Soppimath, K. S.; Kulkarni, A. R.; Aminabhavi, T. M., "Encapsulation of antihypertensive drugs in cellulose-based matrix microspheres: Characterization and release kinetics of microspheres and tableted microspheres", *J. Microencapsulation* 18, 2001, 397.

Steckel, H.; Thies, J.; Müller, B. W., "Micronizing of steroids for pulmonary delivery by supercritical carbon dioxide", *Intl. J. Pharm.*, 152, 1997, 99.

Sudsakorn, K. and Turton, R., "Nonuniformity of particle coating on a size distribution of particles in a fluidized bed coater", *Powder Technol.*, 110, 2000, 37.

Takeo, O.; Koichi, N.; Katsuaki, S., "Formation of carbon nanocapsules with SiC nanoparticles prepared by polymer pyrolysis", *J. Mater. Chem.*, 8, 1998, 1323.

Thies, J. and Müller, B. W., "Size controlled production of biodegradable microparticles with supercritical gases", *European J. Pharm. Biopharm.*, 45, 1998, 67.

Tom, J. W. and Debenedetti, P. G., "Formation of bioerodible polymeric microspheres and microparticles by rapid expansion of supercritical solutions", *Biotechnol. Prog.*, 7, 1991, 403.

Tom, J. W.; Debenedetti, P. G.; Jerome, R., "Precipitation of poly (L-lactic acid) and composite poly (L-lactic acid)-pyrene particles by rapid expansion of supercritical solutions", *J. Supercrit. Fluids*, 7, 1994, 9.

Tsutsumi, A..; Nakamoto, S.; Mineo, T.; Yoshida, K., "A novel fluidized-bed coating of fine particles by rapid expansion of supercritical fluid solutions", *Powder Technol.*, 85, 1995, 275.

Tu, L. S.; Dehghani, F.; Foster, N. R., "Micronisation and microencapsulation of pharmaceuticals using a carbon dioxide antisolvent", *Powder Technol.*, 126, 2002, 134.

Türk, M., "Influence of thermodynamic behaviour and solute properties on homogeneous nucleation in supercritical solutions", *J. Supercrit. Fluids*, 18, 2000, 169.

Vollath D. and Szabó, D. V., "Coated nanoparticles: A new way to improved nanocomposites", *J. Nanoparticle Res.*, 1, 1999, 235.

Walas, S. M., *Phase Equlibria in Chemical Engineering*, Butterworth, Boston, ch. 2 (1985).

Walter, E.; Moelling, K.; Pavlovic, J.; Merkle, H. P., "Microencapsulation of DNA using poly (DL-lactide-co-glycolide): stability issues and release characteristics", *J. Control. Rel.*, 61, 1999, 361.

Wan, S. C. and Lai, W. F., "Multilayer drug-coated cores: A system for controlling drug release", *Intl. J. Pharm.*, 81, 1992, 75.

Wang, D.; Robinson, D. R.; Kwon, G. S.; Samuel, J., "Encapsulation of plasmid DNA in biodegradable poly(D, L-lactic-co-glycolic acid) microspheres as a novel approach for immunogene delivery", *J. Control. Rel.*, 57, 1999, 9.

Wang F. –J. and Wang, C. –H., "Sustained release of etanidazole from spray dried microspheres prepared by non-halogenated solvents", *J. Control. Rel.*, 81, 2002, 263.

Wang, T. J.; Tsutsumi, A.; Hasegawa, H.; Mineo, T., "Mechanism of particle coating granulation with RESS process in a fluidized bed", *Powder Technol.*, 118, 2001, 229.

Wang, Y.; Wei, D.; Dave, R.; Pfeffer, R.; Sauceau, M.; Letourneau, J.-J.; Fages, J., "Extraction and precipitation particle coating using supercritical CO_2", *Powder Technol.*, 127, 2002, 32.

Wang, Y.; Dave, R.; Pfeffer, R., "Nanoparticle encapsulation with heterogeneous nucleation in a supercritical antisolvent process", *J. Supercrit. Fluids*, 28, 2004, 85.

Werling, J. O. and Debenedetti, P. G., "Numerical modeling of mass transfer in the supercritical antisolvent process", *J. Supercrit. Fluids*, 16, 1999, 167.

Werling, J. O. and Debenedetti, P. G., "Numerical modeling of mass transfer in the supercritical antisolvent process: miscible conditions", *J. Supercrit. Fluids*, 18, 2000, 11.

Wieland-Berghausen, S.; Schote, U.; Frey, M.; Schmidt, F., "Comparison of microencapsulation techniques for the water-soluble drugs nitenpyram and clomipramine HCl", *J. Control. Rel.*, 85, 2002, 35.

Winter, M. A.; Frankel, D. Z.; Debenedetti, P. G.; Carey, J.; Devaney, M.; Przybycien, T. M., "Protein purification with vapor-phase carbon dioxide", *Biotechnol. Bioeng.*, 62, 1999, 247.

Winter, M. A.; Knutson, B. L.; Debenedetti, P. G.; Sparks, H. G.; Przybycien, T. M.; Stevenson, C. L.; Prestrelski, S. J., "Precipitation of proteins in supercritical carbon dioxide", *J. Pharm. Sci.*, 85, 1996, 586.

Wissinger, R. G. and Paulaitis, M. E., "Glass transitions in polymer-CO_2 mixtures at elevated pressures", *J. Polym. Sci., Part B*, 29, 1991a, 631.

Wissinger, R. G. and Paulaitis, M. E., "Molecular thermodynamic model for sorption and swelling in glassy polymer-CO_2 systems at elevated pressures", *Ind. Eng. Chem. Res.*, 30, 1991b, 842.

Yamaguchi, Y.; Takenaga, M.; Kitagawa, A.; Ogawa, Y.; Mizushima Y.; Igarashi, R., "Insulin-loaded biodegradable PLGA microcapsules: initial burst release controlled by hydrophilic additives", *J. Control. Rel.*, 81, 2002, 235.

Yang, T. H.; Dong, A.; Mayer, J.; Johnson, O. L.; Cleland, J. L.; Carpenter, J. F., "Use of infrared spectroscopy to access secondary structure of human growth hormone within biodegradable microsphere", *J. Pharm. Sci.*, 88, 1999, 161.

Yates, M. Z.; Li, G.; Shim, J. J.; Maniar, S.; Johnston, K. P.; Lim, K. T.; Webber, S., "Ambidextrous surfactants for water-dispersible polymer powders from dispersion polymerization in supercritical CO_2", *Macromolecules*, 32, 1999, 1018.

Yen, S.-Y.; Sung, K. C.; Wang, J.-J.; Hu, Y.-P., "Controlled release of nalbuphine propionate from biodegradable microspheres: in vitro and in vivo studies", *Intl. J. Pharm.*, 220, 2001, 91.

Yeo, S-D.; Choi, J.-H; Lee T-J., "Crystal formation of $BaCl_2$ and NH_4Cl using a supercritical fluid antisolvent", *J. Supercrit. Fluids*, 16, 2000, 235.

Yeo, S.-D.; Lim, G.-B.; Debenedetti, P. G.; Bernstein, H., "Formation of microparticulate protein powders using a supercritical fluid antisolvent", *Biotech. Bioeng.*, 41, 1993, 341.

Yeo, S. -D.; Debenedetti, P. G.; Patro, S. Y.; Przybycien, T. M., "Secondary structure characterization of microparticulate insulin powders", *J. Pharm. Sci.*, 83, 1994, 1651.

Young, T. J.; Johnston, K. P.; Mishima, K.; Tanaka, H., "Encapsulation of lysozyme in a biodegradable polymer by precipitation with a vapor-over-liquid antisolvent", *J. Pharm. Sci.*, 88, 1999, 640.

Xu, C.Y.; Sievers, R.E.; Karst, U.; Watkins, B. A.; Karbiwnyk, C. M.; Andersen, W. C.; Schaefer, J. D.; Stoldt, C. R., "Supercritical carbon dioxide assisted aerosolization for thin films deposition, fine powder generation, and drug delivery", *Chapter 18 in Green Chemistry: Frontiers in Benign Chemical Synthesis and Processes*, P.T. Anastas and T.C. Williamson (Eds.), Oxford University Press, Oxford, 1998, 313.

Xu, C. Y.; Watkins, B.; Sievers, R. E.; Jing, X.; Trowga, P.; Gibbons, C. S.; Vecht, A., "Submicron-sized spherical yttrium oxide based phosphors prepared by supercritical CO_2-assisted aerosolization and pyrolysis", *Appl. Phys. Lett.*, 71, 1997, 1643.

Xu, J.; Wlaschin, A.; Enick, R. M., "Thickening carbon dioxide with the fluoroacrylate-styrene copolymer", *SPE J.*, 8, 2003, 85.

Zhang, J. X. and Gao, L. Q., "Nanocomposite powders from coating with heterogeneous nucleation processing", *Ceramics International*, 27, 2001, 143.

Zhang, Y.; Zhang, Q.; Li, Y.; Wang, N.; Zhu, J., "Coating of carbon nanotubes with tungsten by physical vapor deposition", *Solid State Communications*, 115, 2000, 51.